Copyright Warning & Restrictions

The copyright law of the United States (Title 17, United States Code) governs the making of photocopies or other reproductions of copyrighted material.

Under certain conditions specified in the law, libraries and archives are authorized to furnish a photocopy or other reproduction. One of these specified conditions is that the photocopy or reproduction is not to be "used for any purpose other than private study, scholarship, or research." If a, user makes a request for, or later uses, a photocopy or reproduction for purposes in excess of "fair use" that user may be liable for copyright infringement,

This institution reserves the right to refuse to accept a copying order if, in its judgment, fulfillment of the order would involve violation of copyright law.

Please Note: The author retains the copyright while the New Jersey Institute of Technology reserves the right to distribute this thesis or dissertation

Printing note: If you do not wish to print this page, then select "Pages from: first page # to: last page #" on the print dialog screen

ABSTRACT

1,4-DIOXANE BIODEGRADATION IN PROPANOTROPHS: MOLECULAR FOUNDATIONS AND IMPLICATIONS FOR ENVIRONMENTAL REMEDIATION

by
Fei Li

1,4-Dioxane (dioxane) has emerged with an escalating concern given its human carcinogenicity and widespread occurrence in groundwater. Bioremediation is promising as an effective and cost-efficient treatment alternative for *in situ* or *ex situ* cleanup of dioxane and co-existing pollutants in the field. Soluble di-iron monooxygenases (SDIMOs) are reputed for their essential roles in initiating the cleavage of dioxane and other pollutants. In this doctoral dissertation, molecular foundations for SDIMOs-mediated dioxane biodegradation are untangled to promote the development and implication of site-specific bioremediation and natural attenuation strategies. This dissertation focused on propanotrophic bacteria given their pivotal roles in dioxane metabolism and co-metabolism.

The first part of this dissertation is centered on investigating the distinctive catalytic behaviors between two archetypical dioxane degrading enzymes, propane monooxygenase (PRM) and tetrahydrofuran monooxygenase (THM), belonging to group-6 and group-5 SDIMOs, respectively. They are compared from kinetics, inhibition, and substrate range. Results reveal that PRM is more profitable in environmental conditions such as low dioxane concentration, co-existing chlorinated solvents, and many other pollutants suggesting that PRM may has been long underestimated.

The second section refines the phylogenies of SDIMOs into six groups. The evaluation sequence of this multi-component enzyme family follows the order: group-4

alkene MO → group-5 propane/tetrahydrofuran MO → group-6 propane MO → group-3 methane/butane MO. Their short-chain gaseous hydrocarbon degradation capabilities evolve from unsaturated to saturated compounds and from low C-H bond to high energy. Results allow a robust bioprospecting of SDIMO.

The third part of this dissertation is aimed to untangle downstream dioxane degradation pathways in metabolic degraders via genome the comparison of metabolic and co-metabolic strains. A putative flavin-containing monooxygenase (*fmo*) gene is cloned and expressed in mc^2-155. Unfortunately, no HEAA transformation activity is exhibited by this transformant. Existence of the complete glycolate transformation pathway in all dioxane metabolizers reveals its essential role in dioxane mineralization.

As trace levels of dioxane (<1 mg/L) are widely detected in contaminated sites, the fourth part aims to tackle such biotransformation hindrance by bioaugmentation with a novel dioxane co-metabolizer, *Azoarcus* sp. DD4. DD4 exhibited formidable adaptability and relatively stable performance on dioxane degradation with the supplement of propane, supporting its feasibility for both *in situ* and *ex situ* treatment of dioxane even when its concentration is below 100 µg/L. Pure strain study reveals DD4 can overcome the inhibition of cVOCs and degrade them when supplied with propane.

Last but not the least, a bioremediation treatment train combining the reductive dehalogenation by halorespiring consortium, SDC-9, and cometabolic oxidation by DD4 to address the commingling contamination of TCE and dioxane. SDC-9 can effectively remove TCE, however, lingering with less-chlorinated but toxic metabolites, vinyl chloride (VC) and *cis*-dichloroethene (cDCE). Subsequent aerobic bioaugmentation with DD4, can concurrently degrade dioxane, VC, and cDCE.

1,4-DIOXANE BIODEGRADATION IN PROPANOTROPHS: MOLECULAR FOUNDATIONS AND IMPLICATIONS FOR ENVIRONMENTAL REMEDIATION

by
Fei Li

A Dissertation
Submitted to the Faculty of
New Jersey Institute of Technology
in Partial Fulfillment of the Requirements for the Degree of
Doctor of Philosophy in Environmental Science

Department of Chemistry and Environmental Science

August 2020

.

APPROVAL PAGE

1,4-DIOXANE BIODEGRADATION IN PROPANOTROPHS: MOLECULAR FOUNDATIONS AND IMPLICATIONS FOR ENVIRONMENTAL REMEDIATION

Fei Li

Dr. Mengyan Li, Dissertation Advisor — Date
Assistant Professor of Chemistry and Environmental Science, NJIT

Dr. Somenath Mitra, Committee Member — Date
Distinguished Professor of Chemistry and Environmental Science, NJIT

Dr. Edgardo T. Farinas, Committee Member — Date
Associate Professor of Chemistry and Environmental Science, NJIT

Dr. Alexei Khalizov, Committee Member — Date
Associate Professor of Chemistry and Environmental Science, NJIT

Dr. Lucia Rodriguez-Freire, Committee Member — Date
Assistant Professor of Civil and Environmental Engineering, NJIT

BIOGRAPHICAL SKETCH

Author: Fei Li

Degree: Doctor of Philosophy

Date: August 2020

Undergraduate and Graduate Education:

- Doctor of Philosophy in Environmental Science,
  New Jersey Institute of Technology, Newark, NJ, 2020

- Master of Science in Fermentation Engineering,
  Tianjin University of Commerce, Tianjin, P. R. China, 2015

- Bachelor of Science in Bioengineering,
  Tianjin University of Commerce, Tianjin, P. R. China, 2012

Major: Environmental Science

Presentations and Publications:

Li, F., Deng, D., and Li, M., Distinct catalytic behaviors between two 1, 4-dioxane degrading monooxygenases: kinetics, inhibition, and substrate range. *Environmental Science & Technology*. 2020, 54(3), 1898-1908

Li, F., Deng, D., and Li, M., Comparison of catalytic behaviors between two 1,4-dioxane degrading monooxygenases. 2019 Bioremediation Symposium. Baltimore, MD

Deng, D., Pham, DN., Li, F., and Li, M., Discovery of an inducible toluene monooxygenase that co-oxidizes 1, 4-dioxane and 1, 1-dichloroethylene in propanotrophic *Azoarcus sp. DD4*. *Applied and Environmental Microbiology*. 2020

Deng, D., Li, F., Ye, L. and Li, M., Complete genome sequence of *Azoarcus* sp. strain DD4, a Gram-negative propanotroph that degrades 1, 4-dioxane and 1, 1-dichloroethylene. *Microbiology resource announcements*, 2019, 8(33), e00775-19.

Deng, D., Li, F., Wu, C. and Li, M., Synchronic biotransformation of 1, 4-dioxane and 1, 1-dichloroethylene by a Gram-negative propanotroph *Azoarcus* sp. DD4. *Environmental Science & Technology Letters*, 2018, 5(8), 526-532.

Deng, D., Li, F. and Li, M., A novel propane monooxygenase initiating degradation of 1, 4-dioxane by *Mycobacterium dioxanotrophicus* PH-06. *Environmental Science & Technology Letters*, 2018, 5(2), 86-91.

To my dearest dad and mom. Thanks for always being there for me.

致我最亲爱的爸爸，妈妈，感谢你们一直陪伴在我身边

ACKNOWLEDGMENT

Over the past four years, I have received support and encouragement from the numbers of individuals. I would not complete my Ph.D. degree without their support, accompanying, and nurturing. Here I would like to express my deepest appreciation to those people who made this journey an unforgettable experience.

I am deeply indebted to my adviser, Dr. Mengyan Li for his critical role in my doctoral work. Professor Li provided me with professional guidance, assistance, and expertise that I needed during my experimental design, troubleshooting, article writing, preparing for conferences, and any other circumstances. His patience, expertise, kindness always impressed and encouraged me, leading my research to the right track. I am always grateful for his help in opening my horizons and mentoring me thinking from various aspects. I have fortunately been involved in many research projects, attended numerous international and regional conferences in the related field, and mentor students. These precious experiences taught me how to be an independent researcher and mentor. I quite simply cannot imagine a better adviser.

I would like to extend my gratitude to my dissertation committee members: Dr. Somenath Mitra, Dr. Alexei Khalizov, Dr. Edgardo Farinas, and Dr. Lucia Rodriguez-Freire. Special thanks to them for finding time in their busy schedules to attend my proposal and dissertation defense, also review this dissertation and provide me constructive advice, critical comments, and valuable feedback.

I gratefully acknowledge all the financial support that made the completion of the dissertation, provided by the National Science Foundation NSF CAREER CBET-1846945, United States Geological Survey (USGS) State Water Resources Research Act

Program (2018NJ400B), Langan Engineering, HDR, and the start-up fund from the Department of Chemistry and Environmental Science at NJIT.

The instrumentation and chemical support from Dr. Pin Gu, Mr. Yogesh Gandhi, Dr. Jeong Shim, Dr. Chaudhery M. Hussain, Dr. Xiaoyang Xu, Mr. Lei Ye, Dr. Hao Chen, Dr. Yuanwei Zhang, Dr. Wen Zhang, and Dr. Yongick Kim cannot be overestimated. They generally provided their best help to support my experiment. Furthermore, Dr. Kathleen M. Gilbert, Genti M. Price, and Sylvana L. Brito provided administrative support that made me a successful graduate. Thanks also to Lingke Zeng, Stewart Abrams from Langan Engineering, Andrew Wadden, Patricia Parvis from HDR for their unwavering supports. I found them particularly helpful to me during the time for sampling from rivers, sediments, and Superfund sites.

I am also grateful to my previous and current group members, Dr. Daiyong Deng, Dr. Qiong Wu, Dr. Guifen Lyu, Wu Chen, Dung Ngoc Pham, Na Liu, Yue Zhang, Jian Wang, Jose Antunes and all the students who worked in our lab. I really appreciate their valuable help and support in my academic life. I would like also to say thanks to my friends: Chunzhao Chen, Na Mao, Wanyi Fu, Zhou Sun, Hongling Deng, Caiwu Ding who provided me an enjoyable life.

Lastly, but most importantly, I am deeply thankful to my family for their love, support, and sacrifices. Without them, I would not succeed in this endeavor. They are providing me long-lasting support, understanding, encouragement, and patience, which accompanied me through all the hardships during this research adventure. Words fail to express my gratitude to them.

TABLE OF CONTENTS

TABLE OF CONTENTS
(Continued)

TABLE OF CONTENTS
(Continued)

Chapter **Page**

TABLE OF CONTENTS
(Continued)

Chapter **Page**

TABLE OF CONTENTS
(Continued)

Chapter **Page**

TABLE OF CONTENTS
(Continued)

Chapter **Page**

LIST OF TABLES

LIST OF TABLES
(Continued)

LIST OF FIGURES

LIST OF FIGURES
(Continued)

Figure **Page**

LIST OF FIGURES
(Continued)

LIST OF FIGURES
(Continued)

Figure **Page**

LIST OF FIGURES
(Continued)

Figure **Page**

LIST OF DEFINITIONS

USEPA	United States Environmental Protection Agency
MNA	monitored natural attenuation
SDIMO	soluble di-iron monooxygenase.
SCAM	short-chain alkane monooxygenase
sMMO	soluble methane monooxygenase
PRM	propane monooxygenase
THM	tetrahydrofuran monooxygenase
TMO	toluene monooxygenase
cVOC	chlorinated volatile organic compounds
PCE	tetrachloroethene
TCE	trichloroethene
1,1,1-TCA	1,1,1-trichlorethane
cDCE	1,2-*cis*-dichloroethene
tDCE	1,2-*trans*-dichloroethene
1,2-DCA	1,2-dichloroethane
VC	vinyl chloride
MTBE	Methyl *tert*-butyl ether
THF	tetrahydrofuran
MDL	method detection limit
MRL	minimum report limit

LIST OF DEFINITIONS
(Continued)

PDX	1,4-dioxane-2-one
HEAA	2-hydroxyethoxyacetic acid, 2-(2-hydroxyethoxy) acetic acid
BSA	bovine serum albumin
AMS	ammonium mineral salts
NMS	nitrate mineral salt
PBS	phosphate-buffered saline
V_{max}	maximum degradation velocity
K_m	half-saturation coefficient
K_I	inhibition constant
qPCR	quantitative polymerase chain reaction
RT-qPCR	reverse transcription- quantitative polymerase chain reaction
GC	gas chromatography
MS	mass spectrometry
FID	flame ionization detector
SDS-PAGE	sodium dodecyl sulfate–polyacrylamide gel electrophoresis
SRB	sulfate reducing bacteria
OD	optical density

CHAPTER 1

INTRODUCTION

1.1 Background Information of 1,4-Dioxane

1,4-Dioxane (further referred to as dioxane) is a six-member diether ring. It has a centrosymmetric molecule, which means it adopts a chair conformation as shown in Figure 1.1, and delivers a highly stable structure and recalcitrant in the environment. It was first synthesized as a stabilizer by A.V. Lourenço[1] in 1863 by the hydration reaction of ethylene glycol with the catalyzer sulfuric acid. It has a molecular weight of 88.11 g/mol including four carbons, eight hydrogens, and two oxygens. The oxygen can form hydrogen bonds with water resulting in hydrophilic. It has quite low volatility above H_2O solution because of the low Henry's Law constant (4.80×10^{-6} atm-m^3 /mol at 25 °C) and fair partitioning to organic absorbents since the low log K_{ow} coefficient (-0.27) (Table 1.1).

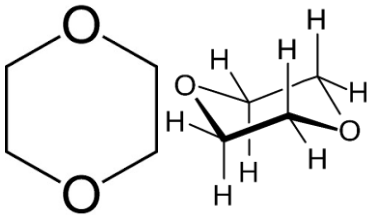

Figure 1.1 Chemical structure of dioxane. Left: structural formula. Right: three-dimensional structural formula.

Historically, dioxane was primarily (90 %) used as a stabilizer for chlorinated solvents typically 1,1,1-trichloroethane (1,1,1-TCA), because dioxane can neutralize the reaction between chlorinated and aluminum which is the main component of transportation containers[2]. Later, dioxane usage as a chlorinated solvent stabilizer was terminated as TCA

was phased out under the 1995 Montreal Protocol. However, dioxane is still being produced as an additive in many other products such as paint strippers, dyes, ink, greases, antifreeze, polyethylene terephthalate (PET) plastic[2, 3] and aircraft deicing fluids[4]. Because of its good solubility for organic compounds, it is used as a purifying agent in the manufacturing of pharmaceuticals and surface treatment agent for high purity metal. It is also an excellent solvent for reaction systems. Trace levels of dioxane can be found in consumer products such as detergents, shampoos, deodorants, and cosmetics. It may be present in food supplements as well, which is expected from the residues from packing adhesive or on food crops treated with a pesticide that contains dioxane[5].

Table 1.1 Physical Properties of Dioxane

Properties	Description
Chemical formula	$C_4H_8O_2$
Molar mass	88.11 g/mol
Appearance	Colorless liquid
Odor	Mild, ether-like
Density (25 °C)	1.033 g/mL
Melting point	11.8 °C
Boiling point	101.1 °C
Solubility (water)	Miscible
Polarity index	4.8
Octanol-water partition coefficient (log K_{ow})	-0.27
Organic carbon partition coefficient (log K_{oc})	1.23
Henry's law constant at 25 °C (atm-m^3 /mol)	4.80×10^{-6}

Unfortunately, dioxane has been widely detected across the world in various aquatic systems such as drinking water systems, municipal wastewater streams, rivers and river beds, coastal marine environment, and groundwater[6-9]. In Japan, research demonstrated that the water from river basin sewerage systems, chemical plants, and effluents from the combined collection treatment from apartment houses serve as the pollutant source discharging dioxane to the aquatic systems[6]. A dioxane concentration

investigation was done in Europe also revealing that the sewage treatment plant cannot remove dioxane, whilst bank filtration and drinking water purification process cannot eliminate dioxane. It marginally degraded from 650ng/L and 670 ng/L to 600 ng/L and 490 ng/L, respectively[10]. Approximately 22% of the public water systems (PWSs) were detected with results higher than the minimum reporting level (MRL) which is 0.07 µg/L. 7% of the PWSs were detected higher than the reference concentration (i.e., 0.35 µg/L) with the cancer risk level of 1:100000[11]. Among the US Air Force (USAF) installations, a total of 732 out of 4196 (17%) groundwater monitor wells (GMWs) were contaminated with dioxane that higher than the reporting limit[4]. Recent site surveys revealed a high co-occurrence frequency of dioxane with 1,1,1-TCA and/or trichloroethene (TCE) at impacted sites nationwide[4, 8, 12].

Dioxane is classified as a possible human carcinogen by the Environmental Protection Agency (EPA), the International Agency for Research on Cancer (IARC), the National Institute for Occupational Safety and Health (NIOSH), and the European Union (EN)[13-15]. Dioxane has also been listed as a "high priority" pollutant in the 2016 amendment of the Toxic Substance Control Act (TSCA)[16]. Although there is limited evidence showing its carcinogenic effect to humans, dioxane's carcinogenicity has been verified with increasing incidences of nasal cavity, liver and gall bladder tumors after a chronic exposure based on animal studies. A short-term exposure to a high concentration of dioxane (> 200 mg/L) causes nausea, drowsiness, headache, and irritation to organisms reported by the Agency for Toxic Substances and Disease Registry (ATSDR), EPA, NIOSH, and EU.

The lack of federal maximum contaminant level (MCL) makes states to legislate varying guideline levels for dioxane. To date, dioxane in drinking water was suggested to

be lower than 50 µg/L accordingly to the lifetime cancer risk of 10^{-5} by WHO[17]. Independently, USEPA also reported a guideline for dioxane in drinking water at the cancer risk level of 10^{-6}, which is 0.35 µg/L[18]. The New Jersey Department of Environmental Protection (NJDEP) released a strict groundwater criterion of 0.4 µg/L for dioxane in groundwater following the cancer risk level at 1:1000000[19]. The most stringent regulation level is 0.25 µg/L in New Hampshire initiated in 2011 (Table 1.2).

Table 1.2 Dioxane Drinking Water or Groundwater Guidelines by States and National or International Organizations

State/Organization	Guideline (µg/L)	Source
Alaska	77	AL DEC 2016
California	1.0	Cal/EPA 2011
Colorado	0.35	CDPHE 2017
Connecticut	3.0	CTDPH 2015
Delaware	6.0	DE DNR 1999
Florida	3.2	FDEP 2005
Indiana	7.8	IDEM 2015
Maine	4.0	MEDEP 2016
Massachusetts	0.3	MADEP 2004
Minnesota	1.0	MDH 2015
Mississippi	6.09	MS DEQ 2002
New Hampshire	0.25	NH DES 2011
New Jersey	0.4	NJDEP 2015
New York	50	NYDOH 2015
North Carolina	3.0	NCDENR 2015
Pennsylvania	6.4	PADEP 2011
Texas	9.1	TCEQ 2016
Vermont	3.0	VTDEP 2016
Washington	0.438	WA ECY 2015
West Virginia	6.1	WV DEP 2009
United States	0.35	US EPA 2010
WHO	50	WHO 2011

1.2 Variety of Bioremediation Strategies for Dioxane Bioremediation

Dioxane poses a current and future threat to human due to its recalcitrance and possible human carcinogen. As a cyclic ether, dioxane exhibits high mobility and persistency once

released to the environment. It is recognized as one of the most frequently detected nonregulated pollutants in our water supplies and sources based on the national survey for the Third Unregulated Contaminant Monitoring Rule (UCMR3)[11]. Dioxane's extreme hydrophilicity and water miscibility may also lead to the formation of large dilute plumes with trace concentrations (e.g., < 1 mg/L[20]) in the subsurface[2, 21]. Due to the miscible solubility and low organic carbon partition coefficient (log K_{OC} = 1.23) of dioxane[22], its efficiency limits the use of GAC in groundwater treatment with high flows and low concentration. Although a novel adsorbent, AMBERSORB™ 560, can effectively remove dioxane over a wide range of concentration down to sub-0.3 µg/L[23], the cost is non-negligible because of the large volume of the dioxane-impacted plume. Same to physical adsorption, AOP is a strategy that needs high cost although it can unbiasedly oxidize many persistent organic contaminants[24]. Typically, capital costs range from $80,000 to $500,000 with operations and maintenance costs ranging from $0.20 to $1.50 per 1,000 gallons of water treated[25]. Some other reasons also significantly limit the application of AOP including the turbidity of aqueous, hydroxyl radical scavenging, unexpected toxic byproducts and acidity of the treated water[26-29]. Biological treatment strategies including monitored natural attenuation (MNA), bioaugmentation, biostimulation, pump-and-treat, membrane bioreactor (MBR) have supported bioremediation as a viable method for dioxane cleanup, especially in terms of cost, feasibility, and destruction of dioxane.

1.2.1 Monitored Natural Attenuation

Monitored Natural attenuation (MNA) generally relies on biological processes, which, unaided by deliberate human intervention, reduce the low concentration of dioxane. However, its feasibility highly dependents on the biodegradation capabilities of indigenous

communities at specific sites[30-32]. Increasingly, stakeholders responsible for cleanup as well as environmental regulators are relying upon natural attenuation as a remediation strategy because it is the most cost-efficient approaches to manage groundwater contamination and also it has the lowest sustainability impacts to the environment[33]. A few of current research revealed that dioxane MNA happens at a significant number of project sites[12, 32]. It relies on the indigenous bacteria harboring propane monooxygenase (PRM), tetrahydrofuran monooxygenase (THM) which can degrade dioxane from the field samples[30-32, 34-38]. With the assistance of modern molecular techniques, such as compound-specific isotope analysis (CSIA)[39], gene biomarker[30, 32, 35, 36], and microarray[32], genes encoding these dioxane degrading monooxygenases were successfully detected at contaminated sites to support the feasibility of MNA.

1.2.2 Biostimulation

Similar to MNA, biostimulation utilizes the indigenous degraders to degrade organic pollutants. It is a biological remediation strategy that involves the modification of the environment to stimulate the indigenous bacteria capable of bioremediation. To our best knowledge, most dioxane-degraders can utilize auxiliary substrate (alkane, alkene, alcohols, and THF) as carbon source and enable the dioxane degradation. The reason underlying is because the involving degrading enzymes, SDIMOs, has a wide range of substrate range. To data, only a handful of field or microcosm studies documented methane, propane, isobutane, and 1-butanol biostimulation in dioxane cleanups. Propane is the most promising stimulation gas for dioxane remediation due to the research found most of the dioxane degraders are propanotrophs. Amendment of 1-butanol (100 mg/L) or THF (300 µg/L) could enhance the trace level dioxane (<300 µg/L) degradation by indigenous

bacteria to some extent[28]. A field study conducted at the former McClellan Air Force Base Operable Unit D contaminated with dioxane (approximately 60 µg/L). Propane stimulated indigenous bacteria that was able to degrade dioxane to below 3 µg/L even without propane and oxygenase addition for a 2-week period[40]. A microcosm study prepared with groundwater from Alaska revealed that 1-butanol could stimulate the biodegradation of 50 mg/L of dioxane[41]. Similar observations were found as to isobutane and methane biostimulation[42-44]. For some specific field conditions, the performance of biostimulation is comparable with bioaugmentation. Rolston *et al.* found with sufficient inorganic nutrients, isobutane biostimulation was as effective as bioaugmentation with *Rhodococcus rhodochrous* strain ATCC 21198[45].

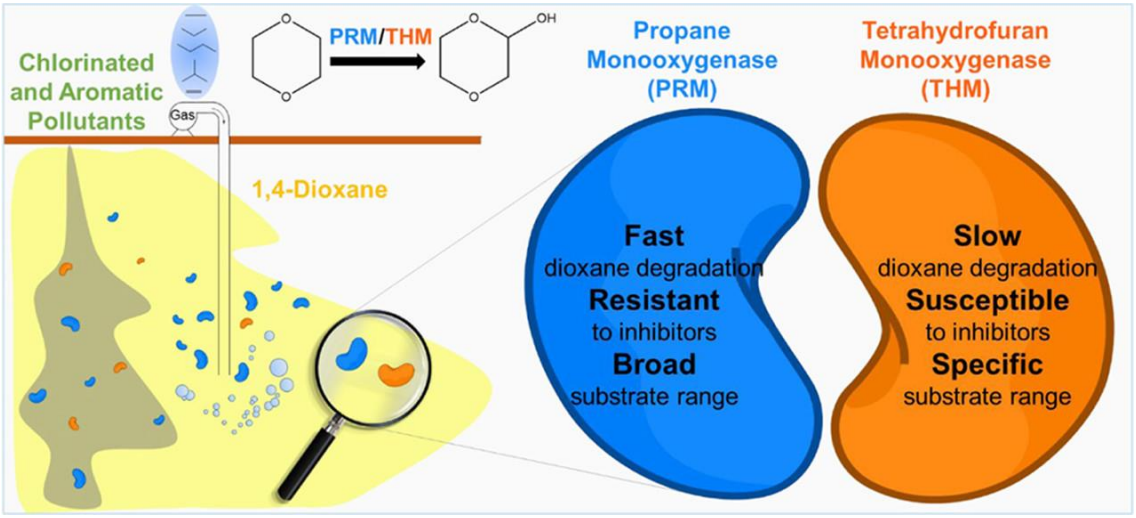

Figure 1.2 Dioxane treatment via biostimulation with short-chain alkane/alkene gases.

1.2.3 Bioaugmentation

Although a number of studies have been reported MNA or biostimulation could remediate dioxane, it typically needs a long period from a few months to decades[33, 46]. Bioaugmentation is a remediation strategy that speeds up the rate of degradation of

contaminants by adding bacterial cultures. Many researches have been studies on dioxane remediation by bioaugmentation technology including the use of CB1190, ENV425, DVS 5a1, and many other strains. Microcosm study revealed that the augmentation of CB1190 or DVS 5a1 could degrade 50 mg/L initial dioxane at the degradation rate of 0.16 ± 0.04 and 0.015 ± 0.006 mg dioxane/d/mg protein at 14 °C, respectively[41]. Results showed that propane biosparging with the addition of *Rhodococcus ruber* ENV425 (4×10^9 cells/mL) can be used for *in situ* treatment of dioxane from 1090 µg/L to below 2 µg/L within 8-month of operating time[47]. He *et al.* indicated PH-06 would be a better bioaugmentation candidate because of the greater cells yield (Y = 0.16 g protein/g dioxane) and higher affinity to dioxane (Km = 78 ± 10 mg/L) in comparison with CB1190 (Km = 145 ± 17 mg/L, Y = 0.11 g protein/g dioxane). Our results also suggested that the PH-06 is a better alternative for bioaugmentation than CB1190 because PRM in PH-06 has a broader substrate range than THM[38] (Figure 1.2). However, the current studies only focused on Gram-negative strains.

1.2.4 Bioreactor

Bioreactor is a manufactured device that supports a biologically active environment. It enables the operation controllable and easily changes the reaction condition depending on different water types and bacterial strains. Entrapped *Afipia* sp. strain D1 in a continuous feeding bioreactor could degrade dioxane from 400-730 mg/L to 3.4-3.6 mg/L with estimated degradation rates of 0.67 and 0.46 kg dioxane/m^3/day at the loading rate ranging from 0.09-0.7 kg dioxane//m^3/day[48, 49]. *Pseudonocardia* sp. D17 were used to replace D1 which could degrade the low level of influent dioxane (5-15 mg/L) and also promote the effluent quality to 0.38-0.49 mg/L at the loading rate of 0.06-0.10 kg dioxane/m^3/day[50]. An

up-flow biological aerated filter (UBAF) was used to treat the wastewater from polyester manufacture containing an average of 31 mg/L of dioxane. A lab-scale bioreactor indicates that maximum of 99.5% dioxane was removed by packed sludge at the loading rate of 0.04 to 0.31 kg dioxane/m^3/day[51]. A full-scale treatment test was conducted at the Lowry Landfill Superfund Site using moving bed bioreactor at the loading rate of 25.2 kg dioxane/m^3/day. Results showed that 99% of dioxane (initial concentration: 10-25 mg/L) was degraded together with THF presence (10-60 mg/L)[52, 53].

1.2.5 Pump-and-treat Treatment

Pump-and-treat approach is a viable *ex situ* contaminant-removal approach due to the high mobility of dioxane. However, its mobility reversely causes the back diffusion from low permeability subsurface which makes pump-and-treat a long-term proposition[46]. This treatment approach particularly suitable for those contaminated sites with limit in situ treatment efficiencies or co-contaminated with other pollutants. Because the following sections after extraction from ground can be various including sorption, advanced oxidation, and biological methods depending on the site properties. However, of significant sites have a relatively large mass of contaminants in the tremendous volume of plumes (e.g., over hundred million liters[54]) comparing with the rate of removal by pump-and-treat option. To this aspect, this treatment approach is best thought of as a management tool to prevent continuation of contaminant migration[54].

1.3 Current Research on Key Enzymes Responsible for Dioxane Degradation

1.3.1 Dioxane Biodegradation Pathways

Dioxane biodegradation pathways in metabolizers and co-metabolizers have been proposed by previous research[55-57]. It is well established that bacterial monooxygenases confer dioxane initialization ability in many dioxane degraders[36, 37, 58]. Hydroxylation firstly happens at any C-H bond in dioxane resulting in production of 1,4-dioxane-2-one and/or 2-hydroxyethoxyacetaldehyde. These two intermediates can be oxidized by alcohol/aldehyde dehydrogenases to 1,4-dioxane-2-one (PDX) and/or 2-hydroxyethoxyacetic acid (HEAA). In metabolizers, CB1190, PH-06, and *Acinetobacter baumannii* DD1, they subsequently oxidize to carboxylic acid, and then cleavage the second ether bond leading to the production of two-carbon intermediates, such as glyoxal, ethylene glycol, glycoaldehyde, glycolate. Further, they become glyoxylate which is another key feature in dioxane degradation pathway besides HEAA. From glyoxylate, it partially converted to oxalate and completely mineralized to carbon dioxide. Results showed that when CB1190 grew on isotope-labelled [^{13}C] dioxane, all detected amino acids also labeled through dioxane assimilation, which directly indicates that dioxane served as a sole carbon source to CB1190. Collectively, dioxane either converted to CO_2 or enter the bacterial central metabolism (Figure 1.3)[55, 57, 59]. Unlike metabolizers, co-metabolizers including *Pseudonocardia* sp. Strain ENV478, *Pseudomonas mendocina* KR1, *Rhodococcus ruber* T1 and T5 cease the degradation process at HEAA[60-62] and accumulated as the end product.

1.3.2 Soluble Di-iron Monooxygenases (SDIMOs)

Soluble Di-iron Monooxygenases (SDIMOs) are multicomponent bacterial enzymes that can incorporate one oxygen atom from O_2 into various substrates such as chlorinated solvents, aromatic hydrocarbons, alkanes, and alkenes to initiate catabolism. They were found in phylogenetically and physiologically diverse bacteria including Actinobacteria (e.g., *Mycobacterium*, *Rhodococcus*, *Pseudonocardia*, *Gordonia*, *Nocardioides*) and Proteobacteria (e.g., *Burkholderiales*, *Xanthobacter*, *Pseudomonas*, *Methylomonas*, *Ralstonia*, *Cupriavidus*)[63]. Six groups of SDIMOs were distinguished on the basis of their component arrangement, substrate specificity, and alpha oxygenase subunit identity. Corresponding to their physiological roles, they were named as phenol monooxygenases (group 1), alkene/aromatic monooxygenases (group 2), soluble methane monooxygenases (sMMO) (group 3), alkene monooxygenases (group 4), tetrahydrofuran monooxygenase (THM) and propane monooxygenases (group 5), and group 6 monooxygenases embracing a collection of MOs that can catalyze a variety of short-chain alkanes/alkenes. SDIMOs are essential enzymes in bacterial oxidation of many pollutants and have broad applications in environmental and industrial biotechnology[63]. Coleman *et al.* did a survey of SDIMO in environmental samples, ethene enrichments, and ethene-degrading bacterial isolates. Results showed the ubiquity and diversity of SDIMOs in theses samples and microorganisms with positive detection of genes encoding ethene (*etnC*), propene (*amoC*, *pmoC*), propane (*prmA*), and butane (*bmoX*) monooxygenases. Given the tight lingkage between SDIMO catalysis and dioxane biodegradation, several SDIMOs have been studied using state-of-the-art molecular tools. With the combination of Geochip and denaturing gradient gel electrophoresis (DGGE), Li *et al.* revealed that *thmA*-like genes coding for

group-5 SDIMOs were detected 2.4-fold more abundant over the background at the source zone of dioxane plume[32]. Recent research discovered a group-6 propane monooxygenase in PH-06 is an alternative dioxane degrading enzyme that can also intiate the dioxane metabolic degradation pathway[35, 36, 63]. Further, some previous studies reported that group-1 and 2 SDIMOs from *Pseudomonas mendocina* KR1, *Ralstonia pickettii* PKO1, and *Burkholderia cepacia* G4 may involve in dioxane biodegradation via cometabolism[64, 65].

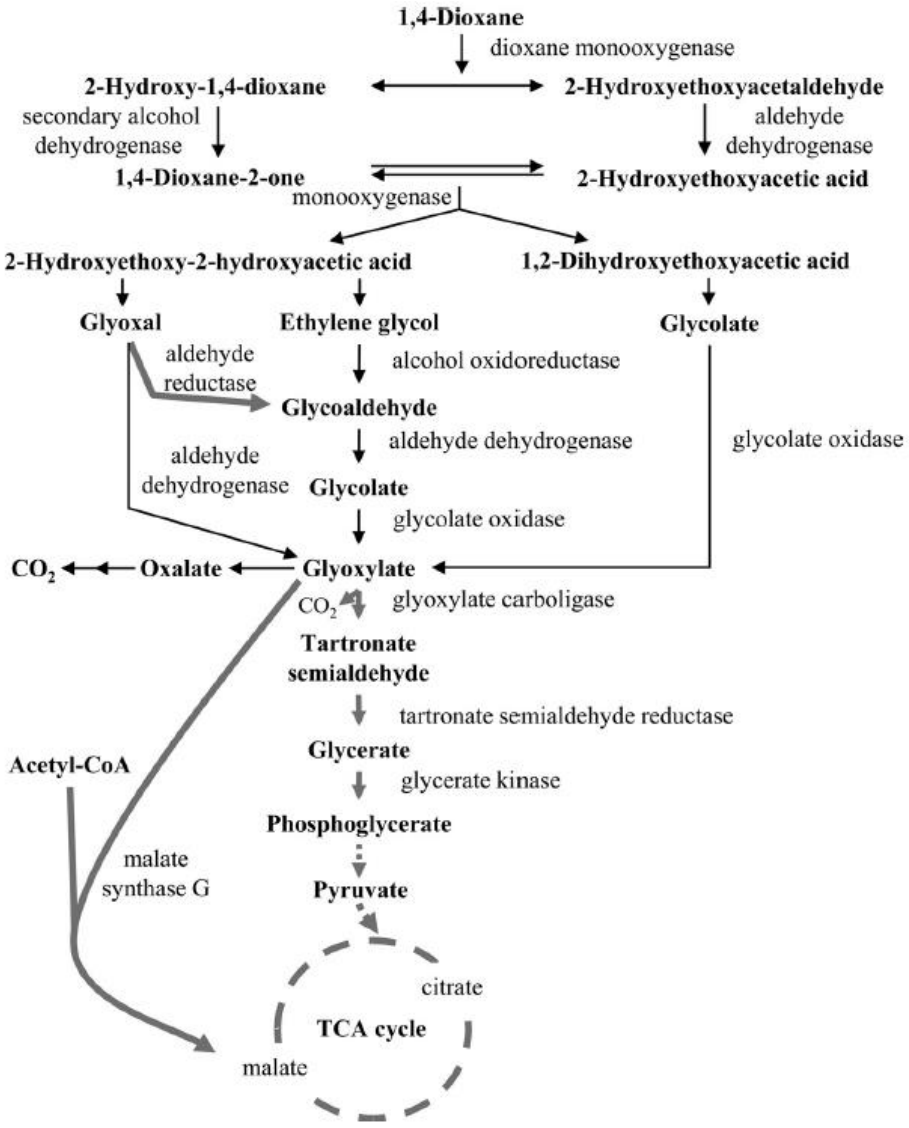

Figure 1.3 Dioxane biodegradation pathway.
Source: Grostern *et al*.[55]

1.3.3 Enzymes Involved in Downstream Dioxane Biotransformation

After dioxane is oxidized by SDIMOs to 2-hydroxy-1,4-dioxane and/or 2-hydroxyethoxyacetaldehyde, further oxidization by dehydrogenases (i.e., alcohol or aldehyde dehydrogenases) forms 1,4-dioxane-one and/or 2-hydroxyethoxyacetic acid. In dioxane metabolizers (e.g., CB1190 and PH-06), these intermediates undergo a further oxidation step catalyzed by an unknown enzyme that can insert another hydroxyl group to 1,4-dioxane-one and 2-hydroxyethoxyacetic acid. Sebsequent cleavage takes place to produce two-carbon intermediates (e.g., glycolate and glyoxylate in Figure 1.3). Some of these two-carbon intermediates will be further converted to glyoxylate by multiple oxidases, such as aldehyde dehydrogenases and glycolate oxidases. The heterologously expressed glyoxylate carboligase encoding gene from CB1190 in *Rhodococcus jostii* RHA1 could activated by the exposure of dioxane. It suggests the participation of this key enzyme in downstream degradation of dioxane[55]. Glyoxylate is further assimilated into the bacterial central metabolism, TCA cycle. It also reported that CB1190 is an autotrophical bacterial strain that can grow using H_2 and CO_2. The results of gene expression microarrays suggested that CB1190 fixes CO_2 through Calvin-Benson-Bassham (CBB) cycle depending on the key enzyme RubisCO and PRK[66].

1.4 Current Challenges in Dioxane Bioremediation

1.4.1 Limited Understanding of Initial Dioxane Oxidation at the Enzymatic Level

To date, two well studied dioxane metabolic degraders CB1190 and PH-06 harbor group-5 tetrahydrofuran monooxygenase and group-6 propane monooxygenase, respectively, for the initialization of dioxane biodegradation. To discern dioxane degradation capabilities

and influence of environmental factors, previous studies have been centered on characterizing type strains (e.g., CB1190[64, 65, 67] and PH-06[35, 58]). By fitting with Michaelis-Menten or Monod model, an array of dioxane degradation kinetic parameters (Table 1.3) have been generated, including the half-saturation coefficients (K_m) and maximum degradation velocities (V_{max}), as well as the inhibition constants (K_I) for common co-occurring chlorinated solvents. However, to interpret the dioxane attenuation naturally occurring in the field, these kinetic parameters may be of limited value for direct implication because (1) the data lack consistency due to variances in experimental operations among different research laboratories and (2) indigenous dioxane-degrading microbes living in the field may behave differently compared to these isolates grown in laboratory culture media. Though expressing the same enzymes (i.e., PRM and THM) to degrade dioxane, indigenous degraders may not only be phylogenetically and functionally disparate, but also display varied physiologies (e.g., biomass growth, nutrient assimilation, membrane transport, and stress resilience) that affect the overall catabolism effectiveness. An additional important impediment is the practice of normalizing the rate of compound removal to the amount of protein associated with the active cells (e.g., V_{max} values in Table 1.3). Wilson *et al.* suggested that the lab-derived kinetic parameters could be used along with data on the abundance of catabolic biomarkers to screen for intrinsic degradation activity[68]. Thus, normalization of degradation rates to the abundance of gene or transcript copies measured by quantitative polymerase chain reaction (qPCR) or reverse transcription- quantitative polymerase chain reaction (RT-qPCR) analyses can be extrapolated to the field system within some useful level of agreement.

Table 1.3. Estimated Dioxane Biodegradation Kinetic Parameters for Transformants Expressing PRM and THM in Comparison with Wild Type PH-06 and CB1190

Strain	Model	K_m (mg/L)	V_{max} (mg/h/mg)	Reference
PRM[a]	Michaelis-Menten	53.0 ± 13.1	0.040 ± 0.003	Li *et al.*[38]
THM[a]	Michaelis-Menten	235.8 ± 61.6	0.055 ± 0.007	Li *et al.*[38]
PH-06	Michaelis-Menten	78 ±10	/	He *et al.*[35]
CB1190	Michaelis-Menten	145 ±17	/	He *et al.*[35]
CB1190	Michaelis-Menten	160 ± 44	0.100 ± 0.008	Mahendra *et al.*[64]
CB1190	Monod Model	6.3 ± 0.2[b]	0.11 ± 0.00[c]	Barajas-Rodriguez *et al.*[69]
CB1190	Michaelis-Menten	63.36 ± 20.24	0.062 ± 0.007	Mahendra *et al.*[65]
CB1190	Michaelis-Menten	12.17	0.085	Zhang *et al.*[67]

[a] PRM and THM represent the transformant cells mc^2-155(pTip-*prmABCD*) and mc^2-155(pTip-*thmADBC*), respectively.
[b] Data converted from mg COD/L based on the theoretical oxygen demand of dioxane (1.82 mg COD/mg 1,4-dioxane).
[c] Data converted from mg dioxane COD/mg biomass COD/d based on the theoretical oxygen demand of dioxane, and bacterial formula of $C_5H_7O_2N$. The protein percentage of bacterial cell is estimated as 65%.

The first group-6 SDIMO was reported in a propane-utilizing bacterium, *Mycobacterium* sp. TY-6[70] in 2006. The gene cluster *prmABCD* encodes for four components, including a α, β hydroxylase, a co-effector, and a oxidoreductase, which are distinguished from the other five groups of SDIMOs. Together with the PRM in PH-06 and many other homologous enzymes compiling as group 6 MOs[35, 71]. Results of RT-qPCR show that all four PRM components can be induced by propane, implying its role in propane oxidation in TY-6[70]. In addition, PRM from *Mycobacterium dioxanotrophicus* PH-06 was verified with a broad substrate range spanning ethane, propane, butane,

isobutane, and ethene[38]. Further, two homologues of group-6 SDIMOs (i.e., Gene IDs of alpha subunits are CRM90_28385 and CRM90_29005) and one SDIMO similar to group-3 sMMO (CRM90_28910) were discovered in *Mycobacterium* sp. ENV421[72]. The comparative proteomics using MALDI/MS revealed that the expression of alpha component, CRM90_29005, was upregulated by propane over three orders of magnitude greater than the control that was grown with succinate[73, 74].

1.4.2 Missing Step in the Dioxane Metabolic Pathway

Though dioxane biodegradation pathways have been investigated in many previous studies with many involved enzymes explicitly uncovered or postulated, it remain to be seen what enzyme is responsible for the oxidation of dioxane-2-one and HEAA. HEAA and dioxane-2-one are spontaneously interconverted by adding or losing a water molecule. As key intermediates in dioxane biodegradation, HEAA and dioxane-2-one were initially reported as accumulating metabolites in dioxane biotransformation mediated by cytochrome P450 monooxygenases in humans[75] and rats[76-78]. Similarly, in dioxane co-metabolic degraders, such as ENV478 and DD4, HEAA was found as a terminal product generated from dioxane oxidation. When ENV478 was exposed to ^{14}C-labeled dioxane, isotopic HEAA was detected as the sole metabolite by HPLC without derivatization[60]. Thus, whether HEAA can be further assimilated or not is the prominent difference that distinguishes dioxane metabolizers and co-metabolizers. To date, little is known regarding the enzyme responsible for this critical step of HEAA oxidation. Mahendra *et al.* firstly proposed that the enzyme initializing dioxane degradation also involved in HEAA hydroxylation[56]. However, later Sales *et al.* heterologously expressed *thmADBC* confirming its encoded group-5 THM can oxidize dioxane and stoichiometrically form HEAA in the transformant

clone. Microarray data suggest that HEAA upregulates the expression of *thmADBC*, but THM is not the enzyme responsible for the degradation of HEAA in CB1190[57]. Thus, a major knowledge gap persists regarding the molecular basis of HEAA biotransformation in dioxane metabolizers, underscoring the needs for further investigation.

1.4.3 Limitations of Dioxane Bioremediation via Metabolism

Although bioaugmentation is generally effective in removing target pollutants under laboratory conditions, performance of inoculating bacteria under natural conditions is less reliable due to the complexity of environmental conditions[79]. A study was conducted to systematically compare the biodegradation via metabolism (i.e., in CB1190) and co-metabolism (i.e., in ENV425). Kinetical fitting by Monod model suggest that co-metabolism of dioxane is faster than metabolism when the initial dioxane concentration is 1 mg/L or lower[69]. A microcosm study also revealed that auxiliary substrate (300 µg/L of THF) temporarily enhanced the degradation of low concentration of dioxane (i.e., <300 µg/L) by the metabolic degrader CB1190. However, addition of this auxiliary carbon source can have counterproductive consequences in long term, since the inducing substrate may exert competitive inhibition to dioxane degradation. When CB1900 is fed with non-inducing substrates (e.g., 1-butanol), it can cure the catabolic plasmid that carries *thmADBC*, leading to the loss of dioxane degradation capacity[28]. Given the fastidious growth condition of microbes imposed in typical environment, including the inhibitory substances and the low concentration of available nutrients, the co-metabolic strains are more profitable to such conditions[80].

1.4.4 Co-existence of Chlorinated Solvents with Dioxane

As the main use of dioxane for stabilizing chlorinated solvents, dioxane therefore commonly found co-occurring with chlorinated solvents including TCE, TCA, and its anaerobic metabolites, cDCE and VC. Co-contamination of TCE and dioxane has been reported across the US and globally. Anderson *et al.*[4] unveiled that 93.5% (730 out of 781) of TCE detectable sites co-exist with dioxane, and 1,1,1-trichloroethane (TCA) co-exist in 29.3% (229 out of 781) of the dioxane-contaminated wells based on the monitoring data from over 4196 United States Air Force (USAF) sites. Similarly, Adamson *et al.*[8] investigated > 2000 sites in California. Among the 605 sites with positive detection of dioxane, 94% had TCE/TCA contamination. Chlorinated volatile organic compounds (cVOCs) are the most prevalently detected organic contaminants in aquifers, overburdens, and soils. Once released to the subsurface, cVOCs interact with aquifer materials through dynamic adsorption and desorption processes governed by their relatively low solubility and high hydrophobicity[81]. Trichloroethene (TCE) in particular is of great concern because it is a potent mutagen and can generate carcinogenic metabolites, such as *cis*-dichloroethene (cDCE), *trans*-dichloroethene (tDCE), vinyl chloride (VC), via biotic and abiotic degradation[82]. Thus, USEPA has enforced a stringent regulation for TCE with a maximum contaminant level (MCL) of 5 μg/L[83], stimulating extensive research and engineering efforts in TCE remediation.

With the discovery of reductive dehalogenation[84, 85], anaerobic bioremediation has emerged as a feasible and economical alternative for *in situ* treatment of chlorinated solvents, particularly TCE. For instance, SDC-9 (Aptim, Inc., Lawrenceville, NJ) is a commercialized consortium consisting of the dehalorinating bacteria belonging to genera

Dehalococcoides (31%) and *Desulfitobacterium* (2.7%) and many other bacteria associated with dehalogenation[86]. Via respiratory dehalogenation, SDC-9 can effectively reduce TCE to cDCE and VC[87], and eventually to the non-toxic ethene[84, 88], under anaerobic condition. SDC-9 thus has been widely used as the bioaugmentation inoculum for *in situ* bioremediation of TCE and other highly chlorinated cVOCs at over 600 impacted sites with varying geochemical conditions[89, 90]. However, dioxane anaerobic biodegradation is elusive at current time. To our best knowledge, only one research reported the anaerobic biodegradation of dioxane, in which an enriched anaerobic sludge with iron-reducing bacteria was operated over the 70-days while being amended with Fe(III) oxide (30 mM) and humic acid (0.5g/L)[91]. Therefore, an effective and feasible *in situ* treatment strategy for chlorinated solvents and dioxane is of urgent needs.

1.5 Research Objectives

Built upon current research progress and challenges in dioxane biodegradation molecular foundations and their implications for groundwater bioremediation, this dissertation is oriented to tackle major knowledge gaps and technology barriers from five aspects listed as follows:

(1) To comprehensively characterize and compare two archetypical dioxane-degrading enzymes, PRM and THM, on their enzyme kinetics, substrate ranges, responses to co-existing chlorinated solvent inhibitors. This study uncovers the differences between group-5 and group-6 SDIMOs at the enzymatic level, revealing their contributions in natural attenuation and biostimulation with short-chain alkanes.

(2) To investigate the evolution, configuration, regulation, and catalytic ability of group-6 SDIMOs. This work sheds light on fundamental understanding of microecological roles of group-6 SDIMOs in natural and engineered environments.

(3) To untangle the genomic divergence between metabolic and co-metabolic dioxane cometabolizers and postulate enzyme candidates that may involve in HEAA oxidation. This study is of great value to underpin and potentially complete the dioxane biodegradation pathway in metabolism.

(4) To assess the treatment efficiency of trace levels of dioxane by a newly isolated co-metabolizer, *Azoarcus* strain DD4, in pure and mixed inocula. This is an exampelary study demonstrating the advantages of co-metabolizers for both *in situ* and *ex situ* treatments of dioxane, particularly when the intial concentration is low at ppb levels.

(5) To develop an anaerobic-aerobic sequential treatment approach for sites impacted by commingled contamination of trichloroethene and dioxane. This novel treatment train doesn't only accelerate the removal of both trichloroethene and dioxane, but also alleviates the issue caused by hazardous byproduct accumulation.

The overview organization of this doctoral research is shown in Figure 1.4.

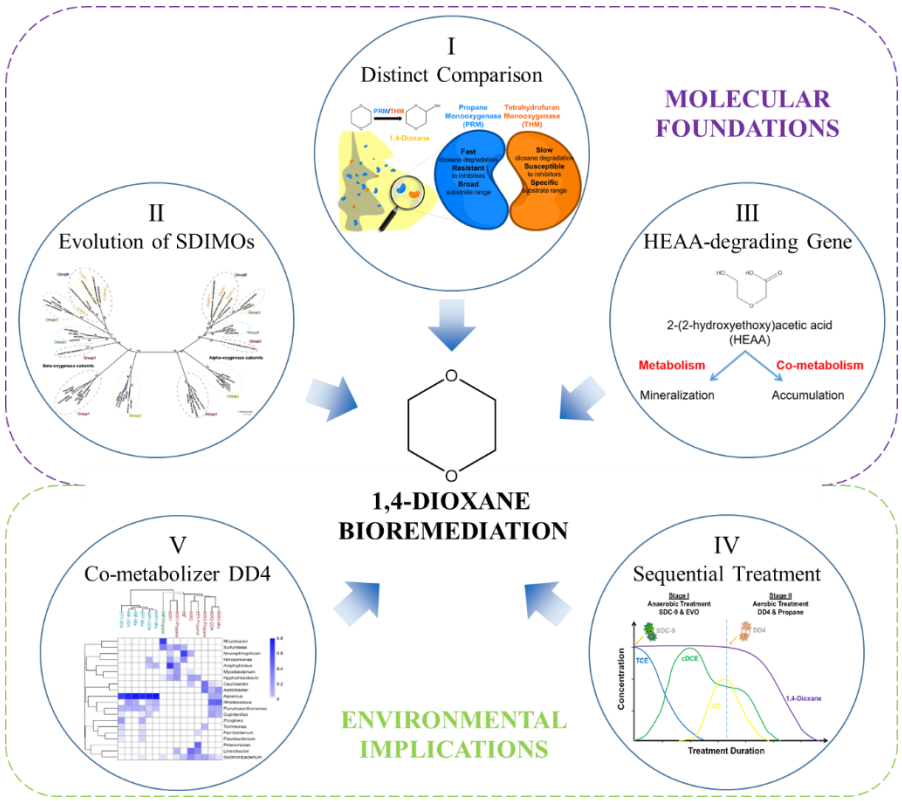

Figure 1.4 Overview schematic of this doctoral dissertation.

CHAPTER 2

DISTINCT CATALYTIC BEHAVIORS BETWEEN TWO 1,4-DIOXANE DEGRADING MONOOXYGENASES: KINETICS, INHIBITION, AND SUBSTRATE RANGE

2.1 Introduction

As the increasing attention to dioxane bioremediation, a number of bacteria have been isolated and identified given their ability of growing with dioxane as their sole carbon and energy source via metabolism[58, 92, 93]. *Mycobacterium dioxanotrophicus* PH-06[36, 58] and *Pseudonocardia dioxanivorans* CB1190[92, 94] are two archetypic dioxane degrading strains which share the same transformation pathway[57, 58]. In PH-06, we recently uncovered and verified the dioxane catalytic function of a novel propane monooxygenase (PRM)[36, 95] encoded by the gene cluster *prmABCD* located on a linear plasmid. In contrast, CB1190 expresses tetrahydrofuran monooxygenase (THM)[57] encoded by *thmADBC* to oxidize dioxane and tetrahydrofuran (THF). Though with relatively low sequence identity (< 40% for α subunits) and different arrangement of core gene components, PRM and THM are phylogenetically related, both belonging to the multi-component bacterial enzyme family, soluble di-iron monooxygenases (SDIMOs)[36, 96, 97]. PRM and THM are categorized as subgroups 6 and 5 SDIMOs[30, 35, 36], respectively, reflecting the potential divergence of their enzyme structures and catalytic behaviors.

Genes encoding THM (e.g., *thmA* and *thmB*) have been detected at sites historically impacted by dioxane, indicating the existence of indigenous dioxane degrading microorganisms by use of modern biotechnologies (e.g., quantitative PCR [qPCR][30, 31, 98, 99] and microarray[32]). Abundance of *thm* genes was positively correlated with the dioxane removal observed in bench-scale microcosm and *in situ* Biotrap assays[30, 31, 99], supporting

the significant contribution of bacteria expressing THM to intrinsic dioxane attenuation in the field. The discovery of dioxane degrading propanotrophs and the essential PRM enzyme in recent field demonstration studies assayed and validated the dominance of *prm* genes after biostimulation with propane[40] and bioaugmentation of some propanotrophs[47]. qPCR[35] and targeted gene sequencing[100] were used to monitor the dioxane degradation by *prm*-harboring *Mycobacterium* spp. in non-contaminated garden soil enrichments. These lines of evidence corroborate the prevalence of bacteria expressing PRM in engineered or enriched environments with or without previous exposure of dioxane. However, the contribution of naturally occurring bacteria expressing PRM to the overall dioxane attenuation at impacted sites remained unknown.

To date, the lack of comparable PRM kenetic data as described in Section 1.4.1 limits our knowledge of it and its application.Therefore, we heterologously expressed PRM and THM in competent cells *Mycobacterium smegmatis* mc^2-155 and compared their kinetic performance at the enzymatic level, which excludes other potentially interfering biological factors (e.g., molecular transport, gene regulation, global stress response). We further investigated the inhibitory effects of three chlorinated compounds (1,1-dichloroethene [1,1-DCE], trichloroethene [TCE], and 1,1,1-trichloroethane [1,1,1-TCA]) given their high co-occurrence frequency with dioxane at impacted sites[4, 7, 8]. In this study, substrate range of both dioxane degrading enzymes was surveyed to investigate their catalytic versatility, particularly toward prevailing chlorinated and aromatic pollutants, as well as short-chain alkane/alkene gases given their association with the success of biostimulation. We hypothesize distinct performances between PRM and THM in regard of dioxane degradation kinetics, susceptivity to environmental inhibitors, and catalytic

versatility given their sequence dissimilarity and evolutionary divergence. The expression of both enzymes is unified in an identical heterologous system and monitored by RT-qPCR, thus allowing kinetic parameters to be normalized based on the transcript copy numbers of their encoding genes, providing useful quantitative data for field assessment. This research is of critical value to advance our fundamental understanding of dioxane degrading enzymes and enable the prediction of their environmental behaviors and contributions to dioxane biotransformation naturally occurring in the field or stimulated with auxiliary substrates.

2.2 Materials and Methods

2.2.1 Chemicals and Cultures

Propane, butane, isobutane, ethane, and ethene were purchased from Airgas (Radnor, PA) with the purity of 99.5% or higher. Dioxane, THF, trichloroethene (TCE), 1,1-dichloroethene (1,1-DCE), *cis*-1,2-dichloroethene (cDCE), *trans*-1,2-dichloroethene (tDCE), vinyl chloride (VC), 1,2-dichloroethane (1,2-DCA), toluene, benzene, methyl tert-butyl ether (MTBE), cyclohexane, chloramphenicol, and thiostrepton were purchased from Sigma-Aldrich (St. Louis, MO). Neat 1,1,1-trichloroethane (1,1,1-TCA) was bought from Ultra Scientific (North Kingstown, RI) and diluted with HPLC-grade (99.9%) methanol (Sigma-Aldrich). Bacterial strains PH-06 and mc^2-155 were originally obtained from Dr. Yoon-Seok Chang (POSTECH, Pohang, South Korea) and Dr. Nicolas Coleman (University of Sydney, Sydney, Australia); CB1190 was bought from DSMZ; *E. coli* DH5α was purchased from Thermo (Carlsbad, CA), and the plasmid pTip-QC2 was acquired from Dr. Tomohiro Tamura at AIST, Japan.

2.2.2 Heterologous Expression of PRM and THM

The 4.0 kb fragment of the *prmABCD* gene cluster in PH-06 was amplified with the forward primer 5'-AAGGAGATATACATATGACTGCATCGGTCACCACAC-3' and the reverse primer 5'-GTATGCGGCCGCCATGAAGCTTCACGCGGATACCGGGG-3', containing NdeI and HindIII sites (underlined), respectively. In parallel, the 4.3 kb fragment of the *thmADBC* gene cluster in CB1190 was amplified with the forward primer 5'-AAGGAGATATACATATGACTGCCCCACCGATGAA-3' and reverse primer 5'-GTATGCGGCCGCCATGGAATTCTACGACTCAGAGTTGATCAGCTCGAT-3', containing NdeI and EcoRI sites (underlined), respectively. Each 50 μL of PCR reaction mixtures consisted of 1 × PCR buffer, 100 nM dNTPs, 250 nM each primer, 1 unit of Pfu polymerase (Thermo, Carlsbad, CA), and 25 ng of the genomic DNA of PH-06 or CB1190 as the template. Thermocycling conditions were: 98 ºC for 5 min, then 30 cycles of 98 ºC for 20 s and 72 ºC for 6 min, and 72 ºC for 10 min at the end. Amplicons with appropriate size were gel-purified using the Zymoclean™ Gel DNA Recovery Kit (Zymo Research Corp, Irvine, CA).

PCR amplicon and vector pTip-QC2 plasmid[36, 57, 101] were both digested with the designed enzyme (New England Biolabs, Ipswich, MA). After purification, the plasmid and PCR insert were ligated at a 1:3 (plasmid:insert) ratio at 16 ºC overnight with T4 DNA ligase (New England Biolabs, Ipswich, MA). The ligation mixture (1 μL) was then used to transform electrocompetent *E. coli* DH5α cells. Colonies with ampicillin (50 μg/mL) resistance were screened for appropriate recombinant constructs, which were designated as pTip-*prmABCD* and pTip-*thmADBC*, respectively. After purification with the Zyppy™ Plasmid Miniprep Kit (Zymo Research Corp, Irvine, CA), 50 ng of plasmid pTip-

prmABCD, pTip-*thmADBC*, or empty vector pTip-QC2 was used to transform electrocompetent mc^2-155 cells using the method as described in Ly *et al.*[102] Electroporation was conducted at 1.8 kV/cm for 4.5 ms by the MicroPulser™ Electroporator (Bio-Rad, Hercules, CA). Successful transformants were selected on LB plates with ampicillin (50 μg/mL) after incubation at 30 ºC for 2 days.

2.2.3 Culturing and Induction of Transformants

Single colonies of mc^2-155 containing the plasmid pTip-QC2 constructs with and without the *prmABCD* or *thmADBC* insert, designated as mc^2-155(pTip-QC2), mc^2-155(pTip-*prmABCD*) and mc^2-155(pTip-QC2), respectively, were inoculated in 5 mL of LB broth dosed with chloramphenicol (34 μg/mL) and grown at 30 ºC while being shaken at 150 rpm. After the initial growth for 48 h, cell culture (5 mL) was then inoculated to a 1-L flask containing 0.2 L of LB broth with chloramphenicol. In addition, 0.1% (v/v) of Tween-80 were added to prevent the formation of cell aggregates during growth[103]. Cells were further incubated at 30 ºC while being shaken at 175 rpm until an OD600 of 0.6 was reached. Then, thiostrepton (EMD Millipore, Billerica, MA) in DMSO was added to a final concentration of 1 μg/mL to induce the heterologous expression. Induced cultures were incubated for a further 48 h. Cells were harvested and the pellets were washed twice with 40 mL of ice-cold phosphate buffered saline (PBS) (20 mM sodium phosphate, pH 7.0, 0.1% Tween-80) prior to the degradation assays.

2.2.4 SDS-PAGE Analysis

After induction by thiostrepton for 48 h, 1 mL of mc^2-155(pTip-*prmABCD*), mc^2-155(pTip-*thmADBC*) and mc^2-155(pTip-QC2) bacterial culture were adjusted to OD around 6. Cells were then lysed by ultrasonication using the Sonic Dismembrator FB-120

(Fisher Scientific, Pittsburgh, PA) for 15 min with 5 s pulse and 5 s of interval. After centrifugation at 15,000 × g for 30 min at 4 ºC, the supernatant consisting ~20 μg of the total protein and SDIMOs fraction was mixed with the Pierce LaneTM Marker Reducing Sample Buffer (Thermo, Waltham, MA) containing 5% of 2-mercaptoethanol (2-ME). After boiling 10 min, 20 μL of the resulted mixture was loaded onto a 4-12% NuPAGE™ Bis-Tris polyacrylamide gel (Thermo, Waltham, MA) according to the method of Laemmli[104]. Pierce™ Unstained Protein MW Marker (Thermo, Waltham, MA) were used for protein size comparison.

2.2.5 Reverse Transcription Quantitative PCR (RT-qPCR) and Expression Level Assay

After induction with thiostrepton, total RNA of mc^2-155(pTip-*prmABCD*), mc^2-155(pTip-*thmADBC*), and mc^2-155(pTip-QC2) transformants was extracted using PureLink™ RNA Mini Kit coupled with PureLink™ DNase Set (Thermo, Carlsbad, CA) to eliminate DNA contamination. The RNA extracts were converted to cDNA using the High-Capacity cDNA Reverse Transcription Kit (Thermo, Foster City, CA). Concentrations of synthesized cDNA were measured by SpectraMax Plus 384 Microplate Reader equipped with a SpectraDrop Micro-Volume Microplate (Molecular Devices, Sunnyvale, CA) and subsequently diluted to 5 ng/μL with nuclease-free water for further qPCR analysis. qPCR reaction (20 μL) consisted of 2 μL diluted cDNA, 10 μL of 2× SYBR Green PCR master mix (Thermo, Foster City, CA), 0.2 μM of each forward and reverse primer, and DNA-free water to a total volume of 20 μL. The primers were designed by He *et al.*[35] and Li *et al.*[30] for *prmA* and *thmA* quantification. RT-qPCR was conducted using QuantStudio™ 3 Real-Time System (Thermo, Carlsbad, CA) with the following temperature setup: 95 °C for 10

min and 40 cycles of 95 °C for 15 s and 60 °C for 1 min. The copy numbers of target genes were quantified using standard curves prepared with serial dilution of genomic DNA of CB1190 and PH-06. The expression levels of PRM and THM were defined as copy numbers of expressed *prmA* or *thmA* over a unit milligram of protein extracted from the induced transformants.

Comparable transcription levels (Figure 2.1) of inserted *prm* and *thm* gene clusters in transformants were checked by reverse transcription quantitative PCR (RT-qPCR) before processing enzyme comparison assays. The heterologous expression procedures were designed and verified to ensure an identical transcription of both PRM and THM expressed with active catalytic functions. First, the sequence accuracy was ensured since high fidelity polymerase was used to amplify the complete *prm* and *thm* gene clusters from the genomic DNA. This greatly reduced the chance of function discrepancies caused by PCR-derived mutations. Second, transcription of the inserted genes was solely regulated by thiostrepton to induce the promoter system embedded on pTip-QC2. Gene clusters were inserted from their start codons (ATG) of *prm* or *thm*'s α-subunits without their original promoters or regulators in wild-type strains PH-06 or CB1190. Third, complete *prm* and *thm* gene clusters were cloned with the same initial restriction site, *Nde*I, at their 5' ends into the expression shutter vector, pTip-QC2. Thus, the start of the *prm* and *thm* transcripts were identical, allowing the consensus of ribosome binding to initiate the translation. Last but not the least, the gene expression shutter vector, pTip-QC2, plasmid proliferation host (*E. coli* DH5α), and expression host (*Mycobacterium smegmatis* mc^2-155), have all been successfully employed to express THM, PRM, and other SDIMOs in our lab and others[36,

[57, 105-107]. This set of expression system enabled effective production of SDIMOs with catalytic functions comparable with wild-type strains.

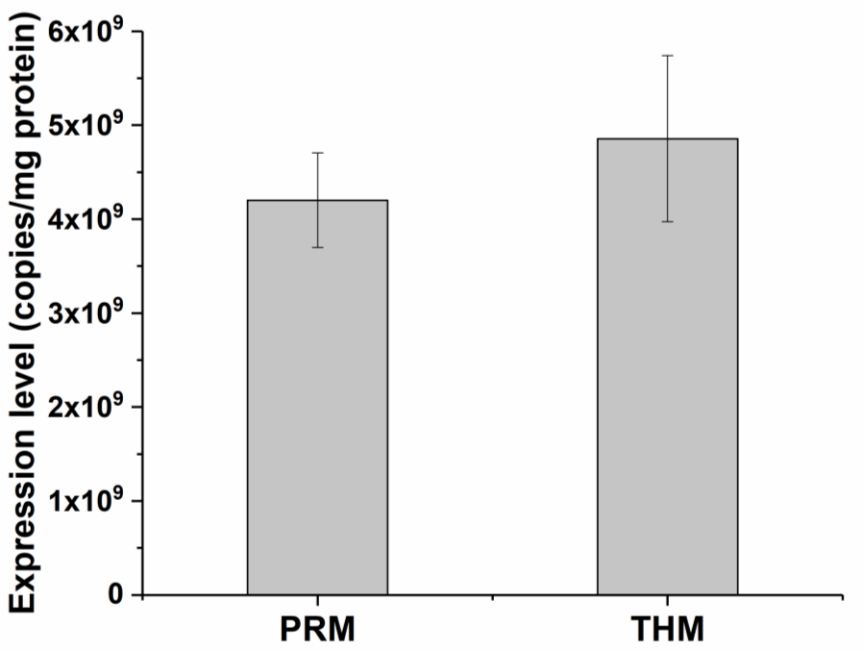

Figure 2.1 RT-qPCR analysis revealed uniform expression in mc^2-155(pTips-*prmABCD*) and mc^2-155(pTips-*thmADBC*) after induction.

2.2.6 Enzyme Kinetics Modeling

Dioxane degradation kinetics were well described by the Michaelis-Menten equation (1.1). Parameters for chlorinated solvent inhibition were estimated using equations (1.2), (1.3), and (1.4)[65], respectively.

Michaelis-Menten equation: $v_0 = \frac{V_{max}[S]}{K_m+[S]}$ (1.1)

Competitive inhibition: $v_0 = \frac{V_{max}}{1+\frac{K_m}{[S]}\left(1+\frac{[I]}{K_{IC}}\right)}$ (1.2)

Uncompetitive inhibition: $v_0 = \frac{V_{max}}{1+\frac{[I]}{K_{IU}}+\frac{K_m}{[S]}}$ (1.3)

Noncompetitive inhibition: $v_0 = \frac{V_{max}}{(1+\frac{[I]}{K_{IN}})+(1+\frac{K_m}{[S]})}$ (1.4)

As experiment had verified the trend of K_m^{app} and V_{max}^{app}, they can be transformed to the following format accordingly (Equation 1.5-1.7):

Competitive inhibition: $K_m^{app} = K_m\left(1 + \frac{[I]}{K_{IC}}\right)$ (1.5)

Uncompetitive inhibition: $K_m^{app} = K_m/(1 + \frac{[I]}{K_{IU}})$ and $V_{max}^{app} = V_{max}/(1 + \frac{[I]}{K_{IU}})$ (1.6)

Noncompetitive inhibition: $V_{max}^{app} = V_{max}/(1 + \frac{[I]}{K_{IN}})$ (1.7)

Where K_m is the half saturation coefficient; V_{max} denotes the maximum degradation rate; *app* means the apparent value based on our experiments; [S] and [I] represent the concentrations of substrate and inhibitor; K_{IC}, K_{IN}, and K_{IU} are competitive, uncompetitive, and noncompetitive inhibition constants, respectively. To estimate the inhibition constant K_I of each model, equations (S5), (S6) and (S7) can be linearized as follows[108, 109]:

Competitive Inhibition: $\frac{K_m^{app}}{V_{max}^{app}} = \frac{K_m}{V_{max}} + \frac{K_m}{V_{max}K_{IC}}[I]$ (1.8)

Uncompetitive Inhibition: $\frac{1}{V_{max}^{app}} = \frac{1}{V_{max}} + \frac{1}{V_{max}K_{IU}}[I]$ & $\frac{1}{K_m^{app}} = \frac{1}{K_m} + \frac{1}{K_mK_{IU}}[I]$ (1.9)

Noncompetitive Inhibition: $\frac{1}{V_{max}^{app}} = \frac{1}{V_{max}} + \frac{1}{V_{max}K_{IN}}[I]$ (1.10)

Therefore, K_I can be computed by the intercept divided by the slope of the regression line drawn by [I] against K_m^{app}/V_{max}^{app}, $1/V_{max}^{app}$, or $1/K_m^{app}$. The experimental data with different concentrations of inhibitors and dioxane were fitted to three possible inhibition models for K_{IC}, K_{IN}, and K_{IU} estimation. The most appropriate model was selected on the basis of the best fitness with the highest R^2 (coefficient of determination).

2.2.7 Enzyme Kinetics and Inhibition Tests

After cultivation and induction as described above, transformant cells were washed twice and re-suspended in phosphate-buffered saline (PBS) to achieve an optical density (OD) of approximately 2.0 at 600 nm. Dioxane was then spiked to achieve the initial concentrations of 10, 40, 80, 160, 320, and 640 mg/L to perform the kinetic assays. Such high initial concentrations were used because PRM and THM both exhibited high K_m and V_{max} values, which were in good agreement with previous studies[35, 64, 67, 69] using wild-type strains (Table 1.3). Two liquid samples (600 µL) were collected, including one at the beginning and the other after 3 h of the enzymatic reaction in each batch test. Samples were then filtered using 0.22 µm Nylon syringe filters and kept in glass vials at 4 °C prior to the gas chromatograph (GC) analysis. Instant degradation rates were calculated by averaging dioxane disappearance in triplicate within the first 3 h, which were further normalized by the initial protein concentration[65] measured by the Bradford Assay[110]. In addition, to evaluate dioxane degradation kinetics under environment-relevant dioxane contaminations, resting cells were exposed to 1.0 and 0.2 mg/L of dioxane, respectively. All treatments were conducted in triplicate and negative controls were prepared with autoclaved biomass.

The significance level among different treatments was statistically determined using the Student's *t*-test.

To assess the inhibition effects from the presence of chlorinated solvent compounds (i.e., 1,1-DCE, TCE, and 1,1,1-TCA), harvested transformant cells were first exposed to the desired concentrations (0-8 mg/L in the aqueous phase) of inhibitors for 20 min, allowing complete portioning of volatile inhibitors in the batch setup and sufficient contact between enzymes and inhibitors. Based on our preliminary tests with varying pre-exposure durations (data not shown), pre-exposure of 20 min is optimal to prevent rapid dioxane degradation by inhibitor-free enzymes without significant impact to enzyme activities, which could greatly affect the estimation of degradation rates. After the pre-exposure, dioxane was spiked at varying initial concentrations and its disappearance was measured at 3 h. Calculation of the concentrations of chlorinated solvents in aqueous phase were based on the mass balance and Henry's law equilibrium using the following equation.

$$V_{stock} \times C_{stock} = V_{aq} \times C_{aq} + V_{gas} \times \frac{C_{aq}}{H_c} \quad (1.8)$$

Where, C_{stock} and C_{aq} are the concentrations of chlorinated compounds in stock solution and aqueous phase; V_{stock}, V_{aq}, and V_{gas} are the volumes of stock solution, aqueous phase, and headspace, respectively. H_c is the dimensionless Henry's constant of a specific chlorinated compound[111]. All dioxane degradation rates were first fitted to the non-linear Michaelis-Menten model (Equation 1.1) to compute apparent kinetic values, which were then fitted with three inhibition equations (Equations 1.1-1.7) (i.e., competitive,

noncompetitive, and uncompetitive) to estimate their inhibition factors and distinguish the dominant inhibition mechanism.

2.2.8 Substrate Range Characterization

Three transformants, mc^2-155(pTip-*prmABCD*), mc^2-155(pTip-*thmADBC*), and mc^2-155(pTip-QC2), were harvested using the procedures as mentioned above. Five milliliters of resuspended cells were transferred to 35-mL sealed serum bottles and then exposed to 19 selected compounds individually to assess if significant degradation occurs in comparison with abiotic controls prepared with PBS with 0.1% Tween 80 as the medium. These tested compounds are categorized into four groups, embracing (1) cyclic and branched ethers (dioxane, THF, MTBE) and a structural analogue (cyclohexane), (2) short-chain alkane/alkene gases (ethane, propane, butane, isobutane, and ethene), (3) aromatic compounds (e.g., toluene, benzene), and (4) chlorinated aliphatic hydrocarbons (1,1-DCE, tDCE, cDCE, 1,1-DCA, 1,2-DCA, VC, TCE, and 1,1,1-TCA). The exposure dosage of each compound is listed in Table 2.1. MTBE, cyclohexane, alkanes, aromatic compounds, and chlorinated solvents were detected in the headspace; dioxane and THF were measured in the filtered aqueous solutions. Concentrations of these compounds were monitored by GC coupled with a flame ionization detector (FID) detector or mass spectrometry (MS) with key analytical details (e.g., retention time and target ions) indicated in Table 2.1. As concentrated non-growing transformant cells were used in these assays, degradation rates were estimated based on the disappearance of each tested compound with the first 4 h of incubation. Samples were also collected at 24 h after the exposure, which were analyzed to verify the occurrence and extent of degradation. All experiments were conducted in triplicate to avoid discrepancy among individual tests and minimize system errors.

Significant degradation was only recognized by the Student's *t*-test when the substrate disappearance in clones expressing PRM or THM within first 4 h is statistically greater ($p < 0.05$) than (1) the abiotic loss observed in negative controls and (2) the biotic loss in mc^2-155(pTip-QC2) transformant cells which contain the empty vector. The degradation ability was verified based on the observation of (1) continuous substrate depletion at 24 h and (2) degradation exhibited by the wild type strains, PH-06 and CB1190. PH-06 and CB1190, which were grown with 50 mL of ammonium mineral salts (AMS) and 500 mg/L of dioxane as a growing substrate in 160 mL serum bottles. Cells were harvested at their exponential phase and diluted to OD_{600} around 1.0 by PBS with 0.1% Tween-80.

Table 2.1 GC-FID or GC-MS Analysis of Tested Substrates

Substrate	Molecular weight (g/mol)	Total molar (μmol)	Retention time (min)	Selected ion (m/z)
Ethers/Analogs				
Dioxane	88.11	5	7.9	GC/FID
Tetrahydrofuran	72.11	5	5.7	
MTBE	88.15	5	11.1	
Cyclohexane	84.16	5	2.7	84
Short-chain Alkanes/Alkene				
Ethene	28.05	5	1.7	GC/FID
Ethane	30.07	5	1.8	
Propane	44.1	5	2.1	
Butane	58.12	5	3	
Isobutane	58.12	5	2.8	
Aromatics				
Benzene	78.11	5	2.7	78
Toluene	92.14	5	5.2	92
Chlorinated Aliphatic Hydrocarbons				
VC	62.5	0.2	1.3	62
1,1-DCE	96.94	0.2	1.6	96, 61
cDCE	96.95	0.2	2.1	96, 61
tDCE	96.95	0.2	1.8	96, 61
1,2-DCA	98.96	0.2	2.5	Full scan
TCE	131.4	0.2	3.3	130, 95
1,1,1-TCA	133.4	0.2	2.5	96,61

2.2.9 Genomic Comparison

Genomes of 10 Actinomycetes in the genera of *Mycobacterium*, *Pseudonocardia*, and *Rhodococcus* that carry complete genes clusters of *prmABCD* or *thmADBC* were retrieved from National Center for Biotechnology Information (NCBI). The sequence alignment was conducted using Mauve 2.4.0[112] with the default parameters.

2.2.10 Analytical Approaches

The total protein content of cells was used to quantify the bacterial biomass by Bradford Assay[36, 64]. Serial dilution of bovine serum albumin (BSA) (Thermo Scientific, Rockford, IL) was made to prepare a linear standard curve for the total protein measurement. The spectral absorbance at 660 nm was measured using the SpectraMax Plus 384 Microplate Reader (Molecular Devices, Sunnyvale, CA).

Dioxane concentration (> 1.0 mg/L) was detected by GC-FID (Trace 1300, Thermo, Waltham, MA) coupled with a TG-BOND Q capillary column (30 m length × 0.32 mm ID × 10 μm film). Direct injection volume of filtered aqueous sample was 1 μL. Helium was used as the carrier gas with a constant flow rate of 6.0 mL/min. The inlet temperature was set as 200 °C, and samples were split at the ratio of 2:1 by the split flow of 12 mL/min. The oven temperature started from 110 °C for 1 min, then ramped to 180 °C at the rate of 15 °C/min, and held for 4 min. The detector temperature was maintained at 250 °C.

For samples with relatively low dioxane concentration (< 1.0 mg/L), dioxane in the aqueous phase was extracted by the frozen micro-extraction (FME) method[113], with dioxane-d_8 and THF-d_8 used as the surrogate and internal standard, respectively. Chemical separation was achieved by a TG-5MS column (30 m × 0.25 mm × 0.25 μm) with a constant helium flow at 1.5 mL/min. The inlet temperature of GC was set at 250 °C. The oven

temperature program was set initially at 40 °C for 2 min, increased to 150 °C at 10 °C/min. Select ion monitoring (SIM) mode was employed to obtain the fingerprint ions of m/z 58, 96 and 80, which were used to represent the ion abundance of dioxane, dioxane-d_8 and THF-d_8, respectively. The retention time of dioxane, dioxane-d_8, and THF-d_8 were 3.66, 3.74, and 2.45 min, respectively.

2.3 Results and Discussion

2.3.1 PRM Exhibits Higher Affinity to Dioxane than THM

In comparision with THM, PRM exhibited a higher affinity to dioxane since the K_m of PRM (53.0 ± 13.1 mg/L) was significantly lower ($p < 0.05$) than that of THM (235.8 ± 61.6 mg/L) (Figure 2.2, Table 1.3). The V_{max} values for PRM and THM were estimated as 0.040 ± 0.003 and 0.055 ± 0.007 mg-dioxane/h/mg-protein, respectively. On the basis of our RT-qPCR analysis (Figure 2.1), V_{max} of PRM and THM can be converted to (9.52 ± 0.71) × 10^{-12} and (1.13 ± 0.14) × 10^{-11} mg dioxane/h/transcript copy, respectively. These values may be of significant value to evaluate real-time dioxane degradation activities in the field when total RNA is recovered from environmental samples. V_{max} of PRM is significantly smaller than THM ($p < 0.05$), indicating PRM has a relatively lower maximum catalytic capacity for dioxane transformation. However, when dioxane concentration is lower than 430 mg/L, PRM surpasses THM in dioxane degradation rate, primarily due to its greater affinity to dioxane. This was evident by the faster dioxane biotransformation observed under two environment-relevant dioxane concentrations commonly found in the field (Figure 2.2B). When the transformant cells exposed to an initial dioxane concentration of 1082.5 ± 29.3 μg/L, the dioxane biotransformation rate by PRM was 0.42 ± 0.01 μg dioxane/h/mg protein, equivalent to (1.00 ± 0.02) × 10^{-13} mg

dioxane/h/transcript copy. This was two times as high as that of THM (0.20 ± 0.01 µg dioxane/h/mg protein, equivalent to (4.12 ± 0.21) × 10^{-14} mg dioxane/h/transcript copy). When we lowered the initial dioxane concentration to around 250 µg/L, PRM (0.11 ± 0.01 µg dioxane/h/mg protein, equivalent to (2.62 ± 0.23) × 10^{-14} mg dioxane/h/transcript copy) retained higher efficiency in dioxane degradation than THM (0.04 ± 0.01 µg dioxane/h/mg protein, equivalent to (0.82 ± 0.21) × 10^{-14} mg dioxane/h/transcript copy). Since dioxane concentration is generally lower than 1 mg/L in groundwater[8] and rarely exceeds 100 mg/L at impacted sites, it can be speculated that bacteria that express PRM are more advantageous compared to those with THM given their higher efficiency in exploiting low or trace levels of dioxane for metabolism (Figure 2.2).

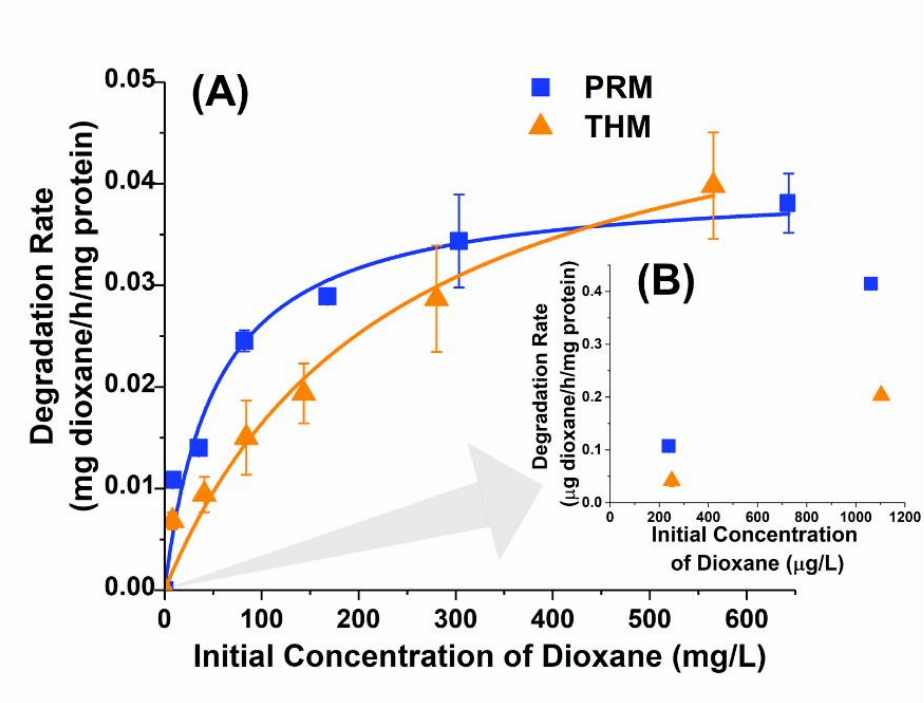

Figure 2.2 (A) Michaelis-Menten curves exhibiting dioxane degradation kinetics by transformant cells expressing PRM (blue square) and THM (orange triangle). Dioxane degradation at environment-relevant concentrations were shown in the inserted figure (B).

Our enzymatic kinetic results are in good agreement with some previous dioxane degradation kinetic studies using wild type model dioxane degraders that actively express these two enzymes essential for dioxane metabolism (Table 1.3). For instance, He *et al.*[35] observed a stronger affinity for dioxane in PH-06 that expresses PRM than CB1190 that expresses THM. Relatively high K_m and V_{max} values were also reported in an early study that characterize dioxane degradation kinetics in CB1190[64]. However, results from some other investigations[65, 67, 69] in CB1190 dioxane degradation kinetics were at variance (Table 1.3). The variation in kinetic coefficients among studies is attributed, at least in part, to the differences in (1) culturing conditions and (2) dioxane exposure duration in the degradation tests[69, 114]. Different culturing media, temperatures, and initial biomass concentrations may affect overall microbial activities and induction of the specific degradation enzyme(s). Dioxane exposure duration is also a critical parameter for the estimation of the kinetic coefficients. These reported studies exposed cells to dioxane for a period ranging from 0.5 to 8 h. Short exposure time may result in an underestimation of degradation rates as cells may take time to acclimate to a new environment. However, long exposure time may cause unwanted biomass growth, as CB1190 cells can grow with dioxane, particularly in the high concentrations dosed in the testing system. In this case, dioxane degradation rates could be overestimated, introducing the extrapolation inaccuracy of V_{max} and K_m using the Michaelis-Menten model that assumes non-growth condition. In our study, we employed expressing cells that do not grow with dioxane and a median exposure duration of 3 h to improve the measurement consistency for dioxane degradation rates.

2.3.2 1,1-DCE is the Most Potent Inhibitor to Both PRM and THM

For both PRM and THM, the inhibitory effects of three tested chlorinated compounds were ranked as: 1,1-DCE > TCE > 1,1,1-TCA (Figure 2.3). The dioxane removal efficiency of PRM dropped from 85.3 ± 12.9% in inhibitor-free PBS solution to 45.8 ± 15.4% with the presence of 2 mg/L of 1,1-DCE. TCE also significantly reduced the dioxane removal efficiency to 52.0 ± 4.1% ($p < 0.05$). However, the influence of 1,1,1-TCA to PRM-catalyzed dioxane degradation was negligible when dosed with the same concentration (i.e., 2 mg/L). A similar inhibitory order of these three chlorinated compounds was also observed in transformant cells expressing THM (Figure 2.3). In PBS solution without any chlorinated inhibitors, cells expressing THM can eliminate 81.2 ± 6.0% of the initial dioxane after 3 h. The addition of 2 mg/L of 1,1-DCE, TCE, and 1,1,1-TCA greatly inhibited the dioxane degradation by THM and reduced the removal efficiencies to 20.0 ± 9.7, 24.0 ± 2.8, and 49.5 ± 8.2%, respectively. This inhibitory order is in concert with previous inhibition tests using growing cells of CB1190 by Zhang *et al.*[67]. The consensus between our enzyme study and their pure culture assay suggest the observed inhibition of chlorinated compounds to dioxane degradation is dominantly governed by the direct interaction between inhibitory molecules and catalytic enzymes, though these inhibitors may also negatively affect the degrading bacteria by inducing universal stress, repressing gene expression, impeding substrate transport, and/or interrupting membrane integrity[67].

1,1-DCE has been well recognized as a potent inhibitor to SDIMOs, such as group-3 methane monooxygenase[115, 116], group-3 butane monooxygenase[117], and group-2 toluene-4-monooxygenase[65], as well as many other bacterial catabolic enzymes (e.g., ammonium monooxygenase[118]). 1,1-DCE can incur an irreversible loss of butane monooxygenase

activity in alkane degrading *Pseudomonas butanovora*[117]. Our study using heterologous expression cells provides the first evidence unequivocally revealing the inhibition of 1,1-DCE to group-6 and group-5 SDIMOs that are responsible for dioxane metabolism. The inhibition of 1,1-DCE may be attributed to its steric and chemical properties (e.g. polarity and degree of unsaturation and chlorination). The double bond in 1,1-DCE confers to a greater reactivity compared to 1,1,1-TCA. Furthermore, 1,1-DCE has a carbon with two chlorine atoms paired with a carbon with no chlorine. In contrast, TCE has a carbon with two chlorine atoms paired with a carbon with one chlorine atom. Such asymmetry of the double bound in 1,1-DCE may result in a higher reactivity than TCE[67].

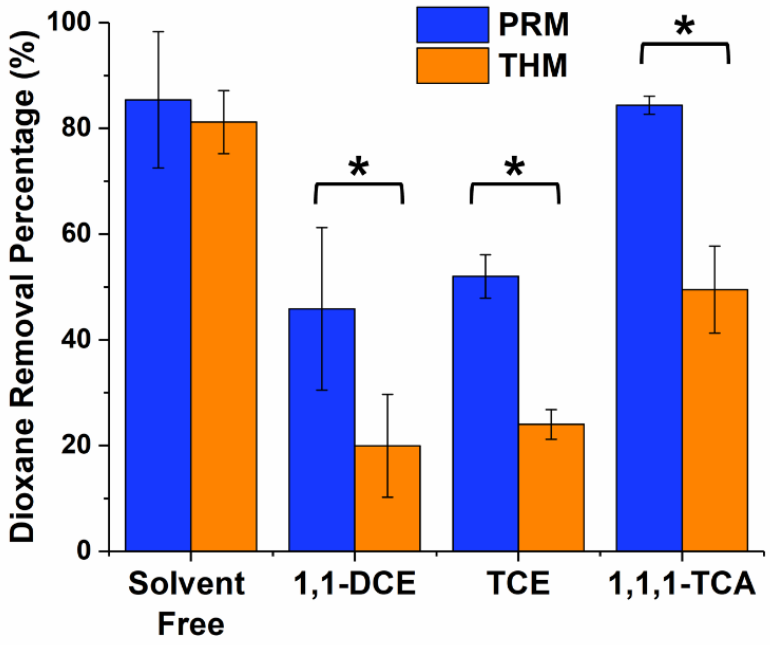

Figure 2.3. Inhibition of dioxane biodegradation by three chlorinated solvents in transformant cells expressing PRM and THM. Cells were pre-exposed to 2 mg/L of each chlorinated solvent and then assessed their dioxane removal efficiencies in the contact time of 3 h with an initial dioxane concentration of 10.0 mg/L. Error bars represent the standard deviation of triplicates. Asterisk marks represent significant ($p < 0.05$) dioxane removal differences between PRM and THM.

2.3.3 PRM is Less Susceptible to Chlorinated Solvent Inhibition than THM

Based on the best fitness (i.e., highest coefficient of determination [R^2]) with the nonlinear Michaelis-Menten model and its derived equations, negative effects of 1,1-DCE and 1,1,1-TCA on dioxane degradation by PRM and THM might be dominated by noncompetitive inhibition (Table 2.2 and Figure 2.4). Previous investigation by Mahendra[65] also revealed noncompetitive inhibition for 1,1-DCE and 1,1,1-TCA on dioxane degradation kinetics using live cells of CB1190 (Table 2.3). Thus, 1,1-DCE and 1,1,1-TCA may bind to an allosteric site (non-active site) on PRM and THM and trigger desensitization of the active site, conducive to the decrease in overall catalytic performance[119]. Unlike 1,1-DCE and 1,1,1-TCA, TCE was inclined to inhibit both enzymes via competitive inhibition (Table 2.2 and Figure 2.4). The presence of TCE may compete with dioxane for the active sites on PRM and THM, resulting in a decreased affinity. Such inhibition may be alleviated when dioxane concentrations are sufficiently high to outcompete TCE. Over the course of dioxane kinetic assays, no significant change was observed in concentrations of three chlorinated compounds (data not shown), precluding negative effects caused by toxic products derived from intracellular reactions of these chlorinated compounds.

It is noted that the R^2 values representing the fitness of empirical data to varying inhibition models were close for some cases in this study and in many previous studies[65, 67, 120-123]. This insufficient resolution inherently presented in kinetic studies may result from the mixed inhibitory mechanisms, systematic errors, and unweighted regression approaches. Our experiments were carried out with whole cells that actively express enzymes of interest, rather than purified enzymes considering the technical challenges in *in vitro* purification. Substrate transport to enzymes and other cellular dynamic processes

may thus influence our inhibition observations[108]. On the other hand, nonlinear regression with the classic Michaelis-Menten model is quite robust in estimating apparent K_m and V_{max} values and can work fairly well even when the errors are not Gaussian-distributed[124]. Comprehensively weighing the shifting of these kinetic parameters in response to a series of inhibitor concentrations, the fitness with different inhibition models is the most frequently used and well-received approach to interpret enzyme-substrate inhibition mechanisms and estimate inhibition constants providing implications for scaling the inhibition potencies.

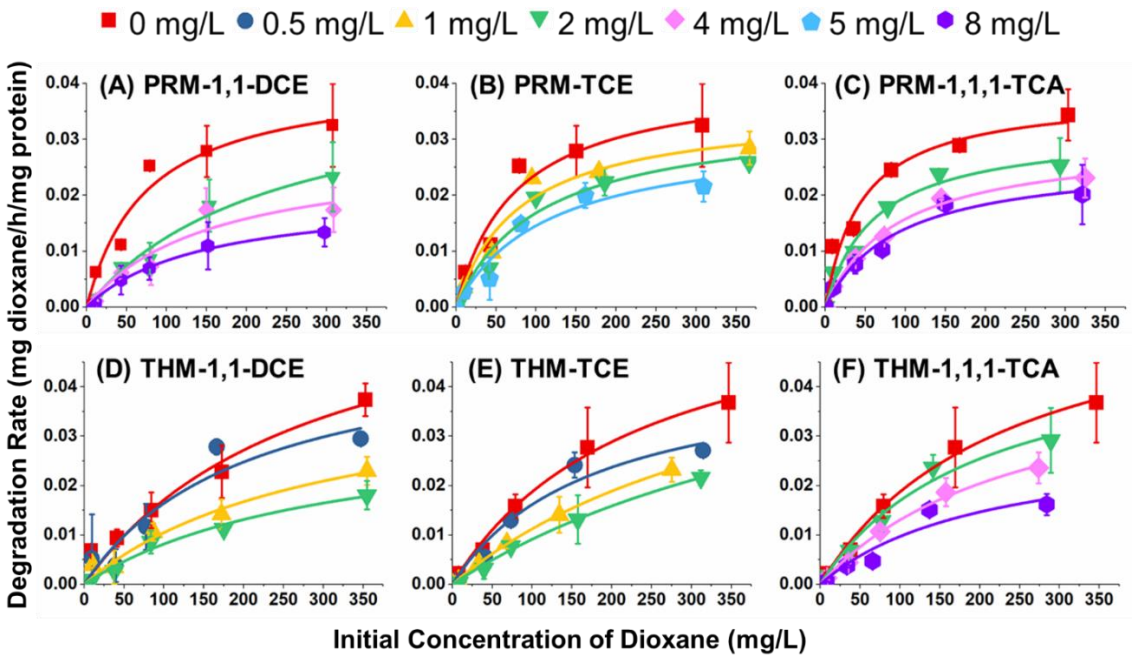

Figure 2.4 Enzyme inhibition kinetics by the Michaelis-Menten model for PRM (A, B, C) and THM (D, E, F) with the presence of 1,1-DCE (A, D), TCE (B, E), and 1,1,1-TCA (C, F). Degradation rates were estimated as the average of the dioxane disappearance among triplicates within the contact duration of 3 h and normalized towards the initial protein concentrations. No significant change in three inhibitor concentrations was observed during these assays.

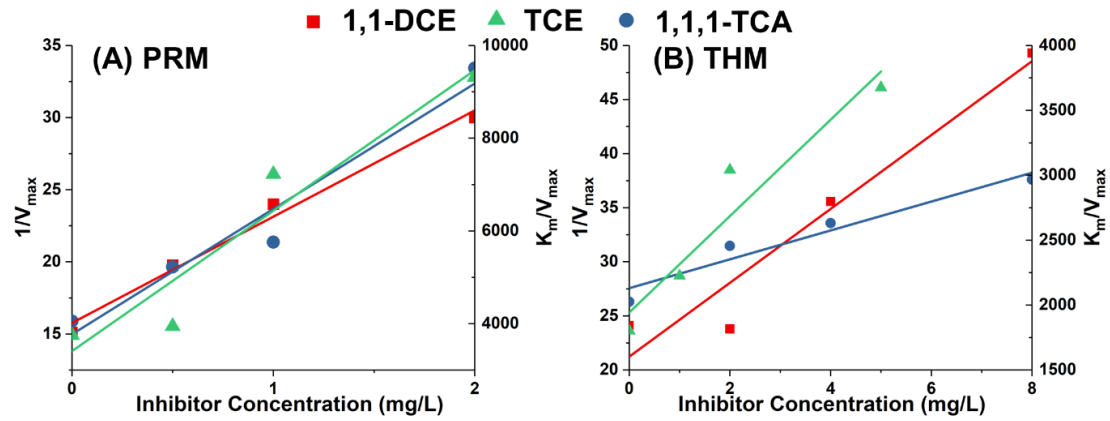

Inhibitor	Equation for PRM	Linear model	Equation for THM
1,1-DCE	y = 3.4x + 21.2 R² = 0.937	$\frac{1}{V_{max}^{app}} = \frac{1}{V_{max}} + \frac{1}{V_{max}K_{IN}}[I]$	y = 7.4x + 15.8 R² = 0.987
TCE	y = 371.3x + 1942.9 R² = 0.919	$\frac{K_m^{app}}{V_{max}^{app}} = \frac{K_m}{V_{max}} + \frac{K_m}{V_{max}K_{IC}}[I]$	y = 3028.8x + 3408.6 R² = 0.921
1,1,1-TCA	y = 1.3x + 27.6 R² = 0.940	$\frac{1}{V_{max}^{app}} = \frac{1}{V_{max}} + \frac{1}{V_{max}K_{IN}}[I]$	y = 8.7x + 15.0 R² = 0.957

Figure 2.5. Regression between the apparent V_{max} and K_m values versus the concentrations of inhibitors fitted by the linearized inhibition model with the highest R^2 value.

Table 2.2 Inhibition Kinetic Parameters for Dioxane Degradation by PRM and THM Expressing Transformants with the Presence of Three Chlorinated Compounds

Chlorinated Solvent	Enzyme	Competitive		Noncompetitive		Uncompetitive	
		K_{IC} (mg/L)	R^2	K_{IN} (mg/L)	R^2	K_{IU} (mg/L)	R^2
1,1-DCE	PRM	5.27	0.745	**6.22**	**0.937**	-19.20	0.216
	THM	1.41	0.901	**2.14**	**0.987**	-10.00	0.172
TCE	PRM	**5.23**	**0.919**	18.43	0.857	-13.00	0.800
	THM	**1.13**	**0.921**	-22.48	0.053	-3.06	0.599
1,1,1-TCA	PRM	5.17	0.888	**20.66**	**0.940**	-15.15	0.747
	THM	2.06	0.951	**1.72**	**0.957**	44.00	0.054

The inhibition model exhibiting the highest R^2 value was selected and bolded.

Table 2.3 Inhibition Constants of Chlorinated Solvents to THM Expressing Transformants in Comparison with CB1190

Inhibitor	Inhibition model	K_I (mg/L)	R^2	Reference
1,1-DCE	Noncompetitive	2.14	0.987	this study
	Noncompetitive	3.3 ± 2.9	0.95	Mahendra *et al.*[65]
	Uncompetitive	1.51 ± 0.26	0.978	Zhang *et al.*[67]
TCE	Competitive	1.13	0.921	this study
	Uncompetitive	8.60 ± 1.74	0.974	Zhang *et al.*[67]
1,1,1-TCA	Noncompetitive	1.72	0.957	this study
	Noncompetitive	1.2 ± 1.0	0.93	Mahendra *et al.*[65]

Remarkably, PRM is less susceptible than THM to the inhibition of all three chlorinated solvents tested in this study. As depicted in Figure 2.3, under a same concentration of any chlorinated solvent (i.e., 2 mg/L), the initial 10 mg/L of dioxane was removed in a significantly greater extent in transformant cells expressing PRM than those that express THM. This was also echoed by the computed inhibition constants K_I based on our experimental results (Table 2.2). For each chlorinated solvent, the best described inhibition mechanism was identical for PRM and THM (Table 2.3); further, K_I values were always greater for cells expressing PRM. These results suggested that PRM is more resistant to the inhibition of chlorinated solvents than THM. Considering that chlorinated solvents are common co-contaminants of dioxane[8, 12], microorganisms expressing PRM may be catalytically more active and enduring in the proximity of the source zone where dioxane and chlorinated solvents co-occur.

2.3.4 PRM has a Broader Substrate Range than THM

As expected, PRM and THM are both efficient in transforming cyclic ethers, including dioxane (0.287 ± 0.010 and 0.171 ± 0.042 μmol/h/mg, respectively) and THF (0.368 ± 0.055 and 0.497 ± 0.036 μmol/h/mg) (Table 2.4). Additionally, both PRM and THM can

degrade cyclohexane, a structural analog of dioxane. This is the first report that aligns PRM and THM with cyclohexane degradation, which was previously observed in wild type dioxane degrader PH-06[58]. However, degradation of this 6-membered carbocyclic alkane was much slower (0.098 ± 0.001 and 0.066 ± 0.011 μmol/h/mg for PRM and THM, respectively) in comparison to the 6-membered heterocyclic dioxane. It is also interesting to notice that PRM exhibited significantly higher degradation rates ($p < 0.05$) for six-membered ring compounds (dioxane and cyclohexane) than THM. Reversibly, THM is faster in degrading the five-membered ring THF. The varied degradation efficiencies on different substrates could partially result from the fitness of substrate molecules with the active site or the transport channel of the catalytic enzyme. MTBE is a highly branched ether pollutant of emerging water concern, since it has been widely used as oxygenate for gasoline[125]. However, neither PRM nor THM can degrade MTBE.

Table 2.4 Substrate Range of PRM and THM and Accordant Degradation Rates

Substrate	Degradation Rate (μmol/h/mg protein)	
	PRM	THM
Ethers/Analogs		
Dioxane	0.287 ± 0.010	0.171 ± 0.042
THF	0.368 ± 0.055	0.497 ± 0.036
Cyclohexane[a]	0.098 ± 0.001	0.066 ± 0.011
MtBE	-	-
Short-chain Alkanes/Alkene		
Ethene	0.487 ± 0.047	-
Ethane	0.127 ± 0.053	-
Propane	0.307 ± 0.045	-
Butane	0.246 ± 0.050	-
Isobutane	0.208 ± 0.084	-
Aromatics		
Benzene	0.106 ± 0.011	-
Toluene	0.345 ± 0.039	-
Chlorinated Aliphatic Hydrocarbons		
VC	0.060 ± 0.007	-
1,2-DCA	0.038 ± 0.005	-
1,1-DCE	-	-
cDCE	-	-
tDCE	-	-
TCE	-	-
1,1,1-TCA	-	-

Green cells represent significant degradation (p<0.05) exhibited by the transformant cells expressing PRM or THM in comparison with both (1) the abiotic control and (2) biotic control with transformant cells carrying the empty vector.

Red cells represent substrate depletion was not observed or not significantly different from either abiotic or biotic control treatment.

[a] Degradation rates for cyclohexane were calculated based on the concentration difference between 4 and 24 h due to a prolonged equilibrium of this chemical in the sealed bottles.

Short-chain (C1-C4) alkanes and alkenes are primary substrates of many subgroups of SDIMOs[126]. They also play an important role in the regulation of SDIMO expression in bacteria. In our transformation surveys (Table 2.4), PRM exhibited exceptional ability to degrade all alkanes (C2-C4) and the C2 alkene (i.e., ethene) tested in this study. Ethene showed the highest degradation rate (0.487 ± 0.047 μmol/h/mg), followed by propane (0.307 ± 0.045 μmol/h/mg), butane (0.246 ± 0.050 μmol/h/mg), isobutane (0.208 ± 0.084

μmol/h/mg), and ethane (0.127 ± 0.053 μmol/h/mg). Homologues to the PH-06 group-6 PRM have been previously identified in dioxane co-metabolizers that grow on propane or isobutane, such as *Mycobacterium* sp. ENV421[127] and *Rhodococcus rhodochrous* 21198[39, 45] (Table 2.5). Further, the presence of propane can also upregulate the polycistronic transcription of the *prmABCD* clusters in PH-06[36] and ENV421[72, 73], which subsequently promoted the activity of dioxane biotransformation. Our study revealed this single PRM enzyme can degrade both dioxane and gaseous alkanes. This novel finding unveiled the plausible linkage between propane/isobutane assimilation and dioxane degradation as evident in the mentioned wild-type strains.

Table 2.5 Bacteria Harboring the Complete Gene Clusters of *prmABCD* and *thmADBC*

Strain Name	Dioxane Degradation	Other Inducible Substrate	Gene Localization	Geographic Location	Gene Cluster Identity (%)	Reference
prm Harboring Bacteria						
Mycobacterium dioxanotrophicus PH-06	m	propane	plasmid	Pohang, South Korea	100	58
Mycobacterium sp. ENV421	ca	propane	ic	New Jersey, US	88.84	47, 72, 127
Rhodococcus rhodochrous strain 21198	ca	propane/isobutane	ic	Japan	86.24	39, 45, 128
Rhodococcus aetherovorans BCP1	u	C2-C7 alkanes	plasmid	Bologna, Italy	86.24	129, 130
Mycobacterium chubuense NBB4	u	ethene/C2-C4 alkanes	plasmid	New South Wales, Australia	86.51	63, 126
thm Harboring Bacteria						
Pseudonocardia dioxanivorans CB1190	m	THF	plasmid	South Carolina, US	100	92, 131
Pseudonocardia sp. N23	m	THF	ic	Japan	97.1	132
Pseudonocardia sp. K1	ct	THF	ic	Göttingen, Germany	94.86	133, 134
Pseudonocardia sp. ENV478	ct	THF	ic	New Jersey, US	96.84	60, 135
Rhodococcus ruber YYL	u	THF	plasmid	Zhejiang, China	99.74	136

m = metabolism
ca = co-metabolism with alkane gases
ct = co-metabolism with THF
u = unknown
ic = incomplete genome with major gaps (precluding the determination of localization of *prm* or *thm* genes

Besides propane and isobutane, PRM can oxidize a greater range of short-chain alkanes and alkenes, including ethene, ethane, and butane. This is in concert with the previous observations that some *prmABCD*-harboring microorganisms can grow on a wide variety of alkane/alkene gases though their ability to degrade dioxane has yet been characterized (Table 2.5). For instance, *Rhodococcus* sp. BCP1[129] can grow on all C2-C7 linear alkanes, which also induced the expression of its group-6 SDIMO. Similarly, *Mycobacterium chubuense* NBB4 can grow on C2-C4 alkanes and ethene[126]. It is noted that these Actinomycetes express a diversity of SDIMOs and other enzymes (e.g. cytochrome P450 and dehydrogenase) that may also contribute to the observed alkane and alkene oxidation[126, 137]. However, this is the first study to ascertain the ability of group-6 SDIMO for the oxidation of C2-C4 alkanes (linear or branched) and ethene.

Chlorinated solvents and aromatic compounds represent two groups of groundwater pollutants commonly found in contaminated aquifers[8, 138, 139]. We assessed the capability of PRM and THM of degrading these common co-contaminants. Notably, PRM degrades both VC and 1,2-DCA, though the degradation rates were relatively low (0.060 ± 0.007 and 0.038 ± 0.005 μmol/h/mg for VC and 1,2-DCA, respectively) (Table 2.4). This suggests the active site of PRM can weakly react with VC and 1,2-DCA, despite of low affinity. Particularly, VC is a carcinogenic pollutant commonly accumulated as an undesirable metabolite via anaerobic dehalogenation in TCE-contaminated aquifers[140, 141]. Thus, presence of bacteria expressing PRM can in addition synchronize the removal of dioxane and VC co-occurring at the chlorinated solvent sites. PRM can also degrade benzene and toluene at the degradation rates of 0.106 ± 0.011 μmol/h/mg and 0.345 ± 0.039 μmol/h/mg, respectively. Ability to degrade these two aromatic compounds was validated

using PH-06 cells actively expressing PRM as they were grown with propane. As major gasoline constituents, benzene and toluene are contaminants prevalently detected in groundwater. Compared with toluene, benzene is more toxic and recalcitrant with strict regulation by EPA[142]. To break the aromatic ring, dihydroxylation is imperative to insert two hydroxyl groups at adjacent aromatic carbon positions. This can be achieved by two sequential oxidations catalyzed by monooxygenases or a simultaneous oxidation by dioxygenases[143]. This is the first study report that PRM has the capability of degrading aromatic compounds, such as benzene and toluene. Overall, PRM's versatile degradation capability of degrading a broad spectrum of common groundwater pollutants (e.g., benzene, toluene, VC, and 1,2-DCA) underscores its value for environmental remediation.

Transformant cells expressing THM did not show degradation capability toward any of the alkanes, alkenes, chlorinated and aromatic compounds in our tests (Table 2.4). This demonstrates that THM is highly specific to cyclic compounds. In contrast, PRM has a much broader substrate range, unveiling greater potential for *in situ* and *ex situ* treatments of commingled contaminations. Even better, expression of PRM may also enable microorganisms to assimilate other carbon sources, such as propane and isobutane, for cell growth, and support decomposition of a variety of pollutants. Collectively, this group-6 PRM displays unparalleled catalytic versatility towards various types of small molecules including alkane, alkene, cyclic, chlorinated, or aromatic[144]. In our previous paper[36], we named this type of group-6 SDIMOs as PRM after its first discovery in the propanotroph, *Mycobacterium* sp. TY-6[70]. They were also designated as "short chain alkane-oxidizing monooxygenase (SCAM)" in other reports[39]. We propose the nomenclature of this group-6 SDIMOs can be unified in the future.

2.4 Implications

2.4.1 Environmental Implications for Monitored Natural Attenuation of Dioxane

Besides PH-06 and CB1190, many other Actinomycetes also harbor *prm* and *thm* genes (Table 2.5). Though not all were verified at the molecular level, it is prudent to assume that these strains can utilize PRM or THM for the initial breakdown of dioxane. It is interesting to note that these *prm* and *thm* harboring bacteria were isolated from geographically disparate locations (e.g., Asian, Europe, and America). However, sequences of their multicomponent gene clusters *prmABCD* and *thmADBC* are highly conservative with minimum identities of 86% and 94%, respectively, even with the consideration of the spacers and overlaps between gene components. It is also notable that most of these gene clusters are localized on plasmids (Table 2.5) and/or adjacent to mobile elements. For instance, the *prmABCD* gene cluster in PH-06 is carried by a transposon cassette flanked by insertion sequences[36]. The meticulous examination (Figure 2.6) revealed all gene clusters are intact without noticeable internal rearrangements. In addition, upstream and downstream sequences (the colored blocks shown in Figure 2.6) of the *prm* or *thm* gene cluster also demonstrated high homology suggesting a consensus origin. These converging lines of evidence corroborate that dioxane degradation genes *prm* and *thm* are disseminated via horizontal gene transfer (HGT), enabling the intercellular spreading of dioxane catabolism across species.

In contaminated aquifers, HGT of *prm* and *thm* may occur among indigenous microorganisms at varying frequencies in response to the concentration of dioxane as the selective pressure[99, 145, 146]. Our enzymatic study suggests that transfer of *prm* may be both physiologically and ecologically more profitable than *thm*. This is because (1) PRM displays a faster dioxane catabolism at field-relevant dioxane concentrations (e.g., < 1

mg/L); (2) such dioxane degradation activity of PRM is also less affected by the inhibition of chlorinated solvents; (3) PRM enables the assimilation of short-chain alkanes and biotransformation of cyclic, chlorinated, and aromatic pollutants which commonly co-occur in the contaminated aquifers. Therefore, it is plausible to postulate that dioxane metabolizing microbes, like PH-06, which express PRM may be more abundant and/or active at sites impacted by commingled contamination of dioxane and chlorinated solvents than those employing THM-mediated catabolism. Note that field environment is staggeringly complexed in comparison with the laboratory condition we conducted in our kinetic assays. For instance, growth substrates other than dioxane may compete with the dioxane degrading enzymes or suppress their expression due to metabolic flux dilution and catabolite repression[99]. On the other hand, availability of other substrates may promote cellular growth in general. Further, intrinsic activities of these dioxane degrading enzymes may also be regulated by a wide spectrum of environmental factors (e.g., inhibiting compounds, temperatures, pH, nutrient, oxygen availability, presence of competitors). However, considering chronic acclimation, all these factors together will, in return, affect the native abundance of dioxane degrading microbes, as well as the frequency of these key catabolic genes (e.g., *prmA* and *thmA*) carried by them, permitting the use of these genes as effective biomarkers to assess dioxane attenuation potentials.

Unfortunately, dioxane attenuation potentials may have been long underestimated as previous efforts have merely focused on the quantification of *thm* genes which code for THM. This underscores the need for the complete molecular survey of both *prm* and *thm* genes to assess the abundance and activity of native dioxane degraders in the field. Together with other lines of evidence (e.g., field monitoring, laboratory microcosm assays,

isotopic fractionation, and geochemical indication), comprehensive biomarker analysis will facilitate the justification to select or reject MNA for the mitigation of dioxane. This may elicit significant reduction of field remediation efforts and associated costs at sites where pump-and-treat is actively employed.

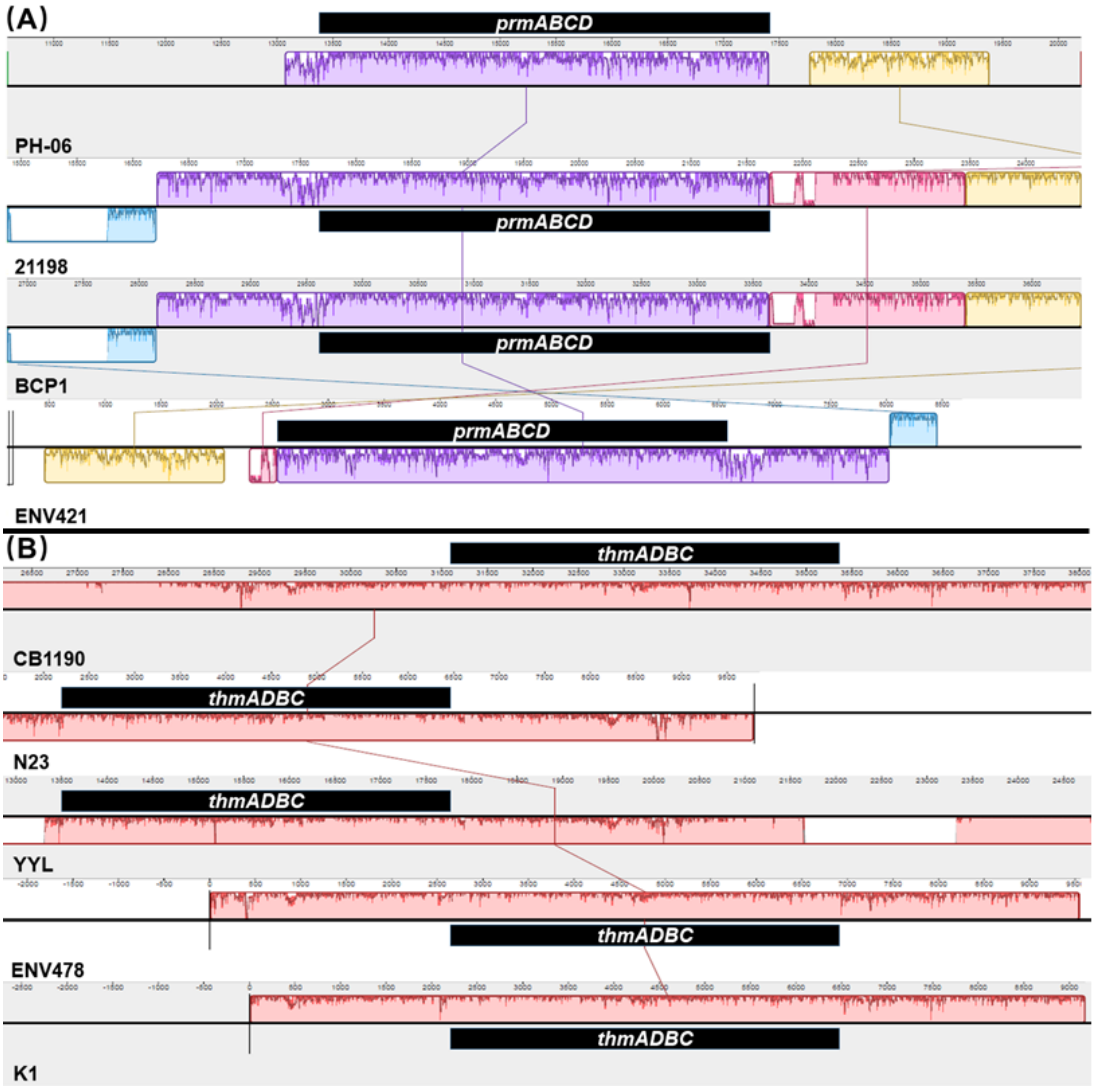

Figure 2.6. Alignment of the nucleotide sequences of (A) five *prmABCD* gene clusters and (B) five *thmADBC* gene clusters from different Actinomycetes generated by Mauve 2.4.0. The *prmABCD* or *thmADBC* gene clusters are indicated by the black bars. The Locally Collinear Blocks (LCB) indicate regions of homology among all five strains; the similarity profiles of the genome sequences are denoted by colored line inside blocks. The blocks depicted above or below the centre line indicate the location of the transcription strand in the forward or inverse orientation.

2.4.2 Environmental Implications for Biostimulation with Short-Chain Alkane/ Alkene Gases

In addition to MNA, biostimulation is an alternative that can effectively accelerate the cleanup of dioxane in the field. A pilot trial lasting over 9 months demonstrated amendment of propane and oxygen into recirculating groundwater sustained an effective removal of dioxane, 1,2-DCA, and other chlorinated compounds at the former air force base site[40]. Ethane and isobutane were also reported for spurring monooxygenase-driven co-metabolism of dioxane in aquifers[45, 147]. In this study, we unequivocally proved that PRM can degrade both dioxane and short-chain alkane/alkene gases, explaining that PRM may contribute to the dioxane co-metabolism observed in previous field and microcosm tests for alkane biostimulation[45, 47, 147]. However, the presence of *prm* genes does not guarantee their ability to carry out catabolic dioxane degradation. Dioxane co-metabolism can be hindered by field factors, such as the lack of inorganic nutrients or inhibition of the auxiliary substrate[45]. Thus, further investigation regarding the PRM-associated dioxane metabolism or co-metabolism are needed to guide for field applications.

We also note that, contribution of bacteria expressing THF to short-chain alkane biostimulation should not be precluded. Though THM is highly specific to heterocyclic ethers, many of *thm* harboring bacteria also carry other SDIMOs genes enabling the assimilation of short-chain alkanes/alkenes. Taking the archetypic THM-mediated dioxane degrader CB1190 as an example, it also carries a group-5 propane monooxygenase gene cluster in the chromosome[131] and its propane degradation capacity was verified in our lab (data not shown). Further investigation is needed to assess the effectiveness of propane and other short-chain alkanes or alkenes for bacteria that carry both *thm* and some other SDIMO genes. However, curing of *thm* carrying plasmids may be of concern. In our

previous study, CB1190 tends to lose redundant plasmids (e.g., the plasmid that carries *thm*) when it is fed with substrates that are readily biodegradable (e.g., 1-butanol and acetate)[99]. Further, in aquifers, the case becomes more intricate, particularly when *prm* harboring bacteria co-exist. Again, this calls for a comprehensive survey of PRM, THM, and other SDIMO genes that are associated with dioxane co-metabolism and the assimilation of the selected auxiliary substrate, which facilitate the design and monitoring of the intrinsic biostimulation. Nonetheless, primary attention is recommended to be made to PRM given their unique and synchronic ability of transforming dioxane and other pollutants and assimilating gaseous alkane/alkene substrates.

CHAPTER 3

CHARACTERIZING THE SOLUBLE DI-IRON MONOOXYGENASE FAMILY: PHYLOGENY, EVOLUTION, SUBSTRATE RANGE

3.1 Introduction

Soluble di-iron monooxygenases (SDIMOs) can catalyze the addition of an oxygen atom to the C-H bond in organic hydrocarbons including aromatics, alkanes, alkenes, chlorinated ethenes/ethanes, and heterocyclic ethers. Given the importance of SDIMOs in the assimilation of various substrates and degradation of different contaminants, catabolic functions of SDIMO are of great interest. Although SDIMOs are found in diverse bacterial strains, their physiological function in each subdivision menifests a remarkable level of specificity according to previous research[96, 97, 148, 149]. For instance, enzymes in group 1 and 2 predominantly function as aromatic monooxygenases and group 3-6 serve as aliphatic monooxygenases. Therefore, the analysis of SDIMOs would provide insights into their evolution and ecology. Bioprospecting of uncharacterized and novel monooxygenases benefits from understanding the principles of SDIMO catalysis on the basis of prior research.

With the advancement of modern molecular techniques, such as metagenomics and biomarker profiling, it is viable to screen the SDIMOs in environmental samples. Alignment of these SDIMOs with characterized enzymes could exploit their potential physiological functions. Metagenomics approaches are state-of-the-art sequencing tools for bioprospecting of pivotal enzymes from diverse environmental samples[150]. Metagenomics also facilitate the idenfication of putative genes encoding SDIMOs from microbial populations, particularly those have relatively low abundances or are

uncultivable but critical in communities. Holmes *et al.*[97] revealed the unprecedented diversity of SDIMOs using nest-PCR with degenerate primers.

This research reviews the existing research about SDIMOs in terms of their phylogeny, evolution, regulation mechanisms. With the inclusion of most-recently discovered SDIMOs, an updated SDIMO phylogenetic tree is constructed which catagorizes the family of SDIMOs into 6 groups. In addition, we re-examine the C-H bond dissociation energies in various common substrates of SDIMOs. This analysis is corherent with the potential evolution direction of SDIMOs. Our updated phylogenetic tree reveals three sub-clusters of group-6 SDIMOs for the first time. Physiological differences of representative group-6 SDIMOs are investigated using transformant clones that heterologously express individual enzymes. Molecular docking is employed to delineate their structural properties and associations with catalytic functions characterized in heterologous expression assays.

3.2 Methods

3.2.1 Construction of Phylogenetic Tree

SDIMOs' α and β hydroxylases have some degrees of similarity in their protein primary and secondary structure, respectively. Leahy *et al.*[96] reported some specific residues located at the catalytic center, "canyon", "handle" and hydrogen-bonding residues are conserved in α and β subunits. Rosenzweig *et al.*[151] characterized the crystal structure of sMMO from *M. capsulatus* Bath by X-ray, revealing 10 α-helices exhibit virtually identical folds. Thus, it is reasonable to surmise that α and β subunits originated with duplication of an ancestral carboxylate-bridged protein with a di-iron center[96]. The deduced amino acid

sequences of α and β subunits were aligned using MUSCLE (3.8.31)[152] with default parameters. The phylogenetic tree was constructed using the maximum likelihood statistical analysis with 1000 Bootstrap by PhyML (version 3.3.20190909)[153]. LG+G+F model was selected as the best substitution model based on the model optimization test ProtTest 3.4.2 (https://github.com/ddarriba/prottest3)[154]. The phylogenetic tree visualization was carried out using the webserver iTOL (version 5.5)[155].

3.2.2 Alignment of Regulation Region Upstream of SDIMOs

The intervals between SDIMOs and their upstream gene were extracted and alignment were aligned using MUSCLE (3.8.31) with default parameters. The regions including the consensus sequences of σ^{54} (-24 and -12) and σ^{70} (-35 and -10) promoters were aligned with the known motifs. The transcription start sites (TSS) were also pointed out on the basis of the known TSS.

3.3 Results and Discussions

3.3.1 Evolution of SDIMOs

According to the alignment of the full-length amino acid sequences of SDIMOs, both α- and β-oxygenase subunits in SDIMOs are distinctly separated into 6 groups using the unrooted maximum likelihood algorithm with 1000 bootstraps. α- and β-oxygenase subunits diverged from a putative common ancestor in the middle region of the phylogenetic tree which is in line with Leahy *et al.*[96] described. *In vivo* degradation capacities of multiple members from each SDIMO group have been characterized in previous studies as listed in Table 3.1. It concurs with their designated names: group 1 as phenol monooxygenases, group 2 as aromatic monooxygenases, group 3 as methane

monooxygenases, group 4 as alkene monooxygenases, group 5 as propane/tetrahydrofuran monooxygenases, and group 6 as propane monooxygenase. However, it should be noted that this nomenclature is somewhat oversimplified due to the substrate promiscuity of SDIMOs. Take propane degradation activity as an example, the propane degradation capability has been found in group 5 and 6. Group-5 SDIMOs compose of two sub-branches as shown in Figure 3.1: one of the branches accommodates well-studied tetrahydrofuran degrading monooxygenase from *P.* CB1190[57], *P.* K1[134], and *P.* ENV478[135]; the other branch accommodates three monooxygenases found in the bacterial strains of *Gordonia sp.* TY-5, *Rhodococcus jostii* RHA1, and *Rhodococcus sp.* RR1. It is reported that TY-5 harbors a gene cluster designated as *prmABCD* that is involved in oxidation of propane to 2-propanol[156]. However, to our best knowledge, the propane oxidation abilities of the other two group-5 homologies in RHA1 and RR1 have not been explicitly explained. It should be noted that both wild-type strains can grow with propane as the sole carbon and energy source[157, 158]. In group 6, PH-06, TY-6, NBB4, ENV421, and BCP1 have been confirmed that can utilize propane and supply energy to their host strains[36, 70, 73, 126, 130].

Our results echo by a number of recent studies which differentiated the enzyme family of SDIMOs into six groups according to their amino acid sequences and discrete physiological roles. Holmes *et al.*[97] constructed a phylogenetic tree by aligning 600 amino acid sequences of α hydroxylase subunits. The phylogenetic tree constructed by He *et al.*[35] using Neighbor-joining algorithm also exhibits the same classification pattern. The distinctive operon arrangements of SDIMOs presented in Figure 3.1B also strongly support that these six lineages in SDIMOs are phylogenetically distinct.

To be noted, the first discovered PRM in TY-6 with its homology forming a sub-branch designed as cluster I. Based on the identity of α subunits, another two group 6 SDIMOs have a distinct distance from the cluster I group 6 SDIMOs. Therefore, group 6 SDIMOs phylogenetically diverged another two sub-branches designed as cluster II and cluster III. Although previous research uncovered the group 6 SDIMOs in term of their high identity of amino acid sequences, the three clusters' physiological properties, evolutionary developments, and substrate ranges are still elusive. Take *Mycobacterium marium* E11[159] as an exemple, its high identical group 6 SDIMO was mentioned in previous study[73]. However, no detailed studies and comparison about degradation capacity, evolutionary pattern, and many other aspects of this monooxygenase. Apart from the scarcity investigations associated within group 6 SDIMOs, the evolution activity of group 6 in the SDIMOs family is ambiguous. Further, it is interesting to learn that group-6 SDIMOs can be distinctly devided into 3 clusters designated as Cluster I, II, and III, respectively (Table 3.1 and Figure 3.1A). However, due to the limited knowledge about group-6 SDIMOs, their physiological properties, substrate range, and evolution remain elucive.

3.3.2 Evidence of Horizontal Gene Transfer (HGT)

SDIMO sequence analysis revealed that distances within a specific group are significantly closer than those between groups. It suggests that SDIMOs evolve through genetic variations (i.e., mutation and recombination) and their coding gene clusters can be spread through HGT. The distances from the branch-off point of each group to the common ancestor decide the evolution order in SDIMOs, following group 1 → 2 → 5 → 4 → 6 → 3 (Figure 3.1). This evolution order indicated group 3 and group 6 likely to have emerged

from most recent evolution events. Previous research[96, 149] also found group-3 SDIMOs represent the most distant branch in SDIMO phylogenetic tree from the "ancestor" and thus surmised their methane oxidization activity may occur in the latest evolutionary stage.

It is likely that SDIMO genes spread through HGT because of the significantly high similarity within each group and their localization on mobile elements. Among the selected 52 monooxygenases in the present study, 13 (25%) have been shown to be plasmid-encoded (Table 3.1). Given the pivotal role of plasmids in HGT in the prokaryotes[160], it is reasonable to speculate that the genes located on plasmid have been obtained via HGT process. Among the rest, 25 (48% of the 52) of them are chromosomal genes and 27% of them are elusive because of their incomplete genome. As persistent vertical transmission which would manifest in the retention of these enzymes in species and genus[161]. However, the strains contain SDIMOs are diverse (Table 3.1); together with the high identity indicating they may from the same origin, it can be surmised that chromosome-encoding genes likely acquired via HGT and ultimately integrated to chromosome[96].

Table 3.1 Subdivisions of SDIMO Enzyme Family, Name of Host Strain, Accession Number, Location of Gene Cluster, and Class and Phylum of Host Strain (Continued)

Group	Strain name	Accession No.	α subunit accession No.	Gene localization (size kb)	Class/Phylum	Reference
Group 1	*Pseudomonas* sp. CF600	M60276	AAA25942	p (>200)	Gamma/P[1]	162, 163
	Pseudomonas putida H	X80765	CAA56743	p (>200)	Gamma/P	164, 165
	Pseudomonas putida P35X	X79063	CAA55663	c	Gamma/P	166
	Acinetobacter calcoaceticus NCIB8250	Z36909	CAA85383	c	Gamma/P	167
	Acinetobacter sp. 20B	D85083	BAA23333	c	Gamma/P	168
	Burkholderia cepacia G4	AF349675	AAL50373	p (108)	Beta/P[2]	169, 170
	Pseudomonas sp. JS150	L40033	AAA88459	p	Gamma/P	171
	Comamonas testosteroni TA441	AB006479	BAA34172	c	Beta/P	172
	Comamonas testosteroni R5	AB024741	BAA87871	c	Beta/P	173
	Ralstonia eutropha E2	AF026065	AAC32455	c	Beta/P	174
Group 2	*Pseudomonas mendocina* KR1	AY552601	AAS66660	NA	Gamma/P	175, 176
	Pseudomonas stutzeri OX1	AJ005663	CAA06654	c	Gamma/P	177
	Pseudomonas pickettii PKO1	U04052	AAB09618	c	Gamma/P	178
	Xanthobacter sp. Py2	AJ012090	CAA09911	p (320)	Alpha/P[3]	179, 180
	Ralstonia eutropha JMP134	AF065891	AAC77380	c	Beta/P	181
	Rhodococcus sp. AD45	AJ249207	CAB55825	NA	Actino/A[4]	182
	Cupriavidus metallidurans CH34	NC_007973	WP_011516082	c	Beta/P	183, 184
	Azoarcus sp. DD4	NZ_CP022958.1	WP_141018170	c	Beta/P	37, 185

Table 3.1 Subdivisions of SDIMO Enzyme Family, Name of Host Strain, Accession Number, Location of Gene Cluster, and Class and Phylum of Host Strain (Continued)

Group		Strain name	Accession No.	α subunit accession No.	Gene location (size kb)	Class/Phylum	Reference
Group 3	Type X	*Methylococcus capsulatus* Bath	M90050	AAB62392	c	Gamma/P	186, 187
	Type I	*Methylomonas* sp. KSPIII	AB025021	BAA84751	NA	Gamma/P	188
		Methylomonas sp. KSWIII	AB025022	BAA84757	NA	Gamma/P	188
	Type II	*Methylosinus trichosporium* OB3b	CP023737	ATQ70365	c	Alpha/P	189, 190
		Methylocystis sp. M	U81594	AAC45289	c	Alpha/P	191
		Methylocystis sp. WI14	AF153282	AAF01268	c	Alpha/P	192
	New cluster	*Mycobacterium* sp. ENV421	NZ_PDHO01000066.1	WP_102810290	NA	Actino/A	72
		Mycolicibacterium chubuense NBB4	GU174751.2	ACZ56334	p (615)	Actino/A	126
		Mycolicibacterium rhodesiae NBB3	NC_016604.1	WP_014211362	c	Actino/A	63
Group 4		*Nocardia corallina* B-276	D37875	BAA07114	p (185)	Actino/A	193
		Mycobacterium chubuense NBB4	GU174752	ACZ56346	p (144)	Actino/A	126
		Mycobacterium sp. JS623	NC_019966	WP_015305852	c	Actino/A	194
		Mycobacterium rhodesiae JS60	AY243034	AAO48576	NA	Actino/A	63
		Nocardioides sp. JS614	AY772007	AAV52084	p (290)	Actino/A	195
Group 5		*Pseudonocardia dioxanivorans* CB1190	CP002597	AEA29037	p (66)	Actino/A	55
		Pseudonocardia sp. ENV478	HQ699618	AEI99544	c	Actino/A	135
		Pseudonocardia sp. K1	AJ296087	CAC10506	c	Actino/A	134
		Pseudonocardia sp. N23	BEGX01000008	GAY07941	c	Actino/A	132
		Rhodococcus ruber YYL	NZ_CP024892	WP_102032065	p (236)	Actino/A	136
		Gordonia sp. TY-5	AB112920	BAD03956	c	Actino/A	156
		Rhodococcus jostii RHA1	NC_008268	WP_011593714	c	Actino/A	101
		Rhodococcus sp. RR1	HM209445	ADM83577	NA	Actino/A	32

Table 3.1 Subdivisions of SDIMO Enzyme Family, Name of Host Strain, Accession Number, Location of Gene Cluster, and Class and Phylum of Host Strain (Continued)

Group		Strain name	Accession No.	α subunit accession No.	Gene location (size kb)	Class/Phylum	Reference
Group 6	Cluster I	*Mycobacterium* sp. ENV421	NZ_PDHO01000068	WP_102810306	NA	Actino/A	[72]
		Mycobacterium dioxanotrophicus PH-06	CP020812	ART74426	p (106)	Actino/A	[35, 36]
		Rhodococcus aetherivorans BCP1	NZ_CM002179	WP_006947300	p (103)	Actino/A	[129]
		Mycolicibacterium chubuense NBB4	NC_018022.1	WP_014805366	p (615)	Actino/A	[126]
	Cluster II	*Mycobacterium* sp. 012931	AOPX01000001	EPQ44813	NA	Actino/A	[196]
		Mycobacterium pseudoshottsii	BCND01000037	GAQ35500	NA	Actino/A	[197]
		Mycobacterium marinum E11	HG917972	CDM74267	c	Actino/A	[198]
		Mycobacterium ulcerans subsp. Shinshuense	NZ_AP017624	WP_096369473	c	Actino/A	[199]
	Cluster III	*Mycobacterium* sp. ENV421	NZ_PDHO01000056	WP_102810202	NA	Actino/A	[72]
		Mycobacterium gordonae 1245752.6	NZ_MAEM01000159	WP_065133219	NA	Actino/A	NA
		Mycobacterium lentiflavum CSUR P1491	NZ_CTEE01000002	WP_090609799	NA	Actino/A	[200]
		Mycobacterium sp. TY-6	AB250938	BAF34294	c	Actino/A	[70]

NA: Not available
p: plasmid
c: chromosome
[1]: Gammaproteobacteria/Proteobacteria
[2]: Betaproteobacteria/Proteobacteria
[3]: Alphaproteobacteria/Proteobacteria
[4]: Actinobacteria/Actinobacteria

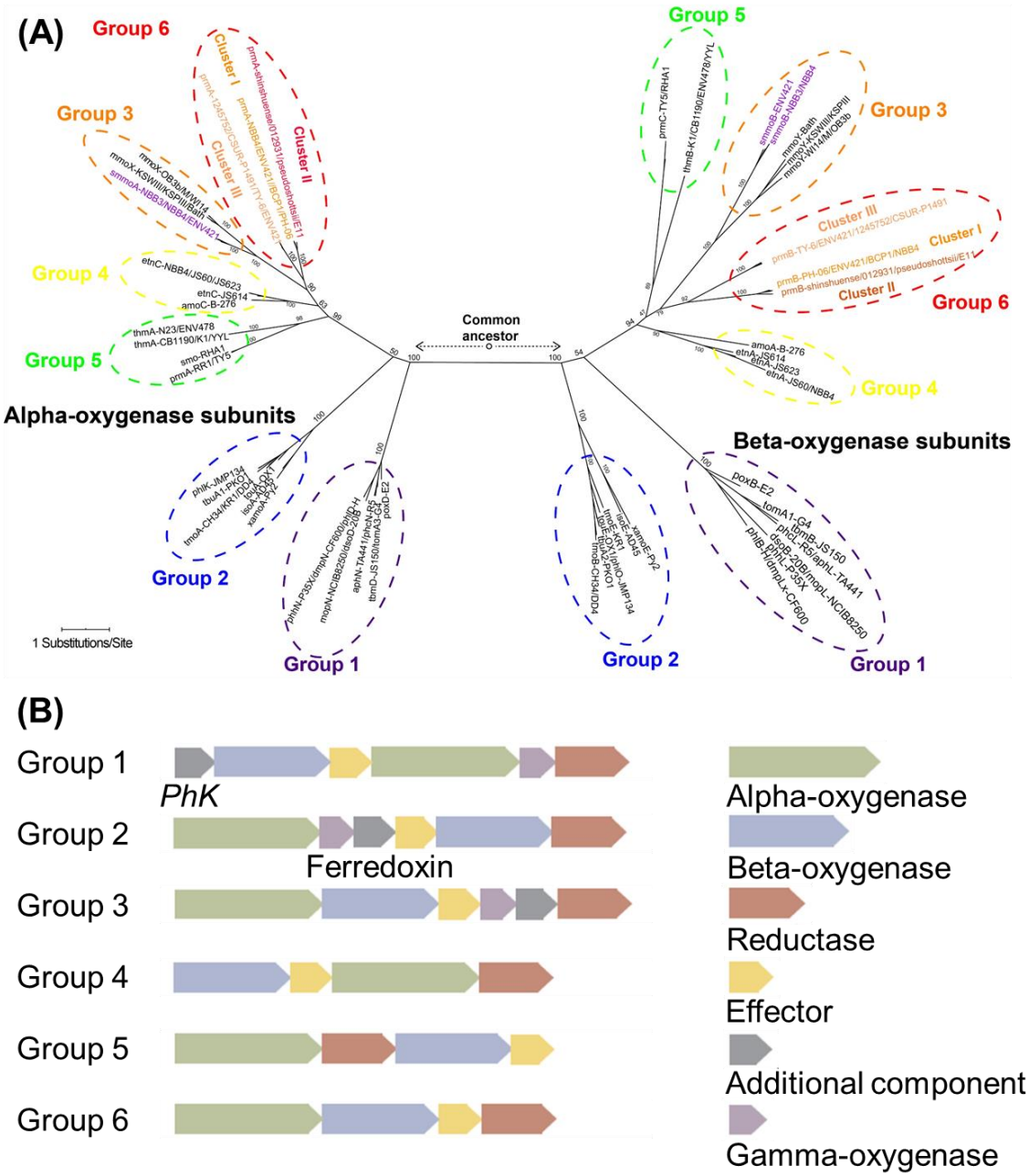

Figure 3.1 Phylogeny and operon organization of SDIMO family. (A) Unrooted maximum likelihood phylogenetic tree of α- and β-oxygenase subunits. (B) Operon organization for each group. Components are indicated in different colors.

3.3.3 SDIMOs Evolve Towards Saturated Substrates with High Dissociation Energy of C-H Bonds

According to the phylogeny analysis, it shows that SDIMOs evolved from unsaturated aromatics or alkenes towards saturated alkanes, ultimately to methane, the most stable hydrocarbon[201]. Alkenes oxidized through the formation of epoxide intermediates while saturated alkanes directly attack the C-H bonds. Thus, the high C-H cleavage energy required for the oxidation of saturated substrates suggests the SDIMO may evolve to attack substrates with the dissociation energies from low towards high. Methane exhibits the highest dissociation energy (i.e., 431.0 kJ/mol) in C-H bond (Table 3.2). The extremely strong C-H bond in methane requires an enzymatic intermediate Q in di-iron core[202] which is an $Fe^{IV}_2O_2$ diomond core structure has extremely high oxidation capability found in nature[203]. C-H bond at the primary location in propane requires 410.0 kJ/mol at the second place of all the alkanes. While with the high dissociation energy for the primary C-H bond, the secondary C-H bond in propane has a relatively low energy (i.e., 395.8 kJ/mol). The whole cell degradation assay revealed that the group-6 propane monooxygenases in TY-6 and BCP1 could oxidize propane through the terminal and sub-terminal oxidation leading to the production of 1-propanol and 2-propanol[72, 129]. On the contrary, the propane monooxygenases belonging to group 5 oxidize propane via sub-terminal oxidation that only produces 2-propanol[129]. These observations support our hypothesis for the correlation between evolution of SDIMOs and the bond cleavage energy of their primary substrates. To be specific, group-6 SDIMOs could cleavage the C-H bond including energy of 410.0 kJ/mol which is the dissociation energy of primary C-H bond in propane. It could surmise that this branch of propane monooxygenases can oxidize most of the C2-C4 gaseous alkanes such as ethane, butane, and isobutane. This prospective in accords with our

substrate assay for the group-6 SDIMO in PH-06[38]. Whilst group-5 propane monooxygenase are capable to oxidize those bonds possessing energy includes 395.8 kJ/mol (the energy of the secondary C-H bond in propane). Of great interest that according to the substrate range of THM in CB1190, the other sub-branch in group 5 SDIMOs exhibits lower capacity that can oxidize C-H bonds possess 393.3 kJ/mol (in cyclohexane) or less[38].

Table 3.2 The C-H Bond Dissociation Energy of Alkanes, Alkene, and Dioxane Analogues

Substrate	Dissociation energy	Reference
Methane	431.0 kJ/mol	Dean *et al.*[204]
Ethene	428.9 kJ/mol	Kerr *et al.*[205]; Gurvich *et al.*[206]
Propane (primary)	410.0 kJ/mol	Kerr *et al.*[205]
Ethane	410.0 kJ/mol	Kerr *et al.*[205]
Butane (primary)	409.9 kJ/mol 431.0 kJ/mol	Gribov *et al.*[207] Dean *et al.*[204]
Isobutane	408.5 kJ/mol	Gribov *et al.*[207]
Propane (secondary)	395.8 kJ/mol	Dean *et al.*[204]
Cyclohexane	393.3 kJ/mol	Kerr *et al.*[205]
Dioxane	389.1 kJ/mol	Battin *et al.*[208]
THF	382.8 kJ/mol	Cruickshank *et al.*[209]; Dean *et al.*[204]

3.3.4 Gene Regulation of SDIMOs

Sequence motifs located upstream of gene clusters are marked as red in Table 3.3 through alignment to the known regulatory regions. As previously reported, group 1, 2, and 3 SDIMOs are regulated by σ^{54}-dependent promoters. In this regulation system, sigma factor 54 can direct RNA polymerase (RNAP)- σ^{54} to bind with the consensus polymerase binding region. The sequences of two hexmars comparing with the sigma factor 70 recognizing

elements (i.e., TTGACA at - 35 hexamer and TATAAT at the - 10 hexamer in *E*.coli[210]) are highly consensus. In groups 1, 2, and 3 SDIMOs (Table 3.3), the typical consensus motifs are TGGCA – 24 and BTGC -12. Activation of σ^{54}-dependent promoters requires the assistance of an activator (also known as bacterial enhancer binding protein, bEBP) that incorporates the energy generated from ATP hydrolysis and enables the isomerization of the RNAP-σ^{54} closed complex (CC) to open complex (OC)[211]. σ^{54}-dependent activators are classified as members of the AAA^+ (ATPases associated with various cellular activities) superfamily[212] on the basis of their structures and functions[213]. Previous investigations regarding groups 1, 2, and 3 SDIMO transcription echoed the prerequisite of an activator. Multiple activators have been discovered, such as DmpR encoded by *dmpR* from *Pseudomonas* CF600, XylR encoded by *xylR* from *Pseudomonas putida*, TbuT encoded by *tbuT* from *Burkholderia pickettii* PKO1, MmoR encoded by mmoR from Bath and OB3b, as well as many other regulatory proteins (e.g., TouR, TbmR, and RhhR). The activator binding site resides upstream of the consensus sequences recognized by polymerase and embodies as a pair of inverted repeats[214, 215]. DNA must be folded up to 180° because activator binding site is relatively far upstream of two transcriptional sites (-24 and -12)[216, 217]. Integration host factor (IHF) often binds between these two transcriptional sites facilitating the formation of the DNA looping[218, 219].

Unlike groups 1, 2, and 3 SDIMOs, group-6 SDIMOs are likely to be regulated by σ^{70}-dependent promoters considering the absence of feature sequences for the σ^{54}-dependent regulation region. This is in line with a previous study that reported the putative -35 and -10 hexamers upstream of group-6 SDIMO gene clusters in BCP1 and NBB4[129]. Researchers reported that RNA polymerase holoenzyme ($E\sigma^{70}$) in *E. coli* recognizes and

binds to the consensus sequences TTGACA at the -35 and positions of TATAAT at the -10, and the spacing between these sequences is crucial for transcription initiation[210, 220]. However, consensus sequences identified as putative transcriptional elements of group-6 SDIMOs are not in good consistence with those reported in *E. coli*. Further, they are weakly conserved for group-6 SDIMOs as compared to those in groups 1, 2, and 3. Unlike σ^{54}-dependent promoters, RNAP-σ^{70} closed complex is an energetic unfavorable structure that is readily converted to the open complex. Thus, the activator is not required by all of the σ^{70}-dependent regulation processes, though this remains unclear and warrents further verification.

Table 3.3 Regulatory Regions Upstream of SDIMOs through Docking Sequence Motifs (Continued)

	Strain Name	Gene	Promoter[a]	Regulatory motif[b]	RBS	References
Group 1	*Pseudomonas sp.* strain CF600	*dmp*	σ^{54}	tggcacagccgttgcttgatgtcctgc**g**	GGAG	221
	Pseudomonas putida H	*phl*	σ^{54}	tggcacagctgttgcactttgtcctgc**g**	GGAG	NA
	Pseudomonas putida P35X	*phh*	σ^{54}	tggcacagctgttgctttatgtcctgc**g**	GGAG	222
	Acinetobacter calcoaceticus NCIB8250	*mop*	σ^{54}	tggcacgactttttggaatatctagagt**a**	AGGA	NA
	Acinetobacter sp. strain 20B	*dso*	miss		AGGA	NA
	Burkholderia cepacia G4	*tom*	miss		GGAGA	NA
	Pseudomonas sp. strain JS150	*tbm*	σ^{54}	tggcacaccttctgcaaaagaggagcg**t**	AGCGGA	NA
	Comamonas testosteroni TA441	*aph*	σ^{54}	tggcacgggctgtgcaattgcaaaggc**c**	AGGAG	NA
	Comamonas testosteroni R5	*phc*	σ^{54}	tggcacgggctgtgcaattgcaaaggc**c**	AGGAG	NA
	Ralstonia eutropha strain E2	*pox*	σ^{54}	tggcacggtcttcgcaatagaccgggc**a**	AGGAG	NA
Group 2	*Pseudomonas mendocina* KR1	*tmo*	miss		CGGAGA	NA
	Pseudomonas stutzeri OX1	*tou*	σ^{54}	tggcatatacattgcttcagatacagat**a**	AAGGAGA	223
	Pseudomonas pickettii PKO1	*tbu*	σ^{54}	tggcaccggccttgcaatggaggacc**g**	AAGGAGA	178
	Xanthobacter sp. Py2	*aam*	σ^{54}	tgggcgcaccttgccgctcatcgca**a**	GGGAGG	NA
	Ralstonia eutropha JMP134	*phl*	σ^{54}	tggcattgcatttgcgaaagggacag**c**	AAGGAGA	NA
	Rhodococcus sp. AD45	*iso*	miss		AGGAAA	NA
	Cupriavidus metallidurans CH34	*dmp*	miss		TGGAGA	NA
Group 3	*Methylococcus capsulatus* strain Bath	*smo*	σ^{54}	tggcacgatccctgtaactaggttgtca**c**	CGGAGGA	214
	Methylomonas sp. strain KSPIII	*smo*	σ^{54}	tggcacgtgtgttgcaatctgccctgcg**a**	AGGAGGA	188
	Methylomonas sp. strain KSWIII	*smo*	σ^{54}	tggcacacgtgttgcaatctgaccaccg**a**	AGGAGGA	224
	Methylosinus trichosporium OB3b	*smo*	σ^{54}	tggcacaggccttgccaaataagaagcg**t**	ACGAGGA	224
	Methylocystis sp. Strain M	*smo*	σ^{54}	tggcacgcgccttgccaaataagtcggg**t**	ACGAGGA	191
	Methylocystis sp. strain WI14	*smo*	miss			NA

Table 3.3 Regulatory Regions Upstream of SDIMOs through Docking Sequence Motifs (Continued)

	Strain Name	Gene	Promoter	Regulatory motif	RBS	References
Group 6	*Mycobacterium sp.* ENV421	*prm*	σ^{70}	taggcaaccgcagagctatgtgtgagcatggtctc**a**	CGGGAG	NA
	Mycobacterium dioxanotrophicus strain PH-06	*prm*	σ^{70}	tgttcgcccgcagatccgcgtgtgatgctggtctc**a**	CGGGAG	NA
	Rhodococcus aetherivorans strain BCP1	*prm*	σ^{70}	tagtcaacccggggtagaaatgtgatggtgatctc**a**	CGGGAG	129
	Mycolicibacterium chubuense NBB4	*prm*	σ^{70}	tagtcgacggcatccgcgcgtgtgacgatgatctc**a**	CGGGAG	129
	Mycobacterium sp. 012931	*prm*	σ^{70}	tagtgcagaccggcgggtggtgtgatcctggtctc**a**	CAAGAG	NA
	Mycobacterium pseudoshottsii	*prm*	σ^{70}	tagtgcagaccggcgggtggtgtgatcctggtctc**a**	CAAGAG	NA
	Mycobacterium marinum E11	*prm*	σ^{70}	tagtgcagaccggcgggtggtgtgatcctggtctc**a**	CAAGAG	NA
	Mycobacterium ulcerans subsp. Shinshuense	*prm*	σ^{70}	tagtgcagaccggcgggtggtgtgatcctggtctc**a**	CAAGAG	NA
	Mycobacterium sp. ENV421	*prm*	σ^{70}	cgcacagctgccaagcctagggtgatctctatcac**c**	GGGGAG	NA
	Mycobacterium gordonae strain 1245752.6	*prm*	σ^{70}	ccgcgaagagagcgccttacagtgacaggcatcac**g**	GGGAAG	NA
	Mycobacterium lentiflavum strain CSUR P1491	*prm*	miss		GGAAG	NA
	Mycobacterium sp. TY-6	*prm*	σ^{70}	ttgccgattcccacccttacggtgatgtctatcac**c**	GGAAG	NA

NA: not available

[a]: The promoters are indicated by σ^{54}- and σ^{70}-dependent polymerases.

[b]: The consensus sequence of polymerase binding sites are marked as red. The transcriptional start sites are bolded.

3.4 Implication

Along with the advent of the next-generation sequencing, an increasing number of SDIMOs are discovered from the environment as they are potent biocatalysts valuable for applications, such as bioremediation and green energy production. However, SDIMOs exhibit eminently diverse and relatively low abundance in environment. Thus, it leads to an intricate process to characterize the physiological roles of newly discovered SDIMOs. For example, the isolation of target SDIMO-expressing strains that are of low abundance is labor-intensive. Even if the isolation is successful, characterization of the target SDIMO involves extensive laboratory efforts. This research reconciles the existing challenges by bioprospecting intrinsic properties and physiological roles of SDIMOs. According to the amino acid sequences of the component that exerts oxidation function (i.e., the α subunit), together with the explicit operonal organization, SDIMOs can be classified into 6 groups as shown. Consequently, for accurate categorization, it is necessary to recover individual SDIMO gene components as well as their entire operons. Though the α subunit of the hydroxylase is the site of hydroxylation, there is evidence that other proteins also affect the catalytic properties of SDIMOs. The bioinformatic profiling of SDIMOs provides the whole picture of this enzymatic family including the novel SDIMOs in group 6, regarding their phylogeny, evolution, and physiological functions. Their physiological roles can be roughly predicted according to characterized enzymes from the same clade. This could provide information in terms of the SDIMOs' substrate range and poteintial properties.

CHAPTER 4

UNTANGLING THE GENOMIC DIVERGENCE BETWEEN METABOLIC AND CO-METABOLIC DIOXANE-DEGRADING ACTINOMYCETES

4.1 Introduction

To date, over 28 bacterial strains have been reported given their capability of degrading dioxane via metabolism or co-metabolism. Based on the taxonomic analysis, many of known degraders are Actinomycetes and can be classified into three genera: *Rhodococcus*[225, 226], *Mycobacterium*[58, 227], and *Pseudonocardia*[60, 228]. Among these dioxane degrading Actinomycetes, 12 of them are dioxane metabolizers that can ultilize dioxane as a sole carbon and energy source to support the growth and fully mineralize it into carbon dioxide. Unlike metabolic degraders, co-metabolic degraders refer to those bacterial strains that can fortuitously degrade dioxane but require the supplement of additional carbon source. Co-metabolizers cannot grow when dioxane is provided as the only carbon source. propane[35, 36], toluene[229], THF[41, 135] are common auxiliary substrates that can not only stimulate the expression of "sloppy" enzymes that concurrently oxidize dioxane, but also sustain the growth of the co-metabolizers.

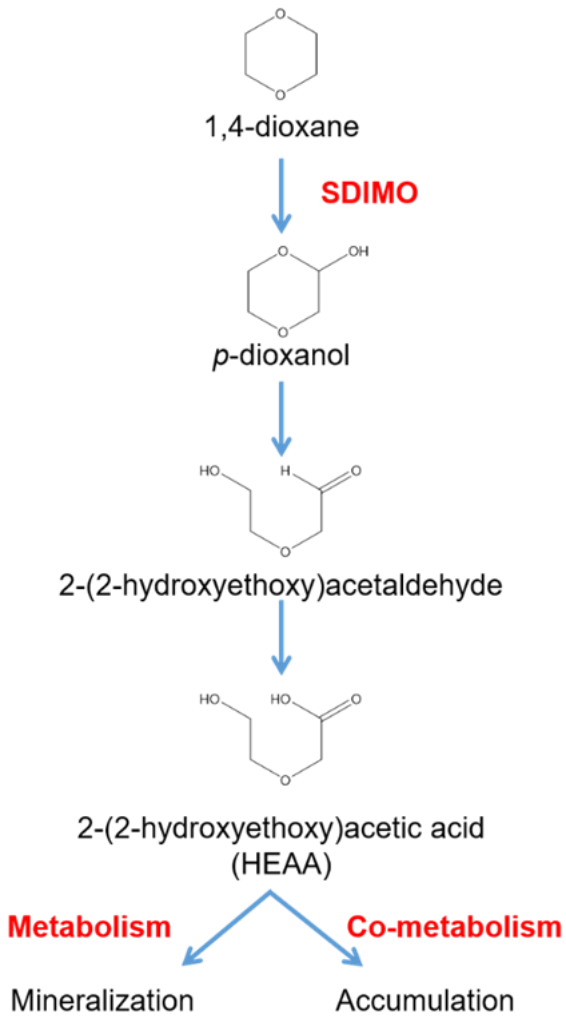

Figure 4.1 Dioxane biodegradation pathways in metabolic and co-metabolic bacterial strains. 2-Hydroxyethoxyacetic acid (HEAA) is mineralized in metabolism pathway. In contrast, HEAA accumulated in co-metabolism degradation pathway.

Increasing attention has been drawn to the biodegradation of dioxane within the last decade. SDIMOs are essential for initiating the dioxane degradation, particularly the group-6 SDIMOs in Actinomycetes as discussed in Chapter 3 of this dissertation. However, as previous studies primarily focused on the first step of dioxane oxidation, limited is known about the downstream degradation pathway after 2-(2-hydroxyethoxy) acetic acid (HEAA) is formed[55, 57]. The initialization of dioxane breakdown is catalyzed by a variety of

SDIMOs including propane monooxygenases, tetrahydrofuran (THF) monooxygenases, toluene monooxygenases, soluble methane monooxygenases[230]. These SDIMOs initialized dioxane degradation by inserting a hydroxyl group to the α-carbon to form *p*-dioxanol. Then it undergoes hydrolysis and forms 2-(2-hydroxyethoxy) acetaldehyde, which is further subject to the oxidation by aldehyde dehydrogenase enzyme forming 2-(2-hydroxyethoxy) acetic acid, which is also named as HEAA[56, 228] (Figure 6-1). Afterward, metabolism and co-metabolism behave divergently regarding to HEAA. Metabolic degraders can continue to transform HEAA into small molecules such as ethylene glycol, glyoxylate, and gylcoaldehyde, which enter central metabolic pathways[55, 57]. Grostern *et al.* revealed that glyoxal, ethylene glycol, and glycolate were the oxidation products after HEAA oxidized by an unknown oxygenase. They underwent sequential oxidation by dehydrogenases and oxidase to glyoxylate, which was approved to be a key downstream product, which is eventually mineralized to carbon dioxide or enter TCA cycle. Thus, glyoxylate assimilation is critical for CB1190 to grow on dioxane as a sole carbon and energy source. Sales *et al.* further explored the degradation pathway of THF. Comparing with the dioxane degradation pathway, the initialization of the ring cleavage of THF was performed by the same dioxane-degrading enzyme THM in CB1190. However, THF was oxidized to 4-hydroxybutyrate without generating HEAA. The succinate was the key metabolite analogous to glyoxylate in the dioxane degradation pathway.

In contrast to dioxane metabolism, HEAA accumulates in co-metabolic degraders without generating downstream metabolites. Thus, HEAA degradation capacity is key to distinguish the dioxane metabolizers with co-metabolizers. Thus, contrasting the genomes of dioxane metabolizers and co-metabolizers may enable the discovery of genes involved

in HEAA biotransformation and other downstream mineralization steps. Heterologous expression of their encoded enzymes can be used to validate their catalytic functions.

4.2 Materials and Methods

4.2.1 Genome Analysis and Comparison

We postulate that genes responsible for the HEAA degradation are only present in dioxane metabolizers but absent in co-metabolic strains. Based on this hypothesis, we investigated the genomic differences between metabolic and co-metabolic strains. The genomic information was retrieved from the database of the National Center for Biotechnology Information (NCBI), which contains the complete genomes of only 4 dioxane metabolic strains and 6 dioxane co-metabolic strains (Table 4.1). CD-HIT algorithm[231, 232] was used to identify specific genes shared only by metabolic strains, but not co-metabolic strains. The comparison was based on the protein sequences to provide a direct linkage with their phenotypes. The cutoff threshold for the identity of protein sequences was 40% to categorize proteins that may exhibit similar functions. The putative functions of the encoded proteins were annotated using the Kyoto Encyclopedia of Genes and Genomes (KEGG) database by the KEGG Automatic Annotation Server (KAAS)[233] and NCBI BLAST. The degradation pathways involving the genes/enzymes of interest were predicted by KEGG orthology (KO) identifiers. Based on the previous study[56], HEAA degradation may be catalyzed by bacterial oxygenases, such as monooxygenase, dioxygenase, ether hydrolase, carbon-oxygen lyase, peroxidase, laccase, and etherase. Thus, we primarily focus on genes encoding these oxygenases to investigate their association with HEAA degradation.

Table 4.1 List of Dioxane Degrading Strains

Metabolism	Co-metabolism
Mycobacterium dioxanotrophicus* PH-06	***Mycobacterium chubuense* NBB4***
***Mycobacterium* sp. D6**	***Pseudonocardia* sp. K1**
***Mycobacterium* sp. D11**	***Pseudonocardia* sp. ENV478***
Pseudonocardia dioxanivorans* CB1190	***Mycobacterium* sp. ENV421***
Pseudonocardia* sp. N23	***Pseudonocardia acaciae* JCM 16707***
Pseudonocardia dioxanivorans* BERK-1	***Pseudonocardia asaccharolytica* JCM 10410***
***Pseudonocardia benzenivorans* B5**	***Rhodococcus aetherivorans* BCP1***
***Pseudonocardia antarctica* DVS 5a1**	***Rhodococcus aetherivorans* JCM 14343T**
***Pseudonocardia* sp. D17**	***Rhodococcus* sp. ENV425**
***Pseudonocardia* sp. RM31**	***Rhodococcus ruber* T1**
***Rhodococcus ruber* 219**	***Rhodococcus ruber* T5**
***Acinetobacter baumannii* DD1**	*Flavobacterium* sp.
Afipia sp. D1	
Rhodanobacter sp. AYS5	
Xanthobacter flavus DT8	
Cordyceps sinensis A	

*Strain with sequenced genomes available in NCBI
Actinomycetes are indicated in bold.

4.2.2 HEAA Degrading Gene Verification

Based on the genome analysis, HEAA degrading gene candidates were selected. To validate their functions, we heterologously expressed the most likely genes in mc^2-155 as described in Section 2.2.2. *Mycobacterium dioxanotrophicus* PH-06 and *Pseudonocardia dioxanivorans* CB1190 are selected as representatives for dioxane metabolism. The ~2.6 kb gene clusters (containing two components) encoding Flavin monooxygenase (FMO) were amplified from PH-06 and CB1190 using the specific primers. PCR was performed using th forward primer 5'-AGATATACATATGGTGGCCGCACCCCACATCG-3' and reverse primer 5'-AGATATAAAGCTTCTAGCCGGTGACCGCGGTC-3' for PH-06 and forward primer 5'-AGATATACATATGGTGCCCGATACCCCCCTTCACC-3' and reverse primer 5'-AGATATAAAGCTTTCAGACGCTCGCGCGGG-3' for CB1190.

Restriction digest sites for NdeI and HindIII are underlined. The expression process was carried out as described in Section 2.2.2. Successful expression of cloned genes in transformants was verified by SDS-PAGE and physiological assay.

4.3 Results and Discussion

4.3.1 Putative HEAA Degrading Genes

Based on the CD-HIT genomic analysis, 637 clusters of protein sequences have been screened out for those that are harbored only by four dioxane metabolizers (i.e., CB1190, PH-06, N23, and BERK-1) but not in the six co-metabolizers. Subsequent annotation showed only 49 genes are relevant to oxidation (Table 4.2). To shorten the candidate list, candidate genes were compared with previous results for screening genes whose transcription was upregulated by dioxane. RNA sequencing (RNA-seq) was employed by He *et al.*[31] to quantify the gene expression fold change during the growth on dioxane relative to glucose in PH-06. Among these genes shown with dioxane upregulation I PH-06, BTO20_RS24595 is the only one found in the candidate list. Further, candidate genes were compared with the results of microarray assays conducted by Sales *et al.* and Grostern *et al.*[55, 57] which surveyed the expression ratio of every single gene induced by dioxane and glycolate relative to growth on pyruvate in CB1190. The gene tagged with Psed_2030 on chromosome was found with 2.2 times induction by dioxane relative to pyruvate. This was the only gene overlapping with candidate genes generated by our comparative genome analysis, though it also induced by the downstream product, glycolate (2.4 time induction). Thus, these two candidate genes are more likely involved in the degradation of HEAA. Cyclohexane is an analog to dioxane, the cyclohexanone monooxygenase participates in the oxidation of cyclohexanone, which is a metabolite of cyclohexane. The cyclohexanone

oxidized by this monooxygenase, which adds a ketone group at the *ortho* location. Thus, this monooxygenase is also a potent candidate.

Table 4.2 The HEAA Degrading Gene Candidates (Continued)

Tag		Description
CB1190	PH-06	
Psed_1410	BTO20_RS12775	4-hydroxyphenylpyruvate dioxygenase
Psed_3175	BTO20_RS33850	alpha/beta hydrolase
Psed_6109	BTO20_RS04180	
Psed_3059	BTO20_RS21400	
Psed_0347	BTO20_RS16920	
Psed_0919		
Psed_2003	BTO20_RS07510	alpha-ketoglutarate-dependent dioxygenase AlkB
Psed_3145	BTO20_RS26460	beta-phosphoglucomutase family hydrolase
Psed_0764	BTO20_RS25720	catechol 1,2-dioxygenase CatA
Psed_3093		
Psed_6065		
Psed_0488	BTO20_RS21890	cyclohexanone monooxygenase
Psed_2233		
Psed_5827		
Psed_0549	BTO20_RS08130	cysteine dioxygenase
Psed_0057	BTO20_RS30275	cytochrome c oxidase assembly protein
Psed_5032		
Psed_2030	BTO20_RS32940	cytochrome P450
Psed_2740	BTO20_RS35755	
Psed_2618	BTO20_RS32300	
Psed_2691		
Psed_5823	BTO20_RS14095	ectoine hydroxylase
Psed_3103	BTO20_RS29675	epoxide hydrolase
Psed_1827	BTO20_RS00490	EthD family reductase
Psed_1828	BTO20_RS32740	FAD-dependent oxidoreductase
Psed_1455	BTO20_RS28730	Glyoxalase
Psed_3315	BTO20_RS31180	
Psed_4204	BTO20_RS13230	
Psed_2367	BTO20_RS26605	iron-containing redox enzyme family protein

Table 4.2 The HEAA Degrading Gene Candidates (Continued)

Tag		Description
CB1190	PH-06	
Psed_4928	BTO20_RS24600	LLM class flavin-dependent oxidoreductase (FMO)
Psed_5838	BTO20_RS34065	
Psed_2056	BTO20_RS05760	
Psed_2622	BTO20_RS12265	
Psed_5837	**BTO20_RS24595**	
Psed_4935	BTO20_RS32215	
Psed_2897	BTO20_RS23965	LysR family transcriptional regulator
Psed_0431	BTO20_RS30790	MBL fold metallo-hydrolase
Psed_3608	BTO20_RS19425	NUDIX domain-containing protein
Psed_1703	BTO20_RS09025	NUDIX hydrolase
Psed_1565	BTO20_RS25650	protocatechuate 3,4-dioxygenase α subunits
Psed_1566	BTO20_RS25655	protocatechuate 3,4-dioxygenase β subunits
Psed_6712	BTO20_RS05975	recombinase family protein
Psed_2573	BTO20_RS35485	SDR family NAD(P)-dependent oxidoreductase
Psed_3999	BTO20_RS08640	
	BTO20_RS10385	
	BTO20_RS24095	
Psed_0988	BTO20_RS14745	VOC family protein
Psed_3302	BTO20_RS09680	

4.3.2 Phylogenetic Analysis of Protein Candidates

Three potential HEAA degrading proteins were screened based on the comparison with transcription data generated by previous studies, as well as the dioxane structure analog degradation pathway analysis. We focused on cyclohexanone monooxygenase (BTO20_RS21890), LLM class flavin-dependent oxidoreductase (BTO20_RS24595 named as FMNH2-dependent monooxygenase in He's paper), and cytochrome P450 (Psed_2030 named as Linalool 8-monooxygenase in Sales's paper) for their potentials in HEAA degradation. Protein sequences with high identities (> 40%) were extracted from all the dioxane degraders to validate their ubiquitous presence and assess their phylogenetic relationships (Figure 4.2).

The phylogentic tree in Figure 4.2A showed LLM class Flavin-dependent oxidoreductases were phylogenetically close in all dioxane metabolizers, though with one found in a dioxane co-metabolizer, BCP1. The four oxidoreductases from the metabolizers exhibited high similarity (> 63%). However, the one harbored by BCP1 is phylogenetically apart from the four harbored by metabolizers with a relatively low identity (55%) to that in CB1190. Thus, it may suggest a distinct physiological role of these enzymes in metabolizers against co-metabolizer. Figure 4.2B showed cytochrome P450 proteins are widely found in both metabolic and co-metabolic degraders. Though three metabolic strains (CB1190, N23, and BERK-1) all harbor cytochrome P450 proteins with high identity (> 88%), the cytochrome P450 protein harbored by PH-06 is distantly related with a low identity of 47% to the one in CB1190. This is also the case for the third enzyme candidate, cyclohexanone monooxygenase (Figure 4.2C). According to these sequence analyses, we postulate LLM class Flavin-dependent oxidoreductases are most likely to be the enzymes that catalyze the HEAA degradation. LLM class Flavin-dependent oxidoreductase is also named as $FMNH_2$-dependent monooxygenase or FMO, representing a common monooxygenase responsible for oxidation of a variety of xenobiotics, such as the sulfonamide degradation in *Microbacterium* sp. strain BR1[234]. Notably, another component of FMO is adjacent to this gene without an interval and was observed in all four metabolizers with high identity. Thus, FMO in metabolizers could be a two-component monooxygenase to exert its physiological function. Research reported that one of them is a NAD(P)H:Flavin oxidoreductase, which provides a reduced flavin to the second component, the proper monooxygenase[235].

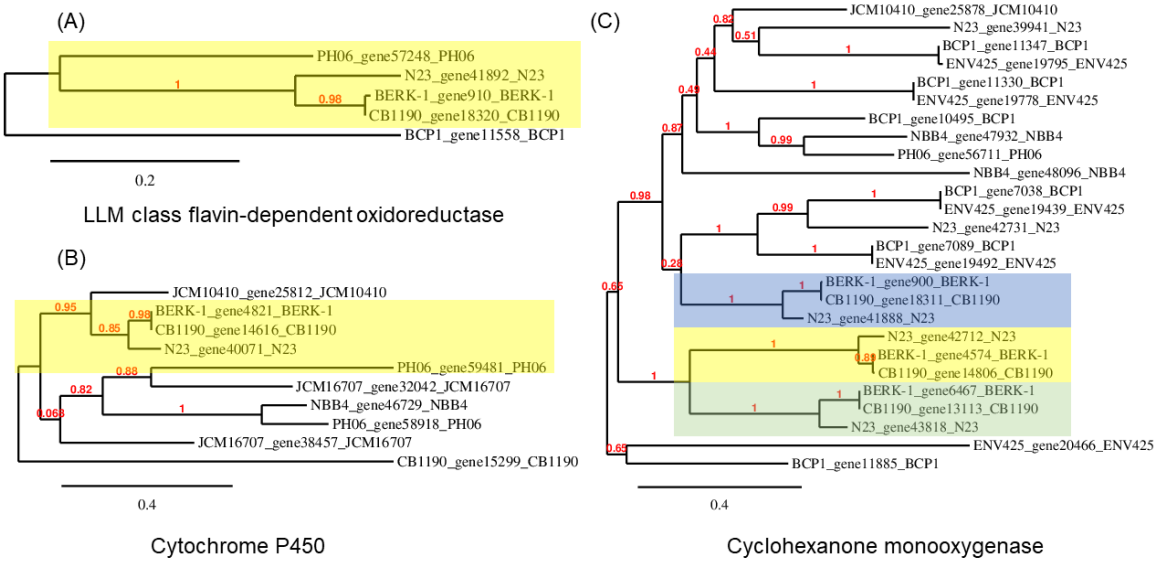

Figure 4.2 Phylogenetic trees of (A) LLM class flavin-dependent oxidoreductases, (B) cytochrome P450, and (C) cyclohexanone monooxygenases in dioxane metabolic and co-metabolic strains.

4.3.3 A Putative FMO Doesn't Have HEAA Degradation Capacity

Heterologous transformation of FMOs from CB1190 and PH-06 to mc^2-155was successful as evident by the overexpression of two FMO components of 47 and 54 kDa in size (Figure 4.3). These transformants were cultured, induced, and harvested as described in Section 2.2.3. Unfortunately, no HEAA degradation was observed in degradation assays with the resting transformants. This may result from several reasons: (1) it indicates that maybe the expressed FMO is not the enzyme in charge of HEAA degradation. (2) or the incorrect fold leading to the abnormal function. To sovle these, we can improve the screening techniques to obtain correct genes. Although we carefully screened the potential HEAA-degrading genes from the list which was acquired from genome comparison, as well as the induced genes from other research, pitfalls are remaining considering the huge gene pools from the dioxane degraders. Transcriptomic analysis of dioxane degraders helps the target gene

screening via comparing the gene abundance with amendment of dioxane or HEAA verses amended with other uninducable substrates, such as succinate, glycolate. Also, some strategies that could result in a correct folded protein may get a protein exerting its function.

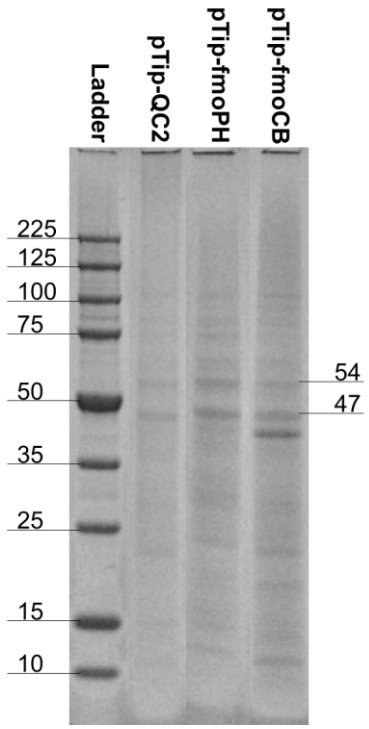

Figure 4.3 SDS-PAGE analysis depicting the increased expression of the FMO proteins in cell extracts from mc^2-155 transformants with pTip-*fmoPH* and pTip-*fmoCB* in comparison with the empty vector (pTip-QC2) control. Band positions indicating two components of FMOs were estimated based on their calculated protein size.

4.3.4 Downstream Genes Involved in Glycolate Transformation Are Essential for Metabolic Biodegradation of Dioxane

Interestingly, a number of genes involved in glycolate transformation were identified in the candidate list, indicating their pivotal role in dioxane mineralization specific for metabolic degraders (Table 4.3). As evident in CB1190, these genes are responsible for generating energy and building blocks for dioxane metabolizers[55]. Glycolate is first oxidized to glyoxylate by GlcF. Glyoxylate is further metabolized through three pathways (Figure 1.3):

(1) glyoxylate is transformed to oxalate, ultimately to carbon dioxide[236] (2) glyoxylate is incorporated with acetyl coenzyme A by malate synthase G and then converted to malate, and (3) two glyoxylate molecules are merged by glyoxylate carboligase, which simultaneously decarboxylates the condensation product to tartronic semialdehyde[237, 238]. Despite the enzyme catalyzing the first pathway remains unknown, enzymes involving the second and third pathways have been identified in metabolic strains, indicating their key roles in dioxane metabolic degradation. Mahendra *et al.*[56] used the isotope-labeled (^{14}C) dioxane to track the mineralization products derived from the degradation of dioxane in CB1190. After 40 h, 40% of 14C was converted to CO_2, and 5% was recovered in CB1190 biomass. Grostern *et al.*[121] carried out isotopomer analysis with ^{13}C-labelled dioxane, results suggest that carbon dioxide and all of the detected amino acids were labeled indicating dioxane was converted to both CO_2 and biomass. They also exploited that CB1190 assimilated carbon partially from atmospheric CO_2 for the generation of amino acids.

Several alcohol and aldehyde dehydrogenases (Figure 4.4), well-known enzymes participating in the secondary step of dioxane biodegradation (Figure 1.3)[239], are present in both metabolizers and co-metabolizers (take group-5 and group-6 SDIMO-containing strains as examples Figure 4.4). It indicates that dioxane is unbiasedly converted to HEAA as a key intermediate products regardless of metabolic or co-metabolic pathways.

Table 4.3 Unique Downstream Genes Involved in Dioxane/HEAA Degradation in Metabolic Degraders

KO No.	EC. No.	Encoded Enzyme	Catalytic Reacion
K11473	1.1.3.15	glycolate oxidase iron-sulfur subunit (*glcF*)	glycolate to glyoxylate
K01608	4.1.1.47	tartronate-semialdehyde synthase (*gcl*)	glyoxylate to tartronate semialdehyde
K00042	1.1.1.60	2-hydroxy-3-oxopropionate reductase	tartronate semialdehyde to D-glycerate
K00865	2.7.1.165	glycerate 2-kinase	D-glycerate to 2-phospho-D-glycerate
K01638	2.3.3.9	malate synthase G	glycolate/Acetyl-CoA to malate
K01816	5.3.1.22	hydroxypyruvate isomerase	hydroxypruvate to tartronate semialdehyde
K00135	1.2.1.16 1.2.1.79	succinate-semialdehyde dehydrogenase / glutarate-semialdehyde dehydrogenase	succinate semialdehyde to succinate
	1.2.1.4	NADP-dependent aldehyde dehydrogenase	adipate semialdehyde to adipate
K01692	4.2.17	enoyl-CoA hydratase	ethene bonds to -OH

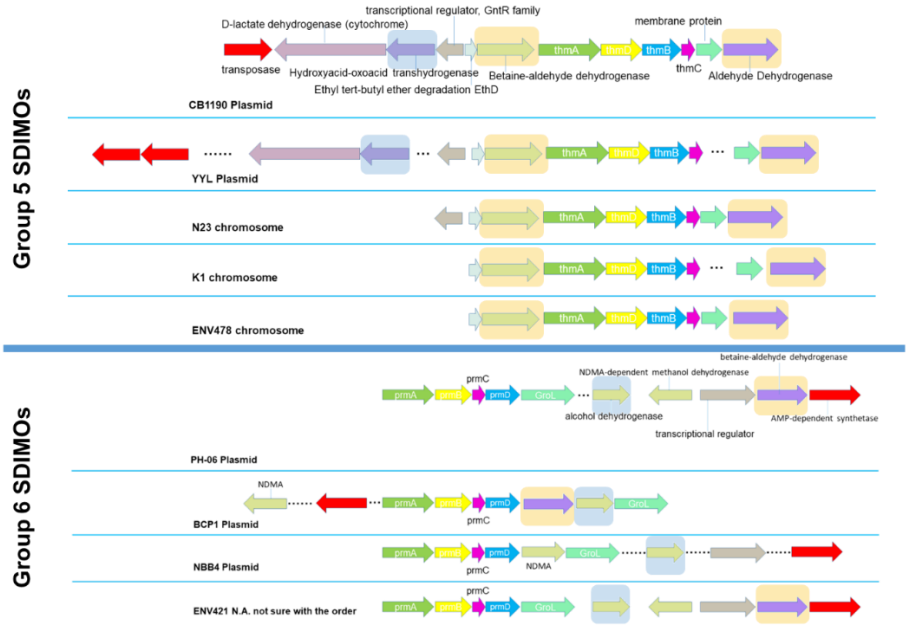

Figure 4.4 Alcohol/aldehyde dehydrogenases involved in dioxane degradation are extensively detected in bacteria that harbor group-5 and 6 SDIMO genes. Alcohol dehydrogenases are shadowed in blue and aldehyde dehydrogenases are shadowed in orange.

4.4 Future Work

Although this study failed for the discovery of the HEAA oxidation gene/enzyme, it provides a feasible strategy for exploiting the novel functions distinct among degradation pathways in phylogenetically related bacteria. In the future, an intricate screening should be conducted by the optimization of the threshold to sort enyzmes of similar functions. Transcriptomic analysis is also recommended as it explicitly points out genes that can be upregulated by HEAA in comparison with downstream intermediates, such as ethylene glycol, glycolate, and other compounds shown in Figure 1.3. Genome sequencing of more dioxane degraders could elevate the availability of genome database, which endows the genome comparison between metabolic and co-metabolic strains a more reliable.

CHAPTER 5

EFFECTIVE REMOVAL OF TRACE LEVELS OF 1,4-DIOXANE BY BIOAUGMENTATION WITH AZOARCUS SP. DD4 AND A PROPANOTROPHIC CONSORTIUM

5.1 Introduction

A growing body of evidence shows monooxygenase-expressing microorganisms such as *Mycobacterium dioxanotrophicus* PH-06, *Pseudonocardia dioxanivorans* CB1190, *Mycobacterium* sp. strain ENV421, *Pseudonocardia* sp. strain ENV478, *Burkholderia cepacia* G4, and *Pseudomonas mendocina* KR1[58, 135, 175, 240-242] are able to degrade dioxane co-metabolically or metabolically. Although the bioaugmentation approach is usually highly efficient in the removal of the target pollutants under laboratory conditions, their performance under natural conditions cannot be predicted because of the complexity of the environmental conditions[79]. Given the severe growth condition of microbes imposed, including more inhibitory substances and the low concentration of available nutrients. The co-metabolic strains involving bioremediation may become prevalent under such fortuitous conditions[80]. A co-metabolic strain *Azoarcus* sp. DD4, the first Gram-negative bacterium, is able to synchronize dioxane oxidation when fueled with propane. It could oxidize dioxane by adding a hydroxyl group to the α-carbon adjacent to oxygen by toluene monooxygenase[37, 229]. Due to the high cell yield and well-distribution, it may likely to degrade low concentration (approximate 100 μg/L) of dioxane to less than New Jersey guidance when feeding with propane.

In the current study, we obtained the influent and effluent water samples from pump-and-treat facility to estimate the DD4 performance in *ex situ* groundwater. Two groundwater samples from near the source zone and middle of the plume were also

collected to evaluate the DD4's feasibility at *in situ* Superfund site. A microcosm assay was set up to evaluate the feasibility of a Gram-negative propanotrophs *Azoarcus* sp. DD4 at authentic Superfund site water samples with low dioxane concentration. To investigate the effects of the co-occurring indigenous or exogenous propanotrophs, propane induced treatment and propane with metabolizers (i.e., CB1190 and PH-06) treatment were conducted in the present study. The molecular microbiology techniques were employed to monitor the survivability and feasibility of DD4 at such groundwater samples and environmental conditions.

5.2 Materials and methods

5.2.1 Sample Collection

Combe Fill South Superfund Site is located at Chester Township, NJ (Figure 5.1). It has been put on the National Priority List (NPL) by USEPA since September 1983 due to the detection of toxic compounds such as benzene, methylene chloride, and chloroform. It is still active for VOCs and dioxane cleanup because of a recent investigation. The ongoing pump-and-treat approach exhibits in Figure 5.2 efficiently remove VOCs to under the NJDEP groundwater quality standards (GWQS) as shown in Table 5.1. Apart from the detected VOCs, many other organic compounds could be efficiently removed by GAC adsorption[243]. The extracted groundwater is pooled together as a composite influent sample (INF). A series of treatments are followed, including equitation, sedimentation, filtration and carbon adsorption to remove recalcitrant VOCs. The effluent (EFF) is discharged after the passage of the effluent monitoring tank. Samples were collected by HDR at this Superfund Site in May 2019 and sent to our laboratory at NJIT with refrigeration on the

same day of the sampling. They were stored at 4 °C in amber glass bottles without headspace prior to the microcosm setup. Four water samples include two groundwater samples from monitoring wells exhibiting typical high- and medium-level dioxane concentrations in the plume at the site (MW1 and MW2 as shown in Figure 5.1), as well as the influent and effluent samples (INF and EFF) from the groundwater extraction and treatment (GWET) facility were collected, aiming to provide potential treatment strategies for *ex situ* or *in situ* bioremediation.

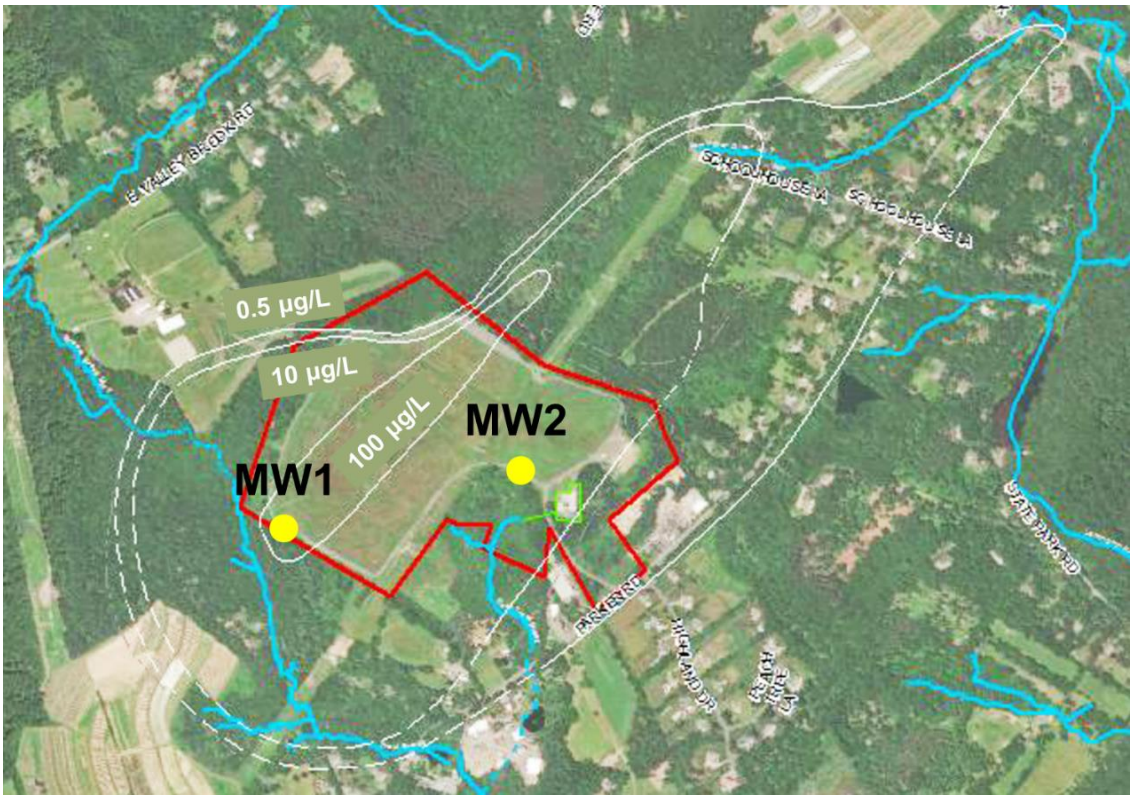

Figure 5.1 The 100, 10, 0.5 µg/L of dioxane isocontours at the Combe Fill South Landfill Superfund site. The two *in situ* sampling points, MW1 and MW2, are indicated as yellow circles.

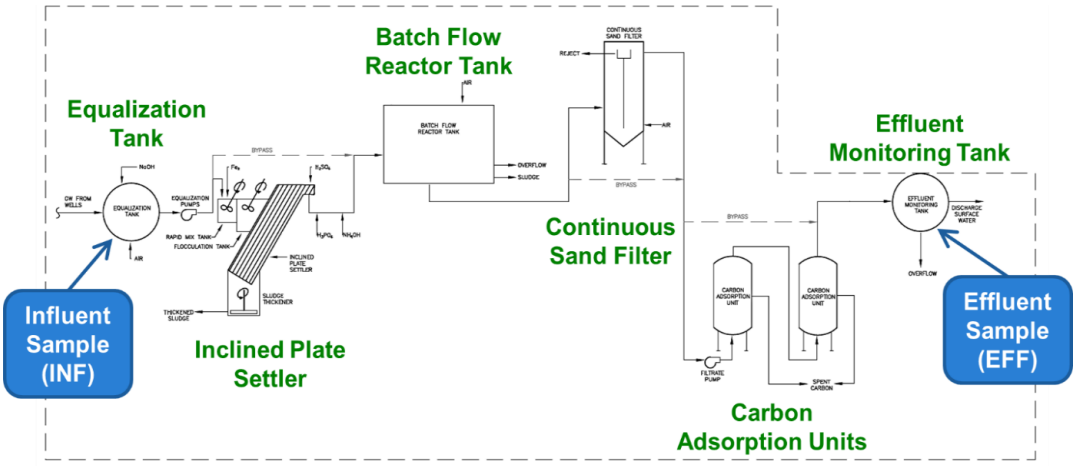

Figure 5.2 The flow chat of groundwater extraction and treatment (GWET) facility.

Table 5.1 Initial Concentrations of VOCs and Metals in Different Groundwater Samples (Continued)

Compounds	Concentration (µg/L)			
	INF	EFF	MW1	MW2
VOCs				
1,1-Dichloroethene	0.13	< 0.50	< 0.50	< 0.5
1,2-Dichlorobenzene	0.40	< 0.50	0.15	0.14
1,2-Dichloroethane	< 0.50	< 0.50	< 0.50	0.5
1,4-Dichlorobenzene	1.2	< 0.50	2.3	0.4
Benzene	0.97	< 0.50	< 0.50	0.64
Chlorobenzene	2.9	< 0.50	0.64	1.5
Chloroform	0.46	0.041	< 0.50	< 0.5
Cis-1,2-Dichloroethylene	1.7	< 0.50	< 0.50	15
Methylene Chloride	0.13	< 0.50	< 0.50	< 0.5
Tert-Butyl Methyl Ether	< 0.50	< 0.50	0.14	0.1
Tetrachloroethylene	0.23	< 0.50	< 0.50	< 0.5
Toluene	< 0.50	< 0.50	< 0.50	0.072
Trans-1,2-Dichloroethene	0.11	< 0.50	< 0.50	0.37
Trichloroethylene	**3.9**	< 0.50	< 0.50	**7.8**
Trichlorofluoromethane	0.59	< 0.50	< 0.50	< 0.5
Vinyl Chloride	0.48	< 0.50	< 0.50	**9.2**
Metals				
Aluminum	34	<20	<20	**330**
Iron	**3100**	<20	**5500**	**40000**
Manganese	**2300**	<1	**1800**	**920**
Magnesium	11000	11000	23000	5600
Sodium	28000	**90000**	**140000**	7800

Table 5.1 Initial Concentrations of VOCs and Metals in Different Groundwater Samples (Continued)

Compounds	Concentration (μg/L)			
	INF	EFF	MW1	MW2
Other				
Dioxane	**34.3±1.1**	**27.4±0.5**	**130.0±3.3**	**83.2±2.3**
TOC	3000	1900	12000	1700

Concentrations that exceed the groundwater quality standards (GWQS) by the New Jersey Department of Environmental Protection (NJDEP) are in bold.

5.2.2 Microcosm Assays

Microcosm assays were conducted in triplicate to discern the rate and extent of dioxane biodegradation occurring in groundwater samples of interest, enabling the assessment of the effectiveness of different bioremediation strategies (e.g., ex situ vs in situ). For each sample, an abiotic control and three biologically active treatments mimicking (1) biostimulation with propane, (2) bioaugmentation with the dioxane co-metabolizer, *Azoarcus* sp. DD4[37], and (3) bioaugmentation with a mixed consortium consisting of two dioxane metabolizers (CB1190[92] and PH-06[244]) and one co-metabolizer (DD4) were conducted as shown in Table 5.2.

Table 5.2 Microcosm Setup

Treatment	**Control**	**Propane**	**DD4+propane**	**Mix+propane**
Propane (0.15 % v/v in headspace)		√	√	√
Groundwater (60 mL in 160 mL serum bottle)	√	√	√	√
DD4 (0.17 mg as total protein)			√	
Mixture of DD4, PH-06, and CB1190 (0.17 mg as total protein)				√

All microcosms were prepared in 160-mL serum bottles sealed with rubber caps. DD4 was cultured in nitrate mineral salt (NMS) media with propane as the growth substrate and harvested at the exponential growth phase. CB1190 and PH-06 grown on 100 mg/L of dioxane in ammonium mineral salts (AMS) media. Cultures were harvested at their exponential growth phases, washed for three times, and resuspended to OD_{600nm} of 2.0 with fresh AMS medium. For the DD4 bioaugmentation microcosms, 0.5 mL of the harvested cells were inoculated to achieve an initial total protein of 0.17 mg per vial. For the mixed inoculum, the seeding mixture was composed of DD4, CB1190, PH-06 with the biomass ratio of 2:1:1. Propane (0.15 % v/v) was amended to all active treatments to supplement carbon and energy. Microcosms were incubated at room temperature (i.e., 24±3 °C) while being shaken at 150 rpm. At selected intervals, liquid and headspace samples were collected for the analysis of dioxane and propane, respectively. Propane was re-amended once when over 95% of the initial propane was consumed.

5.2.3 Quantitative Polymerase Chain Reaction (qPCR)

Total DNA from the original field samples and samples collected after the completion of all microcosm treatments was extracted using the PowerSoil® DNA Isolation Kit (Qiagen, Hilden, Germany) following the manufacturer's instruction. The amount of the toluene monooxygenase gene (*tmoA*) in DD4, the propane monooxygenase gene (*prmA*) in PH-06, and the tetrahydrofuran monooxygenase gene (*thmA*) in CB1190 were quantified by qPCR using designed probe/primers specifically targeting their α subunit components (Table 5.3). A set of generic 16S rRNA primers (341F and 534R) was used to enumerate the total biomass[245]. Each qPCR reaction (20 μL) consisted of 0.1 μL of paired primers (10 μmol/L), 1 μL of 5 ng/μL of the DNA extract, and 10 μL of Power SYBR® Green or TaqMan®

Mastermix (Thermo, Carlsbad, CA). qPCR was run with the Quant Studio3 (Thermo, Carlsbad, CA) following the temperature program: initially held at 10 min for 95 °C, followed by 40 cycles of 15 s at 95 °C and 1 min at 60 °C. The relative abundance of each inoculated strain was calculated as the percentage ratio of the specific dioxane degrading gene number to the total cell number, which is equivalent to the 16S rRNA gene number divided by 4.2 (i.e., average 16S rRNA gene copies per bacterial cell)[246].

Table 5.3 Sequences of Primers and Probes used for qPCR

Target Gene	Primer Name	Sequence (5'-3')	Reference
16S rRNA	341F 534R 806R	CCTACGGGAGGCAGCAG ATTACCGCGGCTGCTGG GGACTACNNGGGTATCTAAT	245
tmoA	*tmoA*_F *tmoA*_R *tmoA*_probe	GGCGGATGGCTGTACTCAACAGAATG AAATCGCCGGAAAGCTTGGGC /FAM/CGACCTGGC/ZEN/CAGGAGTACG AAC/IABkFQ/	229
prmA	*prmA*_F *prmA*_R *prmA*_probe	ACTGCGATGCTGGTTGAC TCAGGTACGCCTCCTGAT /FAM/TTCCTCGCG/ZEN/CAGATGATCGA CG/IABkFQ/	35
thmA	*thmA*_F *thmA*_R *thmA*_probe	CTGTATGGGCATGCTTGT CCAGCGATACAGGTTCATC /FAM/ACGCCTATT/ZEN/ACATCCAGCTC GA/IABkFQ/	30

5.2.4 Microbial Community Analysis

16S rRNA amplicon sequencing was employed to unveil the microbial communities in original and biotreated water samples. Bacterial V3-V4 hypervariable regions of 16S rRNA were amplified by PCR with the primers 341F (5'-CCTAYGGGRBGCASCAG-3') and 806R (5'-GGACTACNNGGGTATCTAAT-3')[247] following the standard MetaVx™ library preparation process. PCR products were examined by gel electrophoresis on 2 %

agarose gel and recovered using the GeneJET^{TM} Gel Extraction Kit (Thermo, Carlsbad, CA). A second round PCR was run for limited cycles for the addition of sample-specific barcodes for multiplexing. Final libraries were pooled together with concentrations quantified by the Qubit® 2.0 Fluorometer (Thermo, Carlsbad, CA). Paired-end sequencing (2×250 bp) was performed using Illumina MiSeq (Illumina, San Diego, CA) at GENEWIZ (South Plainfield, NJ, USA). The raw sequencing data were filtered and analyzed using the Cutadapt (v1.9.1)[248], Vsearch (1.9.6)[249], Qiime (1.9.1)[250]. The sequences after removing the chimera sequences and > 200 bp in length were clustered when sequences' similarity is higher than 97%. Further, representative OTUs were assigned taxonomy based on the > 99% identity using the Ribosomal Database Project (RDP) Classifier[251]. Hierarchical clustering was carried out with *hclust* of stats package in R[252]. the dendrogram to the left is the species cluster and the dendrogram at the top of Figure 5.5 shows clusters of community structures[253].

5.2.5 Analytical Approaches

Low concentration (<1000 μg/L) of dioxane was detected by GC/MS by microfrozen extraction method as described in Section 2.2.10. Propane in headspace was monitored by GC/FID as described in 2.2.10. Concentrations of co-occurring volatilized organic compounds (VOCs) in original water samples were measured at an external commercial lab using the EPA Method 8260C[254]. This is a standard method for quantifying a wide span of VOCs in aqueous samples using purge-and-trap gas chromatography/mass spectrometry (GC/MS).

5.3 Results

5.3.1 Dioxane Degradation and Propane Utilization in Microcosms

Dioxane was detected in INF with an initial concentration of 34.3±1.1 μg/L. Due to the high hydrophilicity of dioxane, it was marginally adsorbed by adsorption units. Dioxane, thus, yet remains 27.4±0.4 μg/L in the effluent of the GWET facility. Bioaugmentation with DD4 can effectively reduce trace dioxane contamination in both INF and EFF samples collected at the GWET facility. In microcosms prepared with the INF sample (Figure 5.3A), dioxane was degraded to 2.5±0.5 μg/L in 3 days, and subsequently to below the method detection limit (MDL, i.e., 0.38 μg/L) within 6 days of incubation. Fast dioxane degradation by DD4 was also observed in the microcosms prepared with the EFF sample (Figure 5.3B). Dioxane was degraded from 27.4±0.5 μg/L to 0.5±0.1 μg/L within 3 days of incubation. Eventually, dioxane concentration was then below our MDL on day 6. At the same time, in both INF-DD4 and EFF-DD4 microcosms, over 300 μL of pure propane was consumed within 6 days (Figure 5.4A and 5.4B). In the microcosm prepared with MW1 field water, dioxane was effectively removed from 130.0±3.3 μg/L to below the MDL within 6 days (Figure 5.3C). Whilst slow dioxane removal was observed in the DD4-bioaugmentation microcosms prepared with MW2 samples (Figure 5.3D), in which dioxane was degraded less than 30% of the initial dioxane concentration (83.2±2.3 μg/L) within 30 days of incubation, leaving a residual concentration of 59.7±2.4 μg/L. The quick propane depletion was observed in MW1 as in INF and EFF (Figure 5.4). Propane consumption in MW2 was greatly decelerated in contrast with the other three types of water. The initially amended propane was not fully consumed until Day 30 (Figure 5.4D).

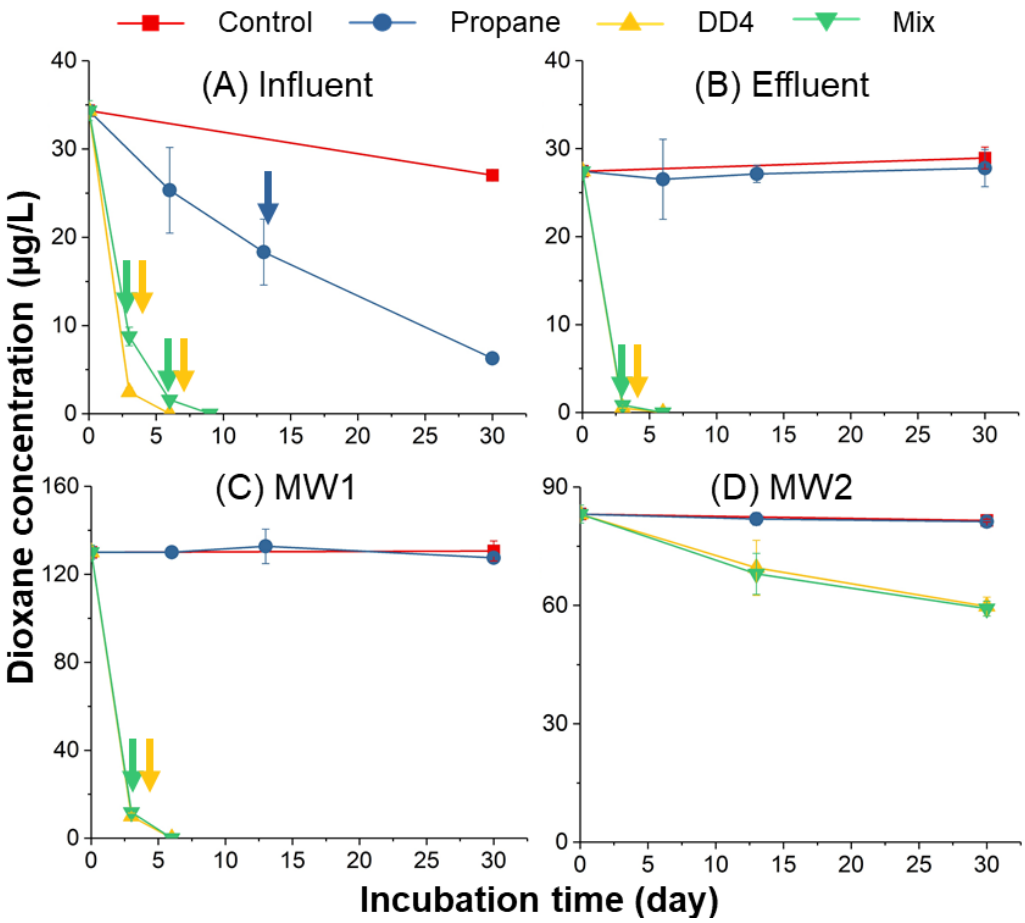

Figure 5.3 Dioxane degradation in microcosms treated with propane, DD4, and propanotrophic consortium in comparison with the abiotic control. Microcosms were prepared with varying groundwater samples, including (A) the influent and (B) effluent of the GWET facility and two monitoring wells (C) MW1 and (D) MW2. Arrows indicate repeated propane amendments when over 90% of propane was consumed. The colors of the arrows are corresponding to the treatment as indicated in the legend.

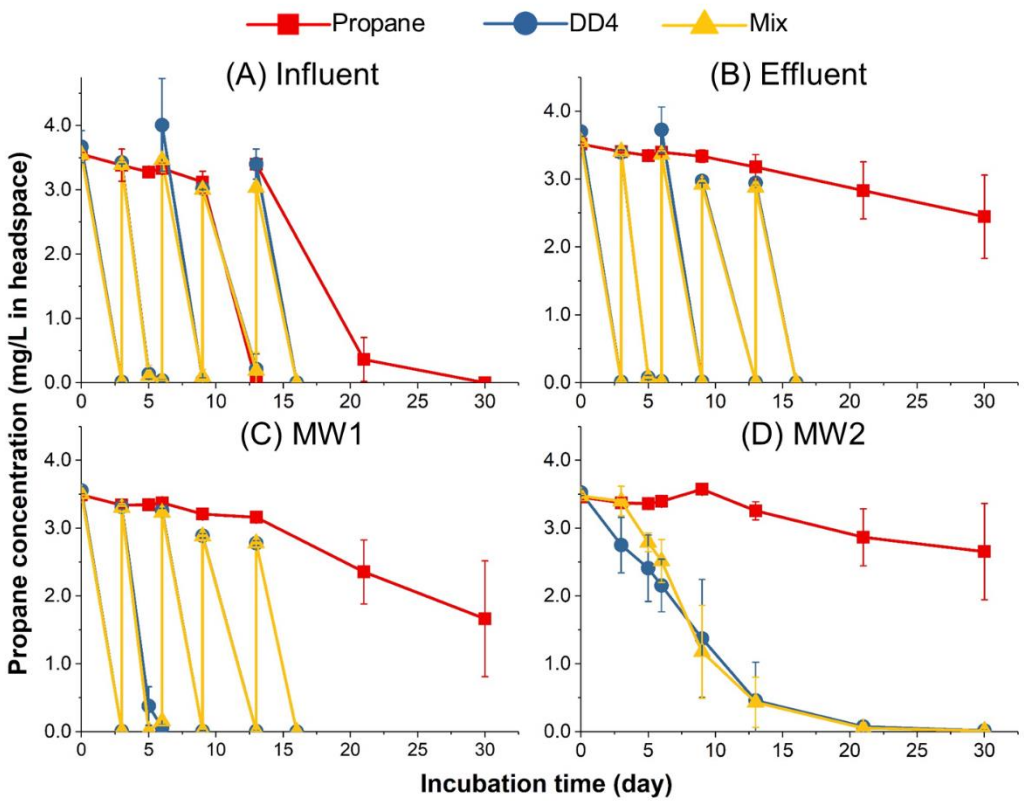

Figure 5.4 Propane consumption in microcosms prepared by (A) Influent, (B) Effluent, (C) MW1, and (D) MW2.

In microcosm degradation assays, the mixed inoculum does not have a significant difference with the corresponding microcosm bioaugmented with single DD4 inoculum in four types of field groundwater samples (Figure 5.3). Dioxane in INF-Mix was degraded from 34.34±1.13 μg/L to 1.59±0.35 μg/L in 6 days and depleted in 9 days; in EFF-Mix dioxane was degraded from 27.42±0.45 μg/L to 0.85±0.10 μg/L in 3 days and completely degraded in 6 days; in MW1-Mix dioxane was degraded from 130.04±3.31 μg/L to 11.77±0.91 μg/L in 3 days and disappeared in 6 days; in MW2-Mix dioxane remained 59.20±1.87 μg/L after 30-days incubation. Propane consumption in mixed inoculum treatment is similar to the single DD4 treatment in all four types of water (Figure 5.4).

Interestingly, in the treatment prepared with INF water samples, without the amendment of exogenous cultures, significant dioxane removal was observed in comparison with the abiotic control. On day 30, dioxane concentration dropped from 34.34±1.13 μg/L to 6.3 ± 0.6 μg/L in the INF-propane treatment, while it remained as high as 27.0 ± 0.6 μg/L in INF-control microcosms (Figure 5.3A). At the same time, propane trends to degrade after 9 days in four types of water, particularly in INF-Propane sample. Over 300 μL of pure propane was consumed (Figure 5.4A) in INF-Propane. Within 30 days, propane was degraded from 3.5±0.0 mg/L to 2.4±0.6 mg/L, 1.7±0.9 mg/L, 2.71±0.7 in EFF-Propane, MW1-Propane, and MW2-Propane, respectively. However, dioxane degradation has not been observed yet within 30 days.

5.3.2 Community Structure Analysis by 16S rRNA Sequencing

Community structure analysis shows that *Azoarcus* is the most abundant genus in DD4 and mixed culture inoculum prepared with INF, EFF, and MW1 (Figure 5.5). Based on the sequences similarity, the representative OTU accommodated in *Azoarcus* genus (i.e., OTU 1) share nearly 100% identity to *Azoarcus sp.* DD4. Thus, according to the 16S rRNA sequencing results, DD4 exhibits as the most abundant strains accounting for 39.6%, 38.3%, 51.4%, 52.4%, 32.9%, 34.9% in INF-DD4, INF-Mix, EFF-DD4, EFF-Mix, MW1-DD4, MW1-Mix (Table 5.4) which agree with the high dioxane degradation in these treatments. DD4 is relatively low in treatment prepared with MW2 with DD4 (3.7%) and mixed culture (3.1%) comparing with the other three types of water. However, it still arises as one of the most abundant ten genera in MW2-DD4 and MW2-Mix.

Table 5.4 The Relative Abundances of the Top 10 Most Abundant Genera in Various Field Samples (Continued)

in situ field sample							
INF							
Taxonomy	INF	Taxonomy	INF-Propane	Taxonomy	INF-DD4	Taxonomy	INF-Mix
Novosphingobium	22.6%	*Rhizobacter*	32.6%	***Azoarcus***	39.6%	***Azoarcus***	38.3%
Nitrosomonas	9.2%	*Sulfuritalea*	17.9%	***Rhodococcus***	9.7%	***Pseudoxanthomonas***	4.5%
Bradyrhizobium	5.2%	*unidentified_Hyphomonadaceae*	4.1%	***unidentified_Hyphomonadaceae***	4.8%	***Rhodococcus***	4.1%
Sphingobium	2.8%	*Coxiella*	3.7%	***Pseudoxanthomonas***	3.6%	***Legionella***	3.5%
Maritimimonas	2.7%	*Reyranella*	2.9%	***Hirschia***	1.9%	***unidentified_Hyphomonadaceae***	3.3%
Methylotenera	2.3%	*Hirschia*	1.9%	*Bryobacter*	1.1%	***Hirschia***	2.8%
Sulfuritalea	2.0%	*Sediminibacterium*	1.1%	***Legionella***	1.0%	*Coxiella*	1.8%
Sediminibacterium	1.6%	*Legionella*	1.0%	*Reyranella*	1.0%	*Reyranella*	1.1%
Parablastomonas	1.1%	*Bryobacter*	1.0%	*Nordella*	0.6%	*Sediminibacterium*	0.6%
Legionella	0.8%	*Hyphomicrobium*	0.8%	*unidentified_Alphaproteobacteria*	0.5%	*Bradyrhizobium*	0.5%
Others	50.7%	Others	33.6%	Others	36.7%	Others	40.0%
EFF							
Taxonomy	EFF	Taxonomy	EFF-Propane	Taxonomy	EFF-DD4	Taxonomy	EFF-Mix
		Polaromonas	33.3%	***Azoarcus***	51.4%	***Azoarcus***	52.4%
		Limnobacter	21.6%	***Zoogloea***	17.7%	***Zoogloea***	5.5%
		Hyphomicrobium	10.1%	***Pseudoxanthomonas***	4.2%	***Pseudoxanthomonas***	4.0%
		Sediminibacterium	7.1%	***Terrimonas***	2.6%	***Ferribacterium***	2.1%
		Ferribacterium	2.2%	***Ferribacterium***	1.9%	*Flavobacterium*	2.1%
		Limnohabitans	2.1%	*Cupriavidus*	1.7%	*Bradyrhizobium*	1.8%
		Reyranella	1.7%	***unidentified_Nitrospiraceae***	1.4%	***Terrimonas***	1.3%

Table 5.4 The Relative Abundances of the Top 10 Most Abundant Genera in Various Field Samples (Continued)

in situ field sample							
EFF							
Taxonomy	EFF	Taxonomy	EFF-Propane	Taxonomy	EFF-DD4	Taxonomy	EFF-Mix
		Curvibacter	1.1%	*Flavobacterium*	1.4%	***unidentified_Nitrospiraceae***	1.3%
		Zoogloea	0.3%	*Terrimicrobium*	0.9%	*Cupriavidus*	1.1%
		Brevundimonas	0.3%	*Brevundimonas*	0.8%	*Sediminibacterium*	1.1%
		Others	20.4%	Others	16.9%	Others	28.4%
ex situ field sample							
MW1							
Taxonomy	MW1	Taxonomy	MW1-Propane	Taxonomy	MW1-DD4	Taxonomy	MW1-Mix
Amphiplicatus	11.2%	*Hyphomicrobium*	8.8%	***Azoarcus***	32.9%	***Azoarcus***	34.9%
unidentified_Gammaproteobacteria	4.0%	*Sulfuritalea*	8.8%	***Nitrosomonas***	2.8%	***unidentified_Cyanobacteria***	2.9%
unidentified_Acidimicrobiia	3.3%	*Amphiplicatus*	7.7%	***unidentified_Cyanobacteria***	2.4%	***Amphiplicatus***	2.5%
unidentified_Nitrospiraceae	3.2%	*Mycobacterium*	7.3%	***Amphiplicatus***	1.8%	***Rhodococcus***	2.3%
Nitrosomonas	2.7%	*unidentified_Acidimicrobiia*	3.7%	***Rhodococcus***	1.7%	***Pseudoxanthomonas***	1.9%
Hydrogenophaga	2.3%	*Pseudomonas*	3.0%	*Cupriavidus*	1.7%	***Bryobacter***	1.5%
Bryobacter	1.4%	*Limnobacter*	2.9%	***Bryobacter***	1.6%	***unidentified_Acidobacteria***	1.2%
Sulfuritalea	1.3%	*Reyranella*	2.6%	***Pseudoxanthomonas***	1.3%	*Reyranella*	0.7%
Reyranella	1.2%	*unidentified_Gammaproteobacteria*	1.9%	***unidentified_Acidobacteria***	1.2%	*unidentified_Acidimicrobiia*	0.6%
Hyphomicrobium	1.0%	*Hydrogenophaga*	1.3%	*unidentified_Alphaproteobacteria*	0.8%	***Nitrosomonas***	0.6%
Others	69.4%	Others	53.3%	Others	52.8%	Others	51.4%

Table 5.4 The Relative Abundances of the Top 10 Most Abundant Genera in Various Field Samples (Continued)

ex situ field sample							
MW2							
Taxonomy	MW2	Taxonomy	MW2-Propane	Taxonomy	MW2-DD4	Taxonomy	MW2-Mix
unidentified_Nitrospiraceae	5.1%	*Caulobacter*	11.6%	***Rhodococcus***	13.6%	***Rhodococcus***	13.2%
unidentified_Hyphomonadaceae	4.6%	*Azotobacter*	11.5%	***Cupriavidus***	5.0%	***Azotobacter***	6.9%
Reyranella	4.6%	*Legionella*	7.1%	***Pseudoxanthomonas***	3.7%	*Legionella*	4.6%
Acetobacterium	2.1%	*Sediminibacterium*	3.9%	***Azoarcus***	3.7%	*unidentified_Hyphomonadaceae*	3.7%
Bradyrhizobium	2.0%	*Haliscomenobacter*	3.1%	*Terrimicrobium*	3.0%	***Hirschia***	3.7%
Paludibaculum	1.3%	*Roseimicrobium*	3.1%	***Hirschia***	2.1%	***Azoarcus***	3.1%
Legionella	1.3%	*Reyranella*	3.0%	*Haliscomenobacter*	2.0%	*unidentified_Gemmatimonadaceae*	2.8%
Haliscomenobacter	0.9%	*unidentified_Hyphomonadaceae*	2.9%	*Sphingopyxis*	2.0%	***Pseudoxanthomonas***	2.7%
unidentified_Gammaproteobacteria	0.8%	*Lacunisphaera*	2.8%	*Reyranella*	1.6%	***Cupriavidus***	1.5%
Polynucleobacter	0.8%	*Terrimonas*	1.9%	***Azotobacter***	1.5%	*Pajaroellobacter*	1.4%
Others	77.3%	Others	50.9%	Others	63.3%	Others	57.9%

The total DNA extracted from EFF sample was insufficient for sequencing.

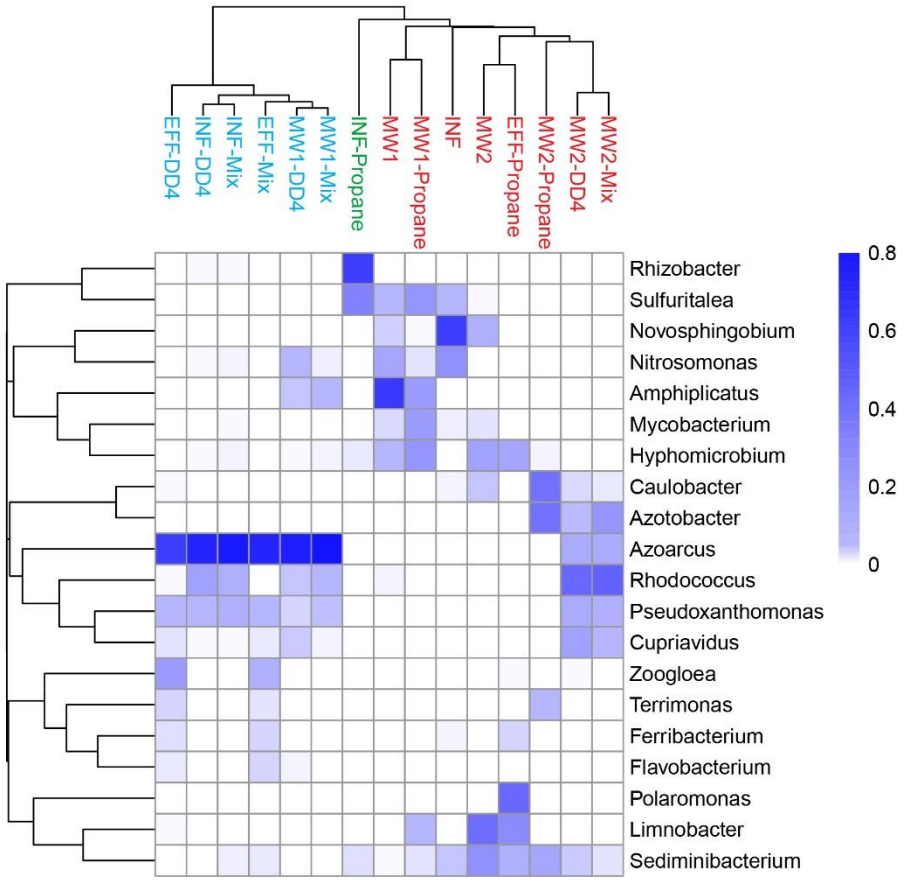

Figure 5.5 Dendrogram depicting the microbial community distribution at the genus level. The columns represent groundwater microcosm treatments and the rows represent genera. Color in the heat map is scaled in accordance with the relative sequence abundance of a specific genus. Treatments that showed complete dioxane removal are highlighted in blue. Treatments with no observable dioxane degradation are highlighted in red. Dioxane in INF-propane (marked in green) was partially degraded by indigenous microorganisms.

Interestingly, *Pesudocardia* genus is absent in all treatments indicating the vanishing of CB1190. While a potential propane and dioxane degrading genus, *Rhodococcus*, was co-occurring with *Azoarcus* in the most abundant 10 genera in treatments prepared with INF, MW1, and MW2 groundwater when augmented DD4 or mixed culture, particularly in MW2. However, *Rhodococcus* was barely detected in the original water samples from INF and MW1, as well as the treatments with propane amendment. Two OTUs (i.e., OTU 5 and 187) accommodated in *Rhodococcus* were

classified into two sub-branch (Figure 5.6). OTU 187 is phylogenetically close to a dioxane degrader *Rhodococcus aetherivorans* 10bc312 (10bc312=JCM 14343=DSMZ 44752)[255] and a propane-utilizing bacteria *Rhodococcus aetherivorans* TPA[256]. It should be emphasized that OTU 187 tends to correlate with *prmA* (Figure 5.6). However, it only occupied 0.05%, 0.02%, and 0.77% of the total microbial communities in INF-Mix, EFF-Mix, and MW1-Mix. While the other representative OTU (i.e., OTU 5) is abundant in INF-DD4 (9.7%), INF-Mix (4.0%), MW1-DD4 (1.7%), MW1-Mix (1.5%), MW2-DD4 (13.6%), and MW2-Mix (13.2%). It was also detected in EFF-DD4 (0.5%), EFF-Mix (0.1%), MW1 (0.2%), and MW1-Propane (0.1%). Both representative OTUs appeared not related to dioxane degradation, but significantly correlated with OTU 1 which represents DD4.

Another potential propane and dioxane degrading genus, *Mycobacterium*, accounts for 0.5% of total biomass in both INF and MW1. It was detected at the range of 0.1% to 0.3% in the control and biological treatments prepared with INF. To be noted, the abundance of *Mycobacterium* is high in MW1-Propane, which occupied 7.3% of the total community. The representative taxa, OTU 52, shares 97.3% sequence identity with PH-06, and has 100% similarity with a *smmo* containing strain NBB3[106, 257] and 99.1% with a dioxane degrading strain JOB5[258-260] indicating it likely to be a propanotrophic *Mycobacterium* (Figure 5.6).

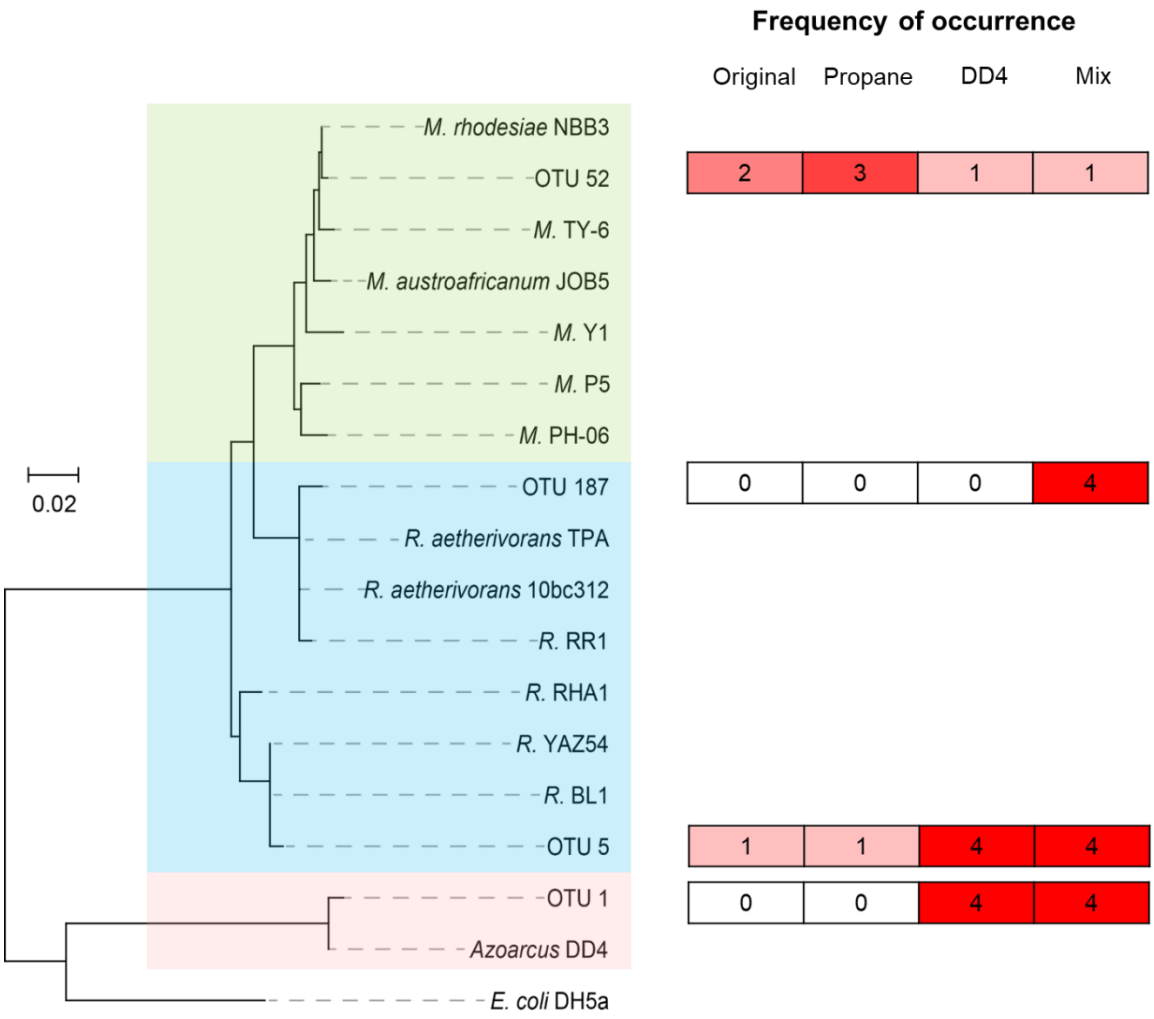

Figure 5.6 Neighbor-joining phylogenetic trees including representative OTUs annotated as *Mycobacterium* (shaded by blue), *Rhodococcus* (shaded by green), and *Azoarcus* (shaded by red), and some known propanotrophs. Phylogeny is calculated in accordance with the V3-V4 region of 16S rRNA sequences. *E. coli* DH5a and some known propanotrophic strains are included as references. The numbers in the right table indicate the occurrence frequency of representative OTUs in four types of water. The first column indicates the occurrences in original water (maximum is 3 because of the missing EFF sample), the second column represents the occurrences after propane inducement. The last two columns indicate the treatments with DD4 and mixed culture augmentations.

5.3.3 *TmoA*, *PrmA*, and *ThmA* Abundances in Microcosms by qPCR Analysis

According to the qPCR analysis, it is plausible to see *tmoA* is found neither in original water samples (i.e., INF, MW1, and MW2) nor propane amended treatments (i.e., INF-

Propane, EFF-Propane, MW1-Propane, and MW2-Propane) (Figure 5.7). It is abundant in the DD4-bioaugmentation microcosms prepared with INF, EFF, and MW1, which occupied 29.9%, 28.6%, and 35.4% of the total microbes. In contrast, *tmoA* only accounts for 2.2% in MW2-DD4 which is in line with the low dioxane degradation and propane utilization rate. The abundances of *tmoA* in mixed treatments prepared by INF, EFF, MW1, and MW2 are comparable with those in DD4 single inoculum bioaugmentation, which are 30.7%, 37.9%, 37.1%, and 4.7%, respectively. These results well agree with 16S rRNA sequencing results that Azoarcus was absent in oringial and propane treated samples, while abundant in DD4 and mixed culture treated samples (Figure 5.5 and 5.6).

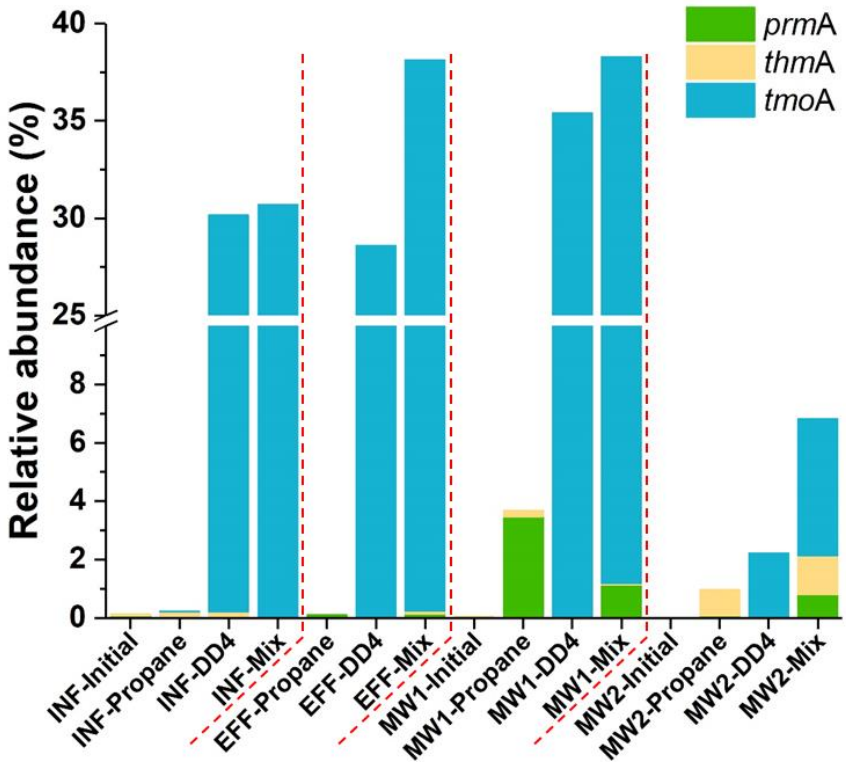

Figure 5.7 The relative abundance of *tmoA*, *prmA*, and *thmA* by qPCR to target the toluene monooxygenase in DD4, propane monooxygenase in PH-06, and tetrahydrofuran monooxygenase in CB1190. All types of gene clusters are normalized by the total bacteria equivalent to the total 16S rRNA gene copies divided by 4.2 according to the qPCR detection.

The gene clusters of *prm* and *thm* were detected by qPCR with specific probe/primers targeting the α oxygenase which is unique and conserved to each gene cluster [96]. The experiment was designed for evaluating the abundance of PH-06, CB1190 in the mixed culture treatments. However, the genes were surprisingly found not only in mixed treatments, indicating the wide presence of these genes in the environment. *prmA* was absent in most natural water samples except in INF (0.1%). With propane amendment, *prmA* was detectable in EFF-Propane (0.1%), MW1-Propane (3.5%), and MW2-Propane (0.1%). However, *prmA* was not detected in the treatments with single DD4 bioaugment because DD4 became the dominant and occupied most of the communities. In the treatments amended with mixed cutlture, the abundance of *prmA* is surprisingly low comparing with the initial inoculation ratio to DD4 (i.e., DD4:PH-06 was 2:1), it is undetectable in INF-Mix, 0.1% in EFF-Mix, 1.1% in MW1-Mix, and 0.8% in MW2-Mix, this may also result from the competition from DD4.

thmA was only barely detected in the microcosm prepared with INF (0.03%) and MW1 (0.05%) suggesting the abundance of *thm* gene cluster is low in natural water without enrichment. With propane amendment, *thmA* abundances elevated to 0.2%, 0.2%, and 0.9% in INF-Propane, MW1-Propane, and MW2-Propane. Like *prmA*, the *thmA* abundances in the treatments with DD4 augmentation are relatively low: 0.2% in INF-DD4, 0.1% in MW2-DD4, it was undetected in EFF-DD4 and MW1-DD4. The abundances of *thmA* in the microcosms treated with mixed culture are not high either, it is absent in INF-Mix, 0.1% in EFF-Mix, 0.1% in MW1-Mix, and 1.3% in MW2-Mix.

5.4 Discussion

5.4.1. *Azoarcus* sp. DD4 Bioaugmentation Is Effective for Dioxane Removal at ex situ and in situ Superfund Site Samples

Results show that dioxane was completely degraded within 6 days in the microcosms prepared with INF, EFF, and MW1 when amended with DD4 and propane. It reveals that DD4 could exert its degradation capability in *ex situ* field samples (i.e., INF and EFF) as well as some specific *in situ* field samples (i.e., MW1), depending on the adaptability to chemical composition and indigenous bacterial community[79]. The field characterization shows the presence of VOCs and metals (Table 5.1). To be noted that some VOCs exceed the standard such as trichlorethlyene and vinyl chloride, it is nevertheless at μg/L level. Although VOCs are reported as important inhibitors for dioxane degradation[38, 62, 65], due to the low concentrations, they may finitely contribute to incomplete degradation in MW2. Some metals such as aluminum, iron and other uncharacterized chemicals existing in MW2 likely involve in inhibition of dioxane-degrading bacteria such as DD4. Furthermore, the community diversity indicated by Shannon Index shows MW2 initially has the highest value (6.00) among all the samples. It decreases to 5.55 after DD4 augmentation indicating bacterial diversity slightly decreased but communities remain highly diverse in comparison with other type of water (Table 5.5). On the contrary, EFF water exhibits the lowest diversity of bacterial community, which is 3.50 for EFF-DD4 suggesting the simplest bacterial community. A similar trend is observed by Simpson Index. There is a consensus that microbial diversity is directly related to ecosystem stability, the high diversity promotes community stability and functional resilience with external perturbation[261]. Thus, the exogenous inoculum DD4 is easy to grow in the water has low diversity (i.e., EFF) than

the high diversity (i.e., MW2). Further, the simple community structure in EFF enabled DD4 becoming the most predominant strain.

Table 5.5 The Community Diversity Analysis Including Shannon and Simpson Index

Sample	Shannon	Simpson
INF	4.81	0.93
INF-Propane	4.13	0.86
INF-DD4	4.17	0.85
INF-Mix	4.53	0.87
EFF-Propane	3.37	0.82
EFF-DD4	3.50	0.76
EFF-Mix	3.79	0.78
MW1	5.72	0.96
MW1-Propane	5.69	0.96
MW1-DD4	4.84	0.90
MW1-Mix	4.83	0.89
MW2	6.00	0.97
MW2-Propane	5.77	0.96
MW2-DD4	5.55	0.95
MW2-Mix	5.49	0.95

16S rRNA sequencing and qPCR analysis independently verified that DD4 is abundant strain after the inoculation. These results well support the dioxane degradation observed in the microcosms, confirming the significant role of DD4 in dioxane biodegradation. It also suggests the adaptability and compatibility of DD4 in these dioxane-impacted water samples. Therefore, single DD4 culture would be effective in treating dioxane in either influent or effluent samples as an addendum to the GAC adsorption system being operated at the site. This straightforward additional strategy renders pump-and-treat technologies economically feasible at many sites for VOCs and dioxane remediation. In addition, DD4 bioaugmentation with propane supplying could degrade the

low concentration of dioxane at some specific *in situ* sites. However, due to the specificity and complexity of *in situ* conditions, feasibility tests are needed for different cases.

5.4.2 Exogenous Metabolizers Vanished but Dioxane-Degrading Gene Clusters Retained in the Communities

With the addition of other two dioxane metabolizers (i.e., PH-06 and CB1190), dioxane degradation did not significantly improve indicating the exogenous metabolizers barely attribute to the degradation. From the genus level, the treatments with or without exegous metabolizers have at least 6 out of 10 are the same genera (bolded in Table 5.4) suggesting the addition of metabolizers has minor change to the main frame of bacterial communities. The similar community structure in two biological treatments (bioaugmentated with DD4 or mixed culture) also embodies in the close cluster distance in Figure 5.8 and Figure 5.5 by the community similarity analysis. DD4 in both treatments appear as the dominant strain owning a comparable abundance. This scenario suggests that DD4 outcompeted these two exogenous dioxane metabolizers. A primary reason is because of DD4 as a co-metabolizer exhibits a faster growth rate (1.95±0.01 day^{-1}) on propane[37] than CB1190 (0.74±0.06 day^{-1}) on dioxane[69]. The growth rate of PH-06 on dioxane is estimated at approximately 0.35 day^{-1} from its growth curve[58], which is comparable with CB1190 (0.74±0.06 day^{-1}) meanwhile lower than DD4 growth rate (1.95±0.01 day^{-1}). Such limit growth rate of metabolizers scants contribution to dioxane degradation when together with co-metabolizer, DD4. There are also some hindrances of metabolic dioxane degraders with their applications. Due to the insufficient energy source in groundwater, propane supposes to be supplied as an auxiliary substrate for dioxane degraders. However, propane is preferentially utilized over dioxane in metabolic strains[69].

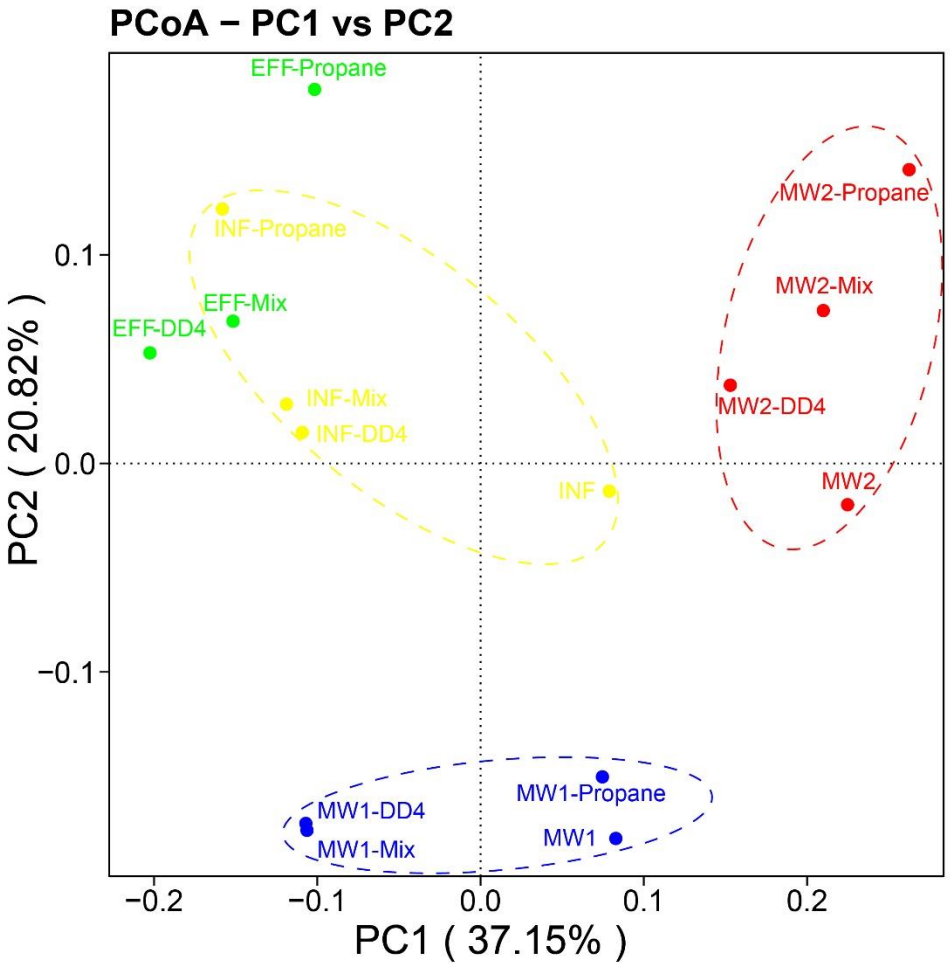

Figure 5.8 The principal coordinates analysis (PCoA) biplot shows weighted-UniFrac based on distances quantitative (i.e., phylogeny) measures of microbial community. PC1, PC2, represent the first and second principal components, respectively. The percentage represents the contribution rate of this component to sample difference. The distance between samples indicates the similarity of the distribution of functional classifications in the sample. The closer the distance, the higher similarity. INF (yellow), EFF (green), MW1 (blue), and MW2 (red).

Since the possible propanotrophic *Mycobacterium*, OTU 52, was frequently detected in original, and propane induced treatments, it suggests that OTU 52 widely exists in natural environment and it could induce by propane especially in MW1-Propane (7.3%). Like 16S rRNA sequencing, qPCR results found the highest abundance of *prm* gene presented in MW1-Propane achieved as high as 3.5% of total community. This suggests that the representative OTU 52 is more likely to be an indigenous strain contining *prm* gene

cluster rather than the exogenous PH-06. Considering that *Pesudocardia* is absent in all samples according to16S rRNA results, PH-06 and CB1190 likely vanished at the end of incubation. However, it is interesting to be noted that the detectable *prmA* and *thmA* in mixed inoculum treatments (EFF-Mix, MW1-Mix, particularly MW2-Mix) suggesting these gene clusters retained in the communities. Given the important role of the plasmid in HGT, *prmA* and *thmA* located on plasmids[131, 262] likely transfer among the phylogenetically close relatives in Actinomycetes[96, 263]. OTU 187 is unique to mixed culture augmented treatments indicating it related with the inoculation of PH-06 and CB1190. It exhibits high similarity with *Rhodococcus aetherivorans* 10bc312 which was isolated as a methyl tert-butyl ether degrading strain[264]. Previous reports have been confirmed that this strain can use dioxane as sole carbon source, although it appeared not to be an effective dioxane degrader considering the low degradation rate (0.0073 mg-dioxane/mg-protein/h) and affinity (59.2 mg/L). *R. aetherivorans* TPA is a propane-utilizing bacteria[256] and *R.* RR1 is a potential propanotroph because it harbors a propane monooxygenase homologous to group 5 propane monooxygenase[265]. Although OTU 5's phylogeny is relative distinct from propanotrophic *Rhodococcus*, it is highly abundant in all mixed culture treatments. Thus, OTU 5 and OTU 187 are likely to be potential catabolic gene recipients.

5.4.3 The Indigenous Propanotrophic Mycobacterium may Participate in Propane Utilization

Propane tended to degrade after 9 days in all propane amending treatments indicating the extensive existence of propanotrophs which in agreement with previous reports[32, 70, 73]. However, no significant dioxane removal was observed in the propane fed treatment or abiotic control prepared by EFF, MW1, and MW2 within the 30-days incubation period except 82% of dioxane degraded in INF-Propane. Correspondingly, 16S rRNA results in

Figure 5.5 suggest that INF-Propane (printed in green) has a distinct microbial community structure that diverges from the well-treated subgroup (printed in blue) and the poorly treated subgroup (printed in red). Thus, INF-Propane posseses a unique indigenous bacterial community associating with propane utilization and dioxane degradation. The most abundant 10 genera in INF-Propane are *Rhizobacter* (32.6%), *Sulfuritalea* (17.9%), unidentified *Hyphomonadaceae* (4.1%), *Coxiella* (3.7%), *Reyranella* (2.9%), *Hirschia* (1.9%), *Sediminibacterium* (1.1%), *Legionella* (1.0%), *Bryobacter* (1.0%), and *Hyphomicrobium* (0.8%). However, to our best knowledge, no relevant research reported their degradation capacities related to dioxane or propane.

Although dioxane degradation was not observed in MW1-Propane, 52% of propane in has been removed from day 9 to day 30. It suggests that indigenous strain may first utilize the relatively high organic carbon (12000 μg/L) in MW1-Propane. After 9 days, propane provided energy to expand the abundance of OTU 52. The co-occurring high abundances of OTU 52 and *prm* gene in MW1-Propane suggest this strain may contain a group 6 SDIMO, which is a group of enzyme could initiate dioxane degradation and propane utilization. Due to the preference of propanotrophic dioxane-degrading strains, propane more likely to be used over dioxane[28, 69], dioxane degradation could be observed if elongate the incubation time. Together with the phylogeny analysis, OTU 52 may involve in propane and dioxane degradation in propane induced treatment. We intend to continue the enrichment and make efforts to identify and isolate the indigenous dioxane degrading propanotroph(s), which may be well suited for both *in situ* and *ex situ* treatments at this site. However, the indigenous propanotroph(s) do not have obvious varies to the degradation pattern and propane consumption comparing with other treatments.

The microcosm assay shows the Rhodococcus strain, OTU 5, existed in propane amended treatments (i.e., MW1-Propane). According to the sequences, OTU 5 has over 99% identity in comparison with a polychlorinated biphenyls (PCBs) degrading species *Rhodococcus* sp. YAZ54[266] and a hexahydro-1,3,5-trinitro-1,3,5-triazine (RDX) degrading species *Rhodococcus* sp. BL1[267]. The phylogenetic tree exhibits this OUT is relatively away from the known propanotrophic *Rhodococcus* (Figure 5.6). However, it was enriched in the treatments with DD4 and mixed culture augmented suggesting this *Rhodococcus* may containing alcohol dehydrogenases[268, 269], which could be stimulated by the metabolites of propane. To our best knowledge, the other abundant OTUs in various genera such as *Pseudoxanthomonas*, *Legionella*, and *Zoogloea* may have minor participation in propane and dioxane oxidization, although *Pseudoxanthomonas* was found as the abundant genus in all the DD4 and mixed treatments.

5.4.4. *TmoA* Is a Suitable Biomarker for the Rapid Assessment of DD4 Bioaugmentation Performance

In light of the correlation analysis in Figure 5.9, the molecular experiments are potent evidence revealing the relation between DD4 and degradation capacity. The abundance of *Azoarcus* is significantly correlated to the abundance of *tmoA* according to Spearman's coefficient[270], which is 0.90. Their relative abundances are nearly fit a curve with the slope of 0.75, and intersection of 0.01. The absolute copy number of *Azoarcus* and *tmoA* also significantly correlated with the dioxane degradation rate, which are 0.81 and 0.85. It indicates that the *tmoA* probe/primers specifically target to *tmo* gene cluster and can accurately reflect the abundance of *Azoarucs* in the environmental samples. Also, the gene cluster *tmo* primarily attributes to dioxane degradation as observed in the present

experiment. The probe/primers of *tmoA*, therefore, is an excellent biomarker for indicating the abundance of *Azoarcus* and assess the performance of DD4 bioaugmentation.

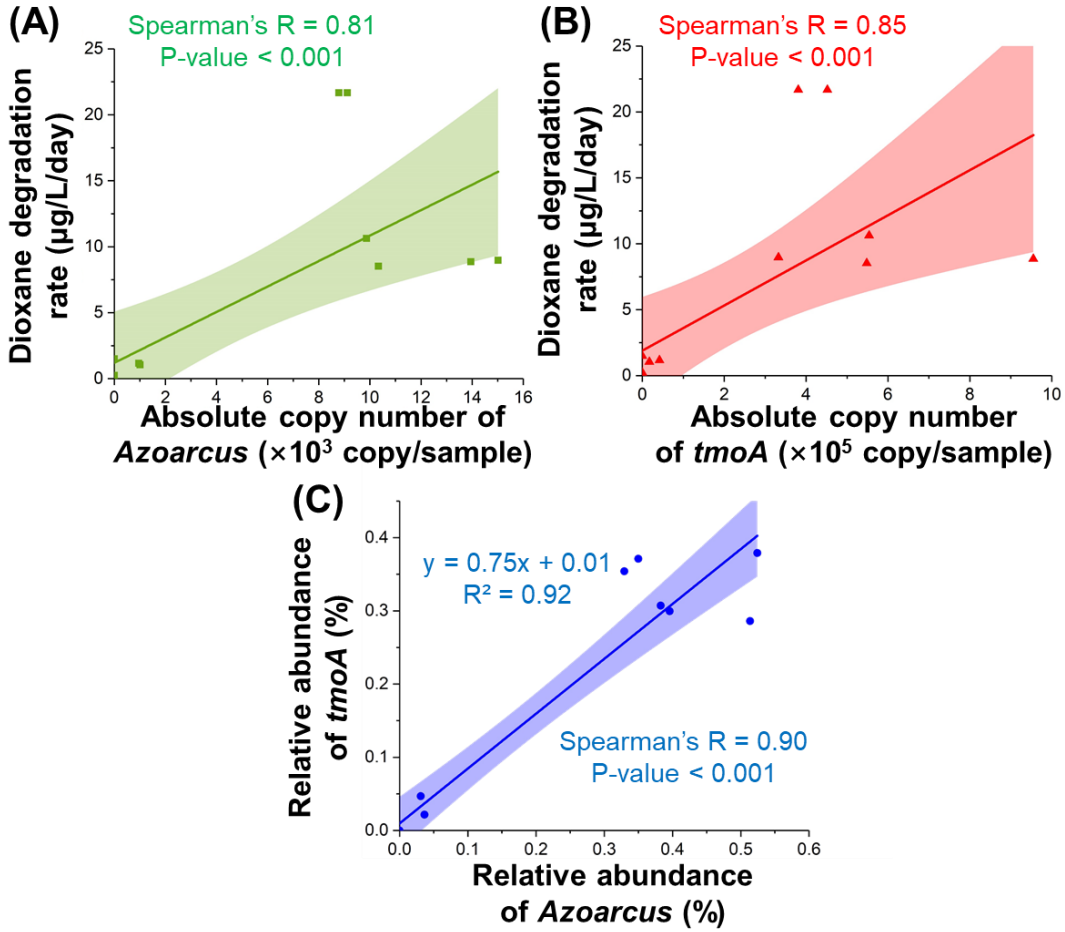

Figure 5.9 Positive linear correlations between (A) dioxane degradation rate (µ/L/day) and absolute copy number of *Azoarcus* (copy/sample), (B) dioxane degradation rate (µ/L/day) and absolute copy number of *tmoA* (copy/sample), and (C) relative abundance of *tmoA* (%) and relative abundance of *Azoarcus* (%). The Spearman's R indicates the correlation of two values.

5.5 Conclusions

Considering the low dioxane concentration at the contaminated plume and treated waters (<100 µg/L), the co-metabolizer, *Azoarcus* sp. DD4 is a potent candidate for dioxane cleanups at in situ or ex situ Superfund site samples. Results show that DD4 efficiently

removed the low concentration of dioxane at a relatively short incubation time (6-9 days) except the groundwater near the source zone due to the complicated chemical and biological compositions. DD4 became the most dominant strain in these microcosms with a relatively high abundance of around 28-52% in light of qPCR and 16S rRNA sequencing analysis. DD4 also exhibits its potent competitive capability to the artificially induced dioxane metabolizers, PH-06 and CB1190. Interestingly, the gene cluster from these two metabolizers have been retained in the communities through HGT. According to the molecular results, two Rhodococcus OTU may involve in revieving catabolic genes. An indigenous propanotrophic Mycobacteri OTU 52 was confirmed that related with propan utilization and dioxane degradation. The significant correlation between the dioxane-degrading gene cluster in DD4 and dioxane degradation rate indicates *tmoA* is a suitable biomarker to evaluate the DD4 bioaugmentation in the future application.

CHAPTER 6

SEQUENTIAL ANAEROBIC AND AEROBIC BIOREMEDIATION OF THE COMMINGLED GROUNDWATER CONTAMINATION OF TRICHLOROETHENE AND 1,4-DIOXANE

6.1 Introduction

As introduced in Chapter 1, the co-occurrences of chlorinated solvents and dioxane were widely detected over US. The current research underscoring an efficient removal of TCE through applications of reductive dehalogenating consortia such as SDC-9 and KB-1 under anaerobic condition[271]. However, two issues have been frequently reported at sites where anaerobic bioremediation is implemented, underscoring the need for effective solutions. First, once TCE is reduced, dehalogenation of cDCE and VC occurs in a slower pace in the field, conducive to the accumulation of these toxic degradation byproducts[141, 272-274]. Though the use of bioaugmentation with halorespiring cultures helps to mitigate daughter product generation at many sites, there are often lingering daughter products. This possibly pertains to the lack of bacteria that are efficient in reducing cDCE or VC to ethene[275], insufficiency of electron donors (e.g., hydrogen)[276, 277], slow kinetic restricted by low concentrations of these intermediate compounds[278], and/or competition with indigenous bacteria for electron acceptors (e.g., sulfate and iron (III))[279, 280]. The other concern is the concurrence of trace levels (typically <1 mg/L) 1,4-dioxane (dioxane), an anthropogenic cyclic ether used for stabilizing chlorinated solvents[4, 8]. Co-contamination of TCE and dioxane has been reported across the US and globally[8, 281]. Anderson *et al.*[4] unveiled that 93.5% (730 out of 781) of TCE-impacted sites was positively detected dioxane, and 1,1,1-trichloroethane (TCA) co-exist in 29.3% (229 out of 781) of the dioxane-contaminated wells based on the monitoring data from over 4196 United States Air Force (USAF) sites.

Similarly, Adamson *et al.*[8] investigated > 2000 sites in California. Among the 605 sites with positive detection of dioxane, 94% had TCE/TCA contamination. Though many Actinomycetes, such as *Pseudonocardia dioxanivorans* CB1190[92] and *Mycobacterium* sp. PH-06[58], have been identified for their capability of metabolizing dioxane as the sole carbon and energy source, their viability and activity are much restricted by the low concentrations of dioxane prevailing in the field[69, 282]. Further, the presence of cVOCs can negatively affect the performance of aerobic dioxane degradation given their potency to inhibit key catalytic enzymes (e.g., soluble di-iron monooxygenases [SDIMOs])[65, 283] and trigger universal cellular stress[67]. Therefore, elimination of co-occurring cVOCs, especially TCE, can be a prerequisite to achieving an efficient biotreatment of dioxane.

In present study, we design and demonstrate a sequential treatment strategy (Figure 6.1) that can effectively reduce TCE first by SDC-9 under anaerobic condition and then oxidize dioxane and other hazardous cVOCs by *Azoarcus* sp. DD4[37] under aerobic condition. Polasko *et al.* reported a consortium mixed with KB-1 and CB1190 can degrade TCE and dioxane (at ~3.5 mg/L) in tandem with no accumulation of cDCE[284]. Unlike this previous work, our treatment train is technologically distinctive, because (1) DD4 is employed as a co-metabolic dioxane degrader that is efficient to remove dioxane at low concentrations (e.g., <1 mg/L) relevant for many contaminated sites, (2) DD4 is inoculated after the completion of the initial anaerobic treatment, in which microcosms are air sparged without exposing DD4 to undesirable anaerobic conditions, and (3) DD4 exhibits superior physiological properties suited for *in situ* applications (e.g., fast planktonic growth and compatibility with aquifer environments)[37] and expresses a diversity of SDIMOs that can degrade cVOCs and other co-existing contaminants[185, 229]. The abundances of key

degraders are monitored using 16S rRNA gene amplicon sequencing and quantitative polymerase chain reaction (qPCR). Collectively, our bioremediation treatment train combining reductive dehalogenation and co-metabolic oxidation has broad application potentials for the cleanup of many sites where TCE and trace concentrations of dioxane co-occur without the concern of accumulating undesirable biotransformation byproducts.

6.2 Materials and Methods

6.2.1 Chemicals and Cultures

The neat TCE (> 99.5%), cDCE (> 99.5%), and dioxane (> 99.8%), as well as VC (2000 μg/mL in methanol), were purchased from Sigma-Aldrich (St. Louis, MO). Propane (>99.5%) was provided by Airgas (Radnor, PA). Slow release substrate (SRS) emulsified vegetable oil (EVO) and SDC-9 bioaugmentation culture commercially marketed as TSI DC™ were supplied from Terra Systems Inc. (TSI, Claymont, DE). The culture has been maintained on sodium lactate and PCE in reduced anaerobic mineral medium (RAMM)[285]. *Azoarcus* sp. DD4 was isolated by our lab from an activated sludge sample from a local wastewater treatment plant in Northern New Jersey[37]. DD4 was grown in nitrate mineral salts (NMS) medium[37] supplemented with propane (0.10 % v/v equivalents to 2 mg/L in headspace) to stimulate dioxane degradation activity.

6.2.2 Anaerobic Microcosm Assays

Groundwater and rock core samples were collected from a site located in central New Jersey in April 2017. This site was operated by a gas company and has been historically impacted by TCE contamination in a deep bedrock aquifer up to 61 m below the ground surface (BGS). Approximately 20 L of groundwater was collected in compliance with the

NJDEP Low Flow Purging and Sampling Guidance from a monitoring well with the highest TCE concentration at the site according to the monitoring data archived in December 2016. The baseline concentrations (Table 6.1) of TCE, cDCE, and dioxane were 296 µg/L, 96 µg/L, and 6.45 µg/L, respectively, as analyzed by a commercial analytical lab. The bedrock cores between 11.0 and 14.6 m BGS were collected during the drilling of the injection well. In order to minimize exposure to oxygen and volatilization of cVOC, the cores were kept with dry ice and crushed under nitrogen blanket into about 2.5 cm pieces. The groundwater and bedrock samples were separately stored in bottles with 10 min of filtered nitrogen purging. Bottles were sealed with PTFE caps on site, preserved at 4 °C on ice, and transported to New Jersey Institute of Technology (Newark, NJ).

Table 6.1 Characterization of VOCs in the Groundwater Sample from the Site (Continued)

VOC	NJDEP GWQS (µg/L)	GCMS Results (µg/L)	Q	MDL (µg/L)
1,1,1-Trichloroethane	30	2.24	U	2.24
1,1,2,2-Tetrachloroethane	1	**1.52**	U	1.52
1,1,2-Trichloro-1,2,2-trifluoroethane	20000	2.72	U	2.72
1,1,2-Trichloroethane	3	0.64	U	0.64
1,1-Dichloroethane	50	3.92	J	1.92
1,1-Dichloroethene	1	**8.00**		2.72
1,2-Dichlorobenzene	600	1.76	U	1.76
1,2-Dichloroethane	0.3	**2.00**	U	2
1,2-Dichloropropane	1	**1.44**	U	1.44
2-Butanone (MEK)	300	24.80	J	17.6
2-Hexanone	300	5.76	U	5.76
4-Methyl-2-pentanone (MIBK)	NA	5.04	U	5.04
Acetone	6000	57.60		8.8
Benzene	1	**1.36**	J	0.72
Bromoform	4	1.44	U	1.44
Bromomethane	10	1.44	U	1.44
Carbon disulfide	700	1.76	U	1.76
Carbon tetrachloride	0	**16.80**		2.64

Table 6.1 Characterization of VOCs in the Groundwater Sample from the Site (Continued)

Chlorobenzene	50	1.92	U	1.92
VOC	NJDEP GWQS (µg/L)	GCMS Results (µg/L)	Q	MDL (µg/L)
Chlorodibromomethane	0.4	**1.76**	U	1.76
Chloroethane	5	2.96	U	2.96
Chloroform	70	62.40		1.76
Chloromethane	NA	1.76	U	1.76
cis-1,2-Dichloroethene	70	**96.00**		2.08
cis-1,3-Dichloropropene	NA	1.28	U	1.28
Dichlorobromomethane	1	**1.20**	U	1.2
Ethylbenzene	700	2.40	U	2.4
Methyl tert-butyl ether	70	1.04	U	1.04
Methylene Chloride	3	**51.20**		1.68
m-Xylene & p-Xylene	NA	2.24	U	2.24
o-Xylene	NA	2.56	U	2.56
Styrene	100	1.36	U	1.36
TBA	100	80.00	*	9.6
Tert-amyl methyl ether	NA	1.28	U	1.28
Tetrachloroethene	1	0.96	U	0.96
Toluene	600	2.00	U	2
trans-1,2-Dichloroethene	100	1.44	U	1.44
trans-1,3-Dichloropropene	NA	1.52	U	1.52
Trichloroethene	0.4	**296.00**		1.76
Vinyl chloride	0.08	**7.60**	J	0.48

Notes:
Sample was collected from the aqueous phase of microcosm bottle within 24 hours of setup.
NJDEP GWQS - New Jersey Department of Environmental Protection Groundwater Quality Standard
Q - Qualifier
MDL - Method Detection Limit
J: Result is less than the RL but greater than or equal to the MDL and the concentration is an approximate value.
U: The analyte was analyzed but not detected.
Bold values are in exceedance of the corresponding NJDEP GWQS values.

Four anaerobic treatments were prepared as Figure 6.1 and Table 6.2, including (1) killed control (I-KC), (2) live control (I-LC), (3) bioaugmentation with SDC-9 (I-SDC), and (4) bioaugmentation with SDC-9 and sulfate amended (I-SDC-SO_4). Considering the iron mineral is rich in the northeast of US, especially in New Jersey[286], we initially

postulate the addition of sulfate may enhance or accelerate the total TCE removal since sulfate can be reduced to sulfide by sulfate-reducing bacteria (SRB) in SDC-9, which couple with ferrous ions leached from the iron-rich bedrocks to form FeS minerals that abiotically react with TCE[287]. Each treatment was prepared in triplicate. TCE concentration in the aqueous phase was spiked to around 20 μM in 410 mL of groundwater and 275 g of bedrock sample, leaving approximately 50 mL of headspace. EVO (1,000 mg/L) and magnesium hydroxide (60 mg/L) were added as the exogenous carbon source and the alkaline reagent to maintain the neutral or slightly basic pH (7.3-7.6), respectively. SDC-9 was inoculated to a final cell density of 2×10^8 CFUs/mL. A high concentration (3,000 mg/L) of sodium azide was added as a biocide in the killed control. Magnesium sulfate heptahydrate (sulfate concentration equivalent to 584 mg/L) was added to investigate the interference of sulfate on TCE degradation. Microcosms were set quiescently at room temperature (i.e., 24±3 °C). Concentrations of TCE, cDCE, and VC in microcosm bottles were analyzed at a commercial lab using the EPA Method 8260C. This is a standard method for quantifying a wide span of VOCs in aqueous samples using purge-and-trap gas chromatography/mass spectrometry (GC/MS). cDCE concentrations in one of the triplicate microcosms were not in good consensus with the others since Week 11 in Treatments I-SDC and I-SDC-SO_4, probably due to variance in bedrock samples. These data were excluded from the analysis.

Table 6.2 Compositions of Anaerobic Microcosms

Amendment	Target amount or concentration	Killed control	Live control	Bioaugmentation	Bioaugmentation + sulfate
Groundwater	410 mL	√	√	√	√
Bedrock	275 g	√	√	√	√
TCE	8,500 µg/L	√	√	√	√
Sodium azide	3,000 mg/L	√			
EVO	1,000 mg/L[a]			√	√
SDC-9	2×10^8 CFUs/mL			√	√
Magnesium hydroxide	60 mg/L			√	√
Magnesium sulfate heptahydrate	1,500 mg/L				√

[a]Amended as TOC concentration

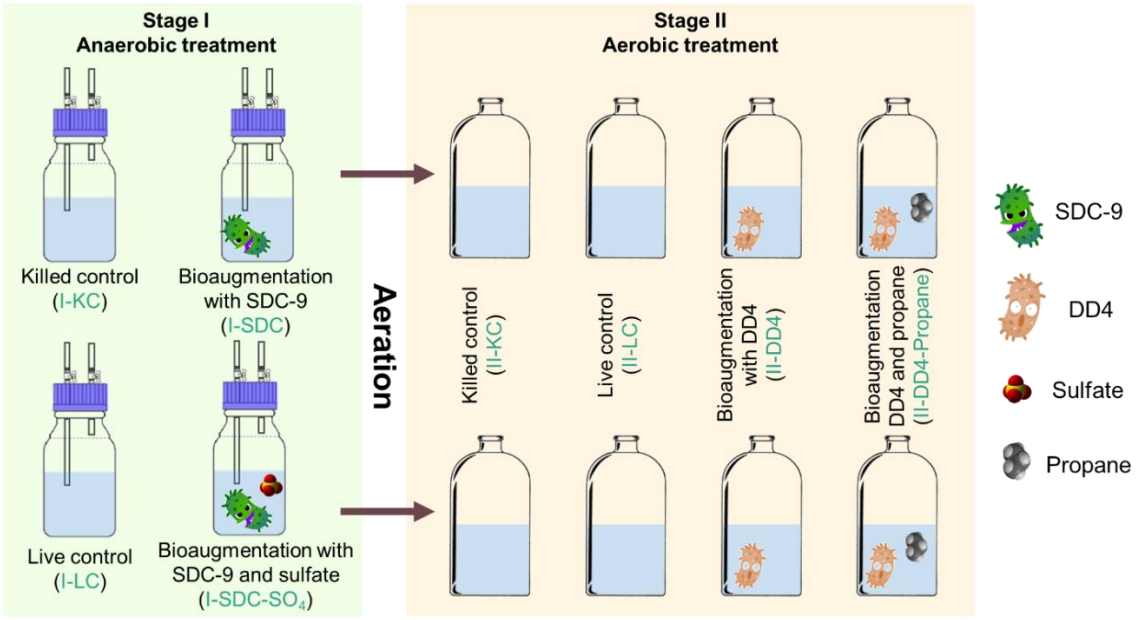

Figure 6.1 Experimental scheme of the sequential anaerobic-aerobic treatment in this microcosm study. Killed control (KC) and live control (LC) were designed for both anaerobic (stage I) and aerobic (stage II) treatments. After the anaerobic treatment, samples from I-SDC or I-SDC-SO_4 were aerated, pooled, and split to prepare the stage II aerobic treatments.

6.2.3 Bacterial Community Analysis after the Anaerobic Treatment

When the anaerobic treatments are terminated, total DNA from treatments I-SDC and I-SDC-SO_4 was extracted for 16S rRNA sequencing and taxonomic analysis using the PowerSoil® DNA Isolation Kit (Qiagen, Hilden, Germany) following the manufacture user protocol. V3-V4 hypervariable region of 16S rRNA was amplified and sequenced as the method in Section 5.1.4.

6.2.4 Aerobic Microcosm Assays

After the removal of TCE, two sets of anaerobic treatments, bioaugmentation of SDC-9 without amendment of sulfate (I-SDC) and bioaugmentation of SDC-9 with amendment of sulfate (I-SDC-SO_4), were selected for sequential treatment of dioxane via aerobic co-metabolism by DD4 (Figure 6.1). First, anaerobic bottles were uncapped and exposed to air for 30 min to induce aerobic conditions. Positive oxidation reduction potential (ORP) (> 50 mV) and high dissolved oxygen (DO) (> 8.0 mg/L) were achieved as measured by Xplorer GLX datalogger (PASCO scientific, Roseville, CA). For either anaerobic treatment (I-SDC or I-SDC-SO_4), groundwater and bedrock samples were removed from these triplicated anaerobic microcosms and pooled to result in approximately 700 mL of anaerobically treated groundwater and 750 g of bedrock.

Each aerobic microcosm was prepared in the 160-mL serum bottle containing 50 mL of water sample and 25 g of bedrock that have been previously treated under anaerobic condition. The aqueous samples were re-spiked with dioxane to achieve an initial concentration of 20 μg/L. As shown in Figure 6.1 and Table 6.3, four treatments were prepared, including killed control (II-KC), live control (II-LC), and DD4 bioaugmentation with (II-DD4-Propane) or without propane (II-DD4) amendment. All treatments were

conducted in triplicate. DD4 was harvested at the exponential phase after being cultured in NMS medium with propane as the sole carbon source. Cells were washed with phosphate-buffered saline (PBS) buffer twice and resuspended to an OD_{600nm} of 2.0. For the two sets of DD4 bioaugmentation microcosms (II-DD4-Propane and II-DD4), 0.5 mL of the harvested cell were inoculated, resulting in an initial protein concentration of 0.17 mg per vial (equivalent to 1.5×10^6 CFU/mL). Propane (0.10 % v/v equivalent to 2.00 mg/L in headspace) was amended to one set of DD4 bioaugmentation microcosms (II-DD4-Propane) as the carbon supplement, while no additional substrates were added to the other bioaugmentation set (II-DD4). Microcosms were incubated at room temperature (i.e., 24±3 °C) while being shaken at 150 rpm. At selected intervals, liquid and headspace samples were collected for the analysis of dioxane and propane by gas chromatography (see supplementary data), respectively. The relative abundance of DD4 was enumerated by quantitative PCR (qPCR) analysis as detailed in supplementary data.

Table 6.3 Compositions of Aerobic Microcosms

Treatment	Target amount or concentration	Killed control	Live control	Bioaugmentation	Bioaugmentation + propane
Autoclave		√			
Pre-treated water sample	50 mL	√	√	√	√
Bedrock	25 g	√	√	√	√
Dioxane	20 mg/L	√	√	√	√
DD4	1.5×10^6 CFUs/mL			√	√
Propane	0.10% v/v				√

6.2.5 qPCR Analysis to Enumerate the Relative Abundance of DD4 after Aerobic Treatment

After aerobic treatments, total DNA in microcosms bioaugmented with DD4 (II-DD4 and II-DD4-Propane) or without amendments (II-LC) were extracted using the PowerSoil® DNA Isolation Kit (Qiagen, Hilden, Germany). qPCR technique was employed to evaluate the abundances of DD4 by targeting the *tmoA* gene using primers, DD4 tmo_F 5'-GGCGGATGGCTGTACTCAACAGAATG -3' and DD4 tmo_R 5'- AAATCGCCGG AAAGCTTGGGC-3', and a TaqMan™ probe 5'-/FAM/CGACCTGGC/ZEN/CAGG AGTACGAAC/IABkFQ/-3'. The detailed method has been described in Section 5.2.3.

6.2.6 Biotransformation of VC and cDCE by DD4 and their Inhibitory Effects to Dioxane Degradation in DD4

Given the observation of cDCE and VC being generated from the anaerobic treatment of TCE, growing and resting cells of DD4 were used to (1) investigate the degradation capability of DD4 on VC and cDCE and (2) assess their impacts on dioxane degradation. DD4 cells were prepared in 20 mL NMS medium in a 160-mL serum bottle with 4 mL propane amended. Cells were harvested and resuspended with fresh NMS medium to an OD_{600nm} of ~2.0. Growing cell assays were prepared with 0.1 mL of resuspended DD4, inoculated to 10 mL groundwater sample spiked with 10 mg/L of dioxane, 1 mg/L of cDCE, and 1 mg/L of VC. As an auxiliary substrate, 150 μL of propane (0.10 % of volume equivalent to 2.0 mg/L in the headspace) was amended at the beginning and when propane concentration was lower than 0.20 mg/L in headspace. In parallel, for resting cell assays, resuspended DD4 with an OD_{600nm} of 2.0 was exposed to dioxane of an initial concentration of 10 mg/L in 5 mL of NMS medium in 30-mL serum bottle. cDCE or VC was amended

to reach an aqueous phase concentration of 0.35 mg/L. Concentrations of dioxane, cDCE, and VC were monitored by the analytical methods described in the Section 2.2.10.

6.3 Results and Discussions

6.3.1 TCE was Transformed to cDCE and VC by SDC-9 in Anaerobic Microcosms

After amendment with SDC-9, TCE was completely reduced to cDCE and VC within 4 weeks of incubation (Figure 6.2). No significant decrease of TCE was observed in killed or live controls. In Week 4, TCE concentration in the SDC-9 augmented treatment (I-SDC) decreased from 24.56±2.46 to 0.47±0.38 µM with the formation of an equivalent molar amount of cDCE (~26.9 µM). SDC-9 was able to continue the reductive dehalogenation and transform cDCE mostly to VC. From Week 4 to Week 11, cDCE concentration decreased from 29.30±0.58 µM to 0.39±0.14 µM, while VC concentration increased from 2.43±0.54 µM to the highest 37.61±2.57 µM. However, VC persisted in the SDC-9-bioagumented microcosms with no further significant removal from Week 11 to Week 16. The accumulation of VC echoes the observations in some of previous studies using SDC-9 and other enriched consortia [89, 288]. Given the time restriction of this project, we terminated the anaerobic microcosm assays in Week 16. It is likely, based on the experience of many others, that VC would be further reduced to ethene, which was not monitored in this study. Such slow or incomplete dehalogenation observed in our microcosms was possibly due to the facts that (1) reduction of VC to ethene is thermodynamically less favorable and thus much slower compared to prior reduction steps (i.e., from TCE to cDCE and from cDCE to VC)[289-291] and/or (2) fastidious growth of VC degrading microbes can be restricted by the competition of indigenous strains[292]. 16S

rRNA gene amplicon sequencing analysis (Figure 6.3) revealed the existence of two well-known halorespiring bacteria, *Dehalococcoides* and *Desulfuromonas*, reflecting their essential roles in reductive dechlorination of TCE to cDCE or VC[86].

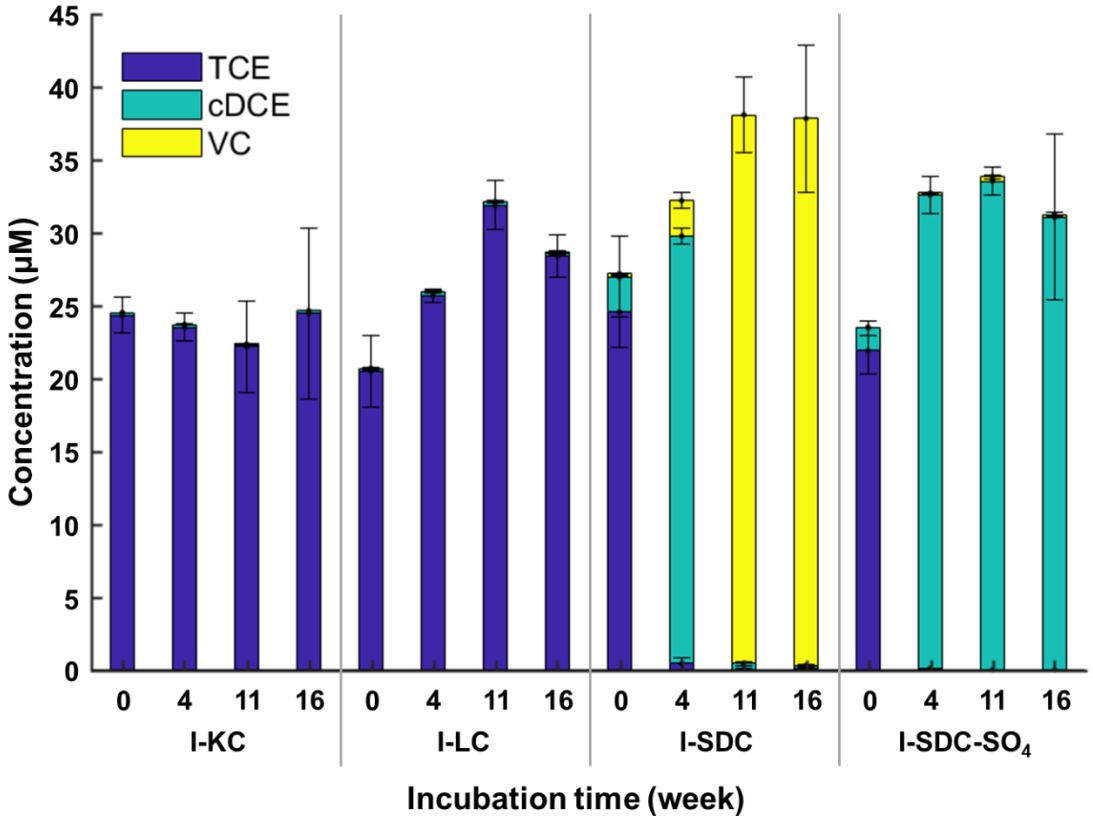

Figure 6.2 cVOCs monitoring during the anaerobic treatments in killed control (I-KC), live control (I-LC), and bioaugmentation microcosms amended with SDC-9 (I-SDC), and with both SDC-9 and sulfate (I-SDC-SO_4), respectively. Blue, green, and yellow bars represent the concentration of TCE, cDCE, and VC in µM, respectively.

6.3.2 Halorespiring Bacteria Prevailed after the Anaerobic Bioaugmentation

16S rRNA gene amplicon sequencing analysis (Figure 6.3) revealed the existence of *Dehalococcoides* and *Desulfuromonas*, two genera well known for their capability of reductive dehalogenation, in SDC-9-bioaugmented microcosms (I-SDC). Genus of *Dehalococcoides* embraces obligatory organohalide-respiring bacteria that are able to

sequentially reduce TCE to cDCE, VC, and ethene [288, 293]. In contrast, *Desulfuromonas* can only catalyze the first dehalogenation step (i.e., TCE to cDCE)[294], rather than transformation of low-chlorinated compounds such as cDCE and VC. Prevalence of these two dehalogenation bacteria have been reported at sites previously treated via bioaugmentation with SDC-9[86]. Despite their relatively low abundance (Figure 6.3), *Dehalococcoides* and *Desulfuromonas* are plausibly pivotal for dehalogenation of TCE to cDCE/VC as observed in the microcosms.

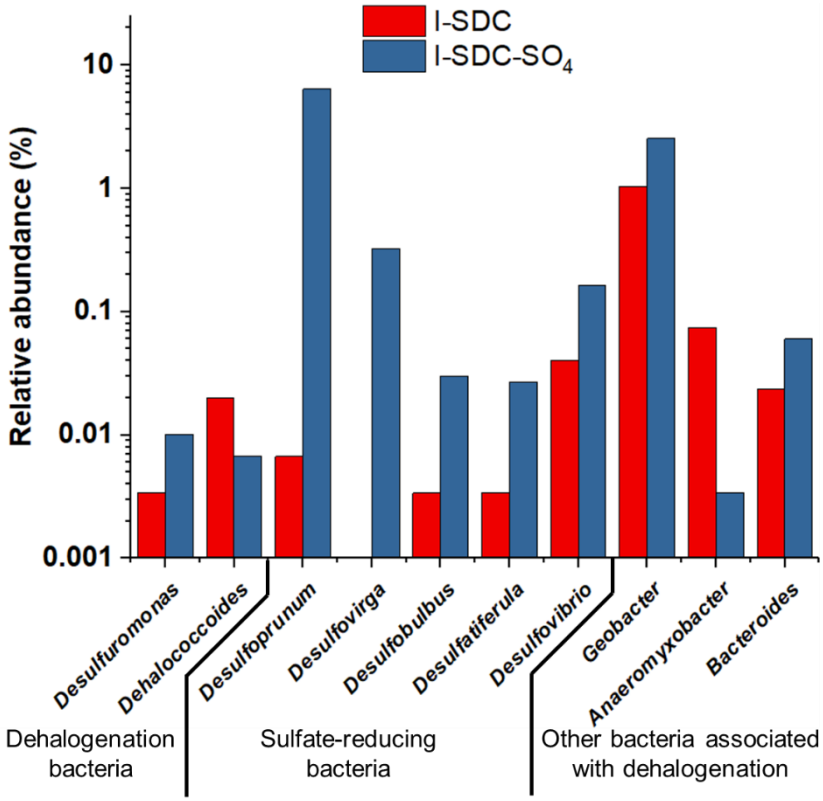

Figure 6.3 Relative abundance (%) of dehalogenation bacteria, sulfate-reducing bacteria, and other genera associated with dehalogenation in anaerobic microcosms after bioaugmention with SDC-9 consortia. Red bars denote the genera relative abundance (%) in anaerobic treatment that was bioaugmented with SDC-9 (I-SDC). Blue bars represent genera relative abundance (%) in the anaerobic treatment which was augmented with both SDC-9 and sulfate (I-SDC-SO_4).

In addition to these organohalide-respiring bacteria, some other microorganisms may also assist in the dehalogenation of TCE observed in the I-SDC microcosms (Figure 6.3). The presence of *Geobacter* species (1.04% in I-SDC) potentially facilitates TCE dehalogenation directly or indirectly. *Geobacter,* a ubiquitous Fe(III)-reducing genus in soil and sediment, has been applied in the anaerobic degradation of aromatic hydrocarbons such as benzene, toluene, and xylene[295]. Some species, such as *Geobacter lovleyi* SZ, exhibit the capability of reducing PCE to cDCE[296]. Further studies showed that *Geobacter* can enhance the dechlorination by *Dehalococcoides* by providing interspecies cobamide as a nutritional supplement[297]. Also known as a halo-respiring genus, *Anaeromyxobacter* accounts for 0.04% in the I-SDC microcosm[298]. *Anaeromyxobacter* has been frequently detected at sites impacted by cVOCs[299]. Based on many previous studies[300, 301], some other bacteria detected in the I-SDC microcosms may act as a supportive role to dehalogenation, such as *Desulfovibrio* (0.04%) and *Bacteroides* (0.02%). It was reported that the production of acetate, hydrogen, and corrinoid cofactors by *Desulfovibrio* can support the reductive dehalogenation by *Dehalococcoides*[300]. Frequent detection of *Bacteroides* implied its association with the reductive dehalogenation process observed in the field[301].

Though successive dehalogenation of TCE to cDCE and then VC was evident in the SDC-9 bioaugmented microcosms, relative abundance of these key dehalogenation bacteria and other contributing bacteria were relatively low. It may result from a number of technical difficulties we have experienced. First, samples were collected at the end of the active dehalogenation treatment without replenishing of EVO or other substrates. Thus, active players for dehalogenation may have decayed to some extent. Second, isolation of genomic DNA from the bedrock samples was challenging. We used the PowerSoil® DNA

Isolation Kit (Qiagen, Hilden, Germany) for DNA extraction, which may cause biased recoveries among different bacteria. Third, specific primers targeting the V3-V4 region of 16S rRNA was amplified by PCR, introducing potential bias for the 16S rRNA gene amplicon sequencing[302]. Fourth, a portion (16.7%) of the sequences were assigned as "unknown" bacteria as no significant homologs were identified within the database (Silva) utilized for annotation. The missing assignment of these sequences may have undermined the roles of bacteria that have been sparsely studied[303].

6.3.3 Contribution of Abiotic Reactions to the TCE Removal was Minimal

In the anaerobic treatment I-SDC-SO_4 that received both SDC-9 and sulfate (584 mg/L), TCE was rapidly transformed from 21.92±1.61 to 0.14±0.03 μM within the first four weeks. Concurrently, cDCE increased from the initial of 1.57±0.50 μM to 32.46±1.26 μM. However, neither reduction of cDCE nor generation of VC was significantly observed after Week 4. Therefore, the addition of sulfate may interfere with the sequential reduction of cDCE to VC, probably due to the outcompetition of halorespiring bacteria by sulfate reducing bacteria (SRB). After the addition of sulfate, the total SRB increased to nearly 7% of the total bacteria (Figure 6.3), including *Desulfoprunum* (6.38%), *Desulfovirga* (0.33%), *Desulfovibrio* (0.16%), *Desulfbulbus* (0.03%), *Desulfatiferula* (0.03%). In contrast, in the I-SDC microcosms where sulfate was not amended, the relative abundance of total SRB was as low as 0.05%. Furthermore, amendment of sulfate also greatly reduced the abundance of *Dehalococcoides* from 0.020% (in I-SDC) to 0.007% (in I-SDC-SO_4) (Figure 6.3). As *Dehalococcoides* are key contributors to the reduction of cDCE to VC[304], the decrease of their abundance could be conducive to the absence of cDCE reduction or VC formation as observed in the I-SDC-SO_4 treatment. In our microcosms, the presence of

sulfate as an alternative electron acceptor exerted a significant selection on SRB, prohibiting reductive dechlorination due to their rapid and competitive utilization of electron donors[305, 306].

The formation of FeS minerals was evident as dark precipitates formed in the I-SDC-SO_4 treatment (Figure 6.4). However, the contribution of abiotic degradation might be minimal to the total TCE removal according to the given evidence. First, there is no significant loss in total molar concentration of cVOCs over the treatment, suggesting little production of dissolved gases including acetylene, which is a dominant abiotic dehalogenation product of TCE. Reports previously found acetylene generated as the primary product (73-78%) of TCE abiotic degradation via reductive β-elimination. Only approximately 7% of the removed TCE was transformed to cDCE and 15-20% was converted to ethene or ethane and other hydrocarbons through hydrogenolysis [287]. Second, the microcosms contained groundwater and rock samples at a ratio of 1.5, while the actual bedrock aquifer could contain groundwater and bedrock at a ratio of 0.02. Therefore, the high water ratio in the microcosms could result in low iron concentrations (due to dilution, Table 6.4) when compared with the concentrations in the Passaic Formation during the field anaerobic treatment. Further, the iron leached from the bedrock typically peaked at 6 to 9 months during the anaerobic treatment (data not shown). Considering that our anaerobic study lasted for less than 4 months, the ferrous iron availability may not reach peak prior to the termination of the study. Therefore, the potential low availability of ferrous iron in the microcosm could limit the formation of FeS at the concentrations that can effectively stimulate abiotic dehalogenation. All these lines of evidence suggest that

dechlorination of TCE to cDCE in the I-SDC-SO_4 treatment was mainly contributed by microbial reduction, rather than the abiotic transformation.

Figure 6.4 Dark particles formed in the anaerobic treatments bioaugmented with SDC-9 and sulfate (I-SDC-SO_4).

Table 6.4 Monitoring of Dissolved Iron During the Anaerobic Treatments

Incubation time (week)	Dissolved iron (mg/L)			
	Killed control	Live control	Bioaugmentation	SDC-9 + sulfate
0	0.2	0.2	0.2	0.7
4	0.2	0.2	0.2	1.4
7	0.2	0.2	0.3	1.4
11	0.2	0.2	0.3	1.4

Dioxane was persistent over the course of anaerobic treatments as no significant dioxane concentration change was observed in all anaerobic microcosms (data not shown). To date, anaerobic treatment of dioxane remains elusive. Thus, a subsequent aerobic

treatment by DD4 was conducted to mitigate dioxane residual after the anaerobic treatment of TCE.

6.3.4 DD4 Effectively Eliminated Dioxane and Sustained its Abundance in Aerobic Microcosms

Dioxane in the field groundwater previously treated anaerobically with SDC-9 was efficiently removed by DD4 when propane was initially supplemented. Within 32 days of incubation, dioxane was degraded from 20.9±0.1 µg/L to below our MDL (i.e., 0.4 µg/L), meeting stringent groundwater cleanup guidance in NJ. Propane (300 µL) was supplemented twice to achieve a complete dioxane removal (Figure 6.5A and 6.6). Absolute qPCR analysis (Figure 6.7) revealed high abundance (6.7%) of DD4 over the course of bioaugmentation treatment with propane supplement.

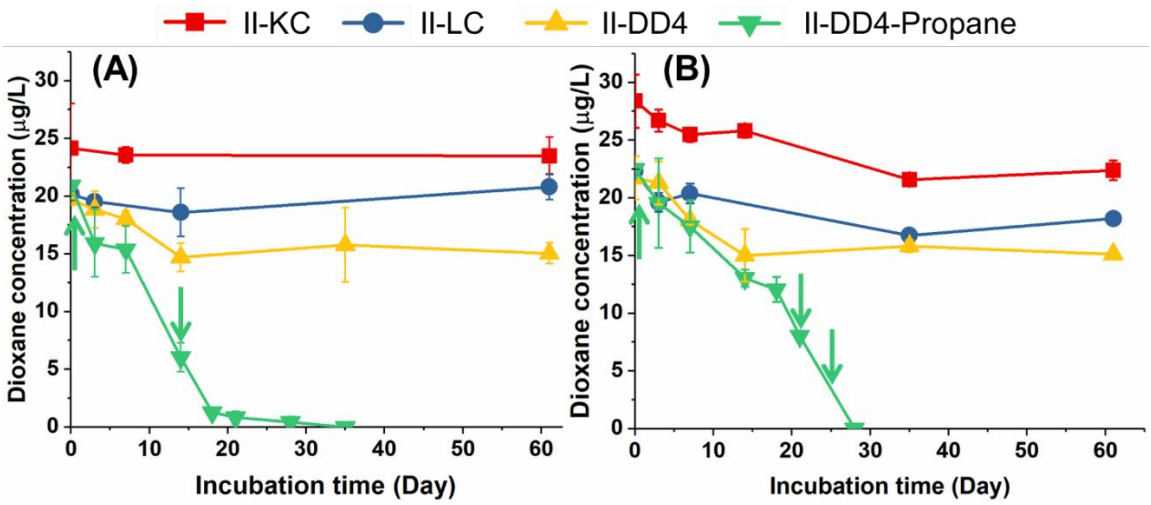

Figure 6.5 Dioxane depletion in the aerobic treatments, including killed control (II-KC), live control (II-LC), bioaugmentation with DD4 (II-DD4), and bioaugmentation with DD4 and propane (II-DD4-Propane). The aerobic microcosms were prepared with samples from the previous anaerobic treatment of (A) SDC-9 without sulfate (I-SDC) and (B) SDC-9 with sulfate amended (I-SDC-SO_4). Green arrows indicate the addition of propane.

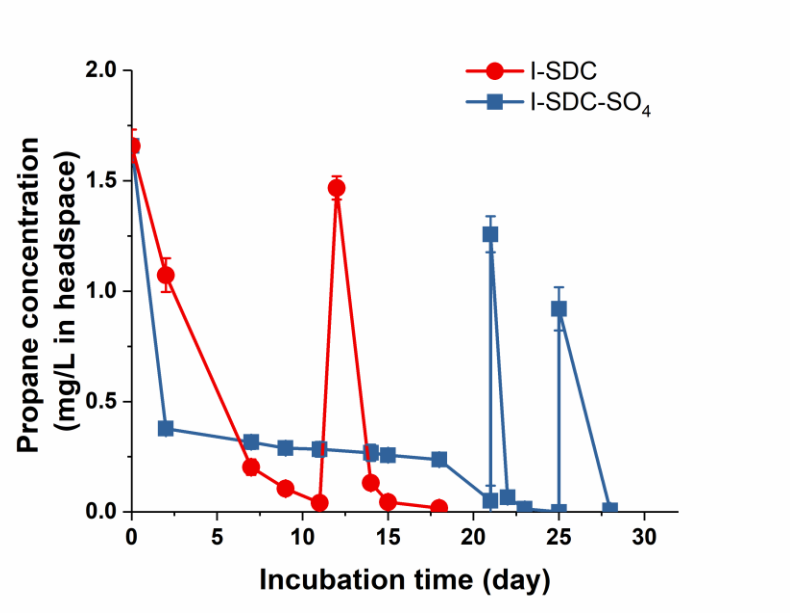

Figure 6.6 Propane consumption (mg/L in headspace) in aerobic treatment (II-DD4-Propane) after anaerobic treatment by SDC-9 bioaugmentation (I-SDC) or SDC-9 with sulfate addition (I-SDC-SO_4).

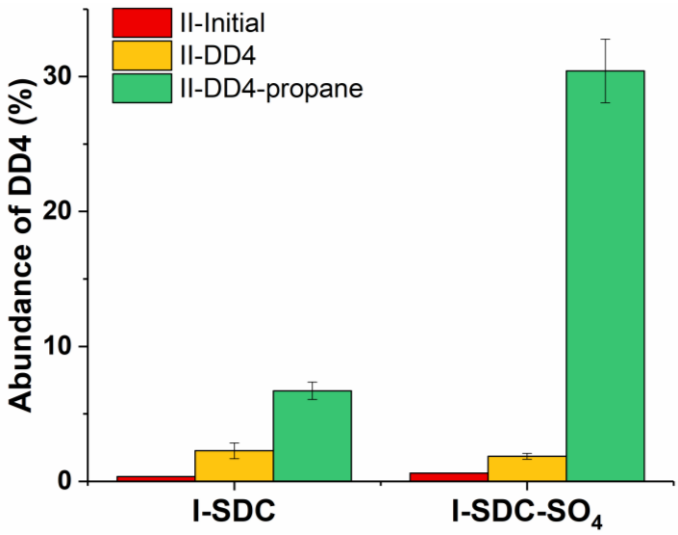

Figure 6.7 Relative abundance of DD4 estimated by qPCR in microcosms at the beginning and end of the aerobic treatments by DD4 and DD4 with propane. The x-axis indicates the samples were previously anaerobically treated by SDC-9 without sulfate (I-SDC) or with sulfate (I-SDC-SO_4).

Though at a slowed degradation rate, complete dioxane was also achieved by propane-fed DD4 in the microcosms prepared with aquifer samples previously treated with both SDC-9 and sulfate (I-SDC-SO_4) (Figure 6.5B). Interestingly, the initial propane consumption was unexpectedly fast. Around 77% of the initially dosed propane was quickly removed in the first 2 days of incubation (Figure 6.6). Later, propane consumption was markedly slowed down, taking 21 days for DD4 to completely degrade the rest of propane that was amended at the beginning (Figure 6.6). Concurrently, dioxane was degraded from 22.5±0.4 µg/L to 8.1±0.1 µg/L (Figure 6.5B). In contrast, in aerobic microcosms prepared with the samples treated with SDC-9 but no sulfate (I-SDC), only 12 days were spent to fully deplete the initial propane, while a similar dioxane removal to 8.4±1.0 µg/L was concurrently achieved (Figure 6.5A). The reason for the transient and fast depletion of propane observed in microcosms prepared with I-SDC-SO_4 samples was unclear. However, the slowed propane consumption and dioxane degradation between Day 2 and Day 18 may be due to some inhibitory factors to DD4 that were derived from previous anaerobic treatment with sulfate supplement (e.g. sulfur chemicals). Within 28 days of active treatment in the aerobic microcosms prepared with the I-SDC-SO_4 samples, propane was added three times resulting in a total amendment of 450 µL (Figure 6.6). This third amendment of propane also greatly accelerated dioxane degradation from Day 25 (Figure 6.5B) and enriched a higher abundance of DD4 is 30.4% in I-SDC-SO_4 in comparison with that in I-SDC (Figure 6.7).

Interestingly, even without the amendment of propane as the exogenous carbon source, there was over 25% disappearance of dioxane in DD4 bioaugmented treatments (II-DD4) within the first 2 weeks of incubation (Figure 6.5). However, dioxane degradation

ceased after 14 days. This suggests DD4 may be able to exploit carbon residuals (e.g., EVO and its fermentation metabolites) from the previous anaerobic treatments to empower the co-oxidation of dioxane. The limited availability of carbon sources was conducive to the relatively low but stable abundance of DD4, which were 2.6% and 2.7% in microcosms that received I-SDC and I-SDC-SO_4 samples, respectively. No significant dioxane degradation was observed in either killed or live controls (Figure 6.5).

Alkane (e.g., propane, isobutane, ethane) biostimulation has been examined and employed at many sites as an economically-efficient approach for *in situ* treatment of dioxane[40, 45, 47, 230]. In this study, we verified that propane as an auxiliary substrate can provide sufficient energy for DD4 enabling it becomes the dominant bacteria among the indigenous community. As in previous field investigation, such biostimulation with propane can accelerate the elimination of low concentrations of dioxane (e.g., 60, 135, and 1000 µg/L) at varying degradation rates ranging from 0.021 to 2/d, depending on (1) the types of substrate delivery methods (solubilization in recirculated groundwater or sparging); (2) different propane concentrations or phase; and especially (3) the microorganisms responsible for biodegradation[40]. Unlike the Gram-positive propanotrophs ENV425, CB1190, DD4 is planktonic Gram-negative microorganism which may exhibit better distribution and thus greater remediation radius once injected at contaminated sites[37].

6.3.5 DD4 Entailed Co-metabolic Degradation of cDCE and VC, two main Accumulating Products from TCE Dehalogenation

During the aerobic treatments by DD4, it was unanticipated that residual cDCE and VC were also removed along with dioxane degradation. After the primary anaerobic treatments by SDC-9 and aeration, we detected 1.4 µg/L of VC and 6.7 µg/L of cDCE remained in

the aqueous phase of the aerobic microcosms prepared with treated samples from I-SDC and I-SDC-SO_4, respectively. Notably, neither VC nor cDCE was detectable after the II-DD4-Propane treatment. Thus, biotransformation assays with resting cells of DD4 were further conducted to verify the ability of DD4 to co-metabolize cDCE or VC. Notably, cDCE and VC were both fully degraded by DD4 within 20 h and 5 h, respectively, when their initial concentrations were dosed at around 0.35 mg/L (Figure 6.8A). No significant loss of cDCE or VC was observed in the abiotic control treatments. Additional biotransformation assays revealed propane-fed DD4 was not able to co-metabolize TCE (data not shown).

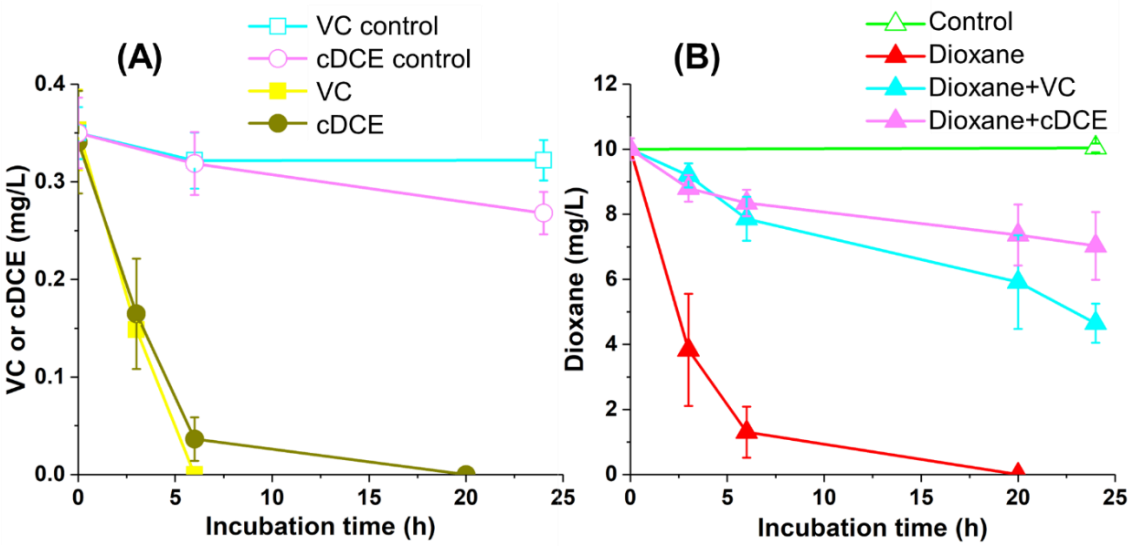

Figure 6.8 Degradation of dioxane by DD4 resting cells with or without the presence of VC and cDCE. The concentrations of cDCE and VC were shown in (A) and dioxane concentration was shown in (B).

To further mimic the commingled contamination observed in the field, microcosms were further prepared with the presence of co-contaminants, VC (1 mg/L), cDCE (1 mg/L), and dioxane (10 mg/L). DD4 was inoculated at a relatively low concentration (0.0034 mg

protein/mL) of DD4 and fed with 2 mg/L propane. Within the first 9 days of incubation, VC was primarily degraded from 1.11±0.02 mg/L to 0.13±0.08 mg/L, achieving 88.3% removal (Figure 6.9A). VC was fully depleted on Day 15. Concurrently, cDCE and dioxane were degraded much slower than VC. cDCE was degraded from 1.06±0.02 mg/L to 0.80±0.02 mg/L on Day 9, and 0.39±0.11 mg/L on Day 15. Only 18.1% of dioxane was removed in the first 15 days. After cDCE was degraded to as low as 0.03±0.01 mg/L on Day 18, dioxane degradation greatly accelerated. Dioxane was then degraded to below 0.1 mg/L on Day 30. This is the first report of a gram-negative propanotroph that can synchronize the removal of dioxane, cDCE, and VC.

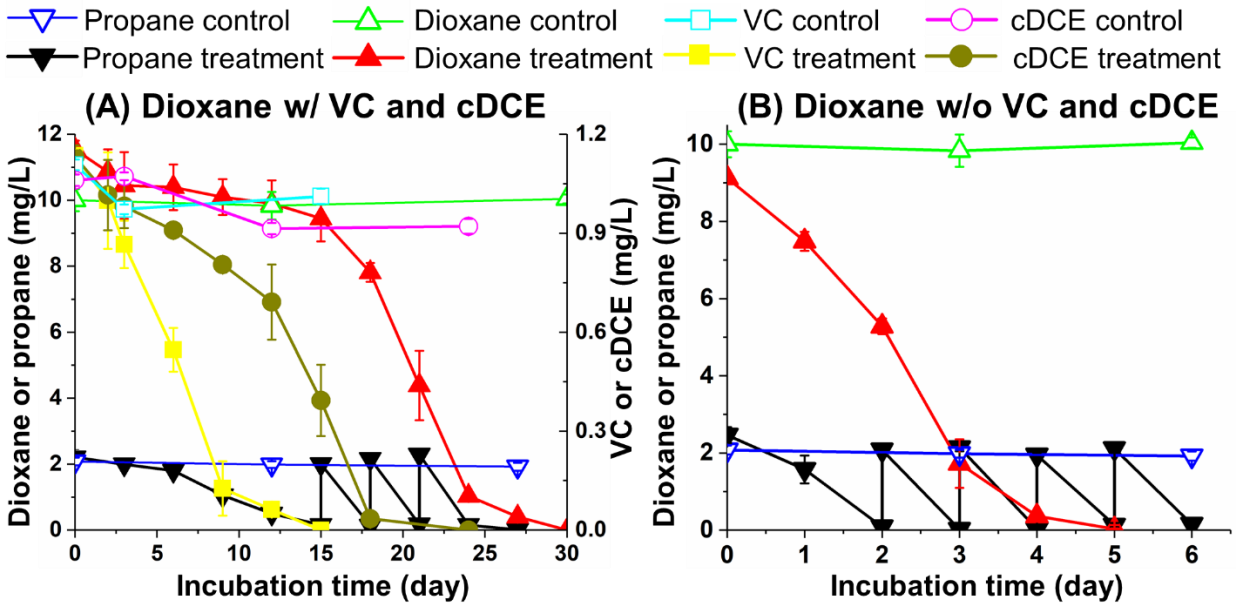

Figure 6.9 Co-metabolic degradation of dioxane (10 mg/L) by DD4 in anaerobically pretreated groundwater with (A) or without (B) the presence of VC (1 mg/L) and cDCE (1 mg/L).

A parallel treatment was dosed only with dioxane. Without the presence of cDCE or VC, complete dioxane removal was achieved within 5 days (Figure 6.9A). The

consumption of propane was also much faster, suggesting a greater growth of DD4 and steady enzyme expression. The initial dose of propane was fully depleted in 2 days when DD4 was not exposed to cDCE or VC. However, when both cDCE and VC were present, it took 15 days for the complete consumption of the same amount of propane. The prolonged propane consumption and dioxane degradation reflect the potential inhibitory efforts of cDCE and VC to DD4, even though both cVOCs can be fortuitously degraded by this propanotrophic bacterium.

According to previous studies, the observed VC and cDCE co-metabolism in DD4 may be attributed to the catalysis of SDIMOs[307]. There exist five putative SDIMO-encoding genes in DD4[185, 229]. Contributions of these SDIMOs to cDCE and VC oxidation underscores further molecular characterization. It is also interesting to observe VC degradation occurred prior to cDCE degradation. This tandem degradation order for VC and cDCE may be attributed to their difference in enzyme affinity as reported in some previous studies[308, 309]. For instance, *Pseudomonas aeruginosa* MF1 degraded VC faster than cDCE as it exhibited a much smaller half-saturation coefficient (K_m) of 0.26±0.037 μM for VC[310] than 22.0±0.8 μM for cDCE[309].

6.3.6 cDCE was More Potent in Inhibiting Dioxane Degradation by DD4 than VC

To assess the inhibitory effects of cDCE and VC, either compound was exposed to DD4 resting cells at an initial dosage of 0.35 mg/L. Significant inhibition to dioxane degradation was observed for both compounds in comparison with the control that received no cVOCs (Figure 6.8B). Without the presence of VC or cDCE, the resting cells of DD4 completely degraded 10.0±0.3 mg/L of dioxane in 20 h. However, in 24 h of incubation, dioxane concentration remained as high as 4.7±0.6 mg/L and 7.0±1.0 mg/L for VC-exposed and

cDCE-exposed DD4 cells, respectively. Thus, cDCE posed a more potent inhibition to DD4 since the dioxane degradation rate was significantly slower ($p < 0.05$) than that observed in VC-exposed cells.

A number of previous investigations have reported the inhibitory effects of cDCE and VC on aerobic biodegradation of dioxane or other groundwater contaminants. It was reported that 5 mg/L of cDCE showed significant inhibition to dioxane degradation by CB1190, and dioxane degradation completely halted at 50 mg/L of cDCE. Inhibitory effects of cDCE may be attributed to universal stress triggered by this compound [67]. To date, no previous studies have reported the inhibitory effects of VC on dioxane biodegradation. As a mutagen, VC can disrupt bacterial metabolism and their abilities to degrade cVOCs. A prior microcosm study observed reversible and irreversible inhibitions by VC (~5.0 mg/L) to aerobic co-metabolism of TCE and cDCE, respectively[311]. Similarly, Zhao *et al.* reported that the rate of cDCE (60 µM) degradation decreased with the increase of VC concentrations (from 10 to 110 µM)[312]. Collectively, degradation of VC that occurred prior to cDCE and dioxane as observed in our microcosms may result from the combination of high affinity to its degrading enzyme in DD4 and potent inhibitory effects (so the cells need to overcome first via co-metabolic decomposition).

6.4 Conclusions

Co-contamination of TCE (~ ppm level) and dioxane (~ ppb level) in groundwater is prevailing at sites in the US and globally. This study demonstrates an anaerobic and aerobic treatment train as a feasible and economical solution to mitigate this challenging co-contamination issue. Subsequent to the primary anaerobic treatment using reductive

dehalogenation by SDC-9, aerobic co-metabolism by DD4 can not only remove trace levels of dioxane but also eliminate undesirable metabolites (e.g., cDCE and VC) commonly generated from reductive dehalogenation. As indicated in our previous work, DD4 has also demonstrated a spectrum of properties compatible with *in situ* remediation technologies (e.g., biosparging), spanning fast planktonic growth, and the ability to exploit trace nutrients and adapt to diverse aquifer environments. The endured viability and activity of this strain in environmental samples pretreated with anaerobic procedures was also validated in this study. Though significant inhibition was observed by cDCE and VC, DD4's versatile catalytic capability allowed it to decompose these inhibiting compounds. This aerobic decomposition of cDCE and VC also avoids the undesired competition of electron acceptor in anaerobic degradation. Through engineering approaches (e.g., recirculation and air injection), the ability of DD4 to conquer field inhibitory factors can be reinforced to accelerate the site remediation and meet stringent cleanup goals for both cVOCs and dioxane.

At many bedrock formations like the one tested in this study, iron can be leached to the aqueous phase in the aquifer to supplement biotic and abiotic processes. Previous studies have demonstrated FeS can mediate abiotic transformation of TCE, contributing to the removal of this resistant compound. Through the addition of excessive sulfate, we intend to integrate this abiotic TCE removal into the anaerobic treatment. Unfortunately, our bench-scale tests revealed that benefits from sulfate amendment might be minimal for this bedrock formation. First, sulfate stimulated the growth of SRB in SDC-9. The dominated SRB outcompeted the halorespiring bacteria, especially those in charge of reducing cDCE to VC. Second, the production of reducing minerals may also hinder the

growth and activity of DD4 in the subsequent aerobic treatment. Combining these lines, SDC-9 without sulfate is suggested in the sequential treatment for TCE and dioxane bioremediation.

CHAPTER 7

CONCLUSIONS AND FUTURE WORK

This dissertation presents five parts oriented to innovate bioremediation for an environment-recalcitrant contaminant, dioxane, from the molecular foundation to two field applications.

Firstly, two dioxane degrading enzymes, PRM and THM, were compared based on their degradation kinetics, susceptibility to inhibition, substrate range. Our results reveal PRM may be more advantageous than THM particullary when dioxane concentration is low (xx μg/L) in the field. PRM also exhibits higher resistance to chlorinated solvents' inhibition and broader substrate range. However, due to the scarcity of previous research about PRM, its contribution to dioxane biodegradation has been long underestimated in the field. Thus, a comprehensive detection covering both PRM and THM could be more accurate for the assessment of dioxane MNA occurring at impacted sites. On the other hand, the extensive substrate range of PRM provides more options for stimulating the PRM-expressing bacteria native in the field. Thus, both MNA and biostimulation will benefit greatly from this study which extends our fundamental understanding of key enzymes that can degrade dioxane.

This dissertation also investigates the SDIMO enzyme family including phylogeny, evolution, substrate range, and regulation mechanisms using bioinformatics analysis. According to the amino acid sequences, operon arrangement, and physiological roles, SDIMOs are distinctly catagorized into 6 groups. Catalytic function of SDIMOs evolves from unsaturated compounds to saturated compounds, ultimately, to methane. According to the dissociation energy of C-H bonds in alkanes, SDIMOs exhibit an evolution direction

of oxidizing bonds with low energy toward high energy. Unlike, group-1,2, and 3 SDIMOs, whose transcription is regulated by the σ^{54}-dependent promoter, group-6 SDIMOs are regulated by the σ^{70}-dependent promoter, suggesting an activator is not essential to initiate the transcription of group-6 SDIMO genes. The profiling of the SDIMO family allows the bioprospecting of new SDIMOs recovered from the environment.

Driven by the necessity to complete the dioxane biodegradation pathway, a study that unravels the genomic differences between metabolic and co-metabolic degraders is conducted. Although it fails to figure out the key enzymes in charge of the HEAA oxidation, several downstream enzymes involved in glycolate transformation are unique to metabolic strains. This indicates that the downstream degradation pathway is also necessary for metabolic strains to obtain energy and carbon source form dioxane. We recommend some further transcriptomic and genomic analysis embracing additional dioxane degraders so that the gene library and analysis can be constructed in a more comprehensive and accurate fashion, which will facilitate the discovery of HEAA degrading gene(s) in the future.

In addition, we investigate the practical application of a new isolate, *Azoarcus* sp. DD4, with two sets of microcosm assays mimicking different *in situ* and *ex situ* treatment strategies. The first microcosm was set up with groundwater from a Superfund site located in the Northern New Jersey, where dioxane is prevailing low at concentrations ranging from 30 to 130 μg/L. After bioaugmentation with DD4 and propane, DD4 outcompetes other indigenous bacteria and becomes dominant in communities in tested groundwater, suggesting its robust adaptability for field application. However, the artificially inoculated dioxane metabolizers (i.e., PH-06 and CB1190) disappeared according to the qPCR and 16S rRNA sequencing analysis. Further analysis also confirmed that the gene encoding

the α subunit of dioxane degrading toluene monooxygenase in DD4, *tmoA*, is a suitable biomarker to monitor and assess the DD4 bioaugmentation as its abudance is positively correlated with the dioxane removal rates observed in the microcosms.

The other microcosm assay is conducted using samples from a site with commingled contamination of TCE and trace dioxane. An anaerobic-aerobic sequential treatment is employed to eliminate TCE by SDC-9 and remove dioxane by DD4. Though TCE was effectively removed, less-chlorinated products, vinyl chloride (VC) and *cis*-dichloroethene (cDCE), were generated over 16 weeks of incubation. During this anaerobic biotreatment, no significant dioxane degradation was observed. Subsequently, the microcosm materials were exposed to air and inoculated with *Azoarcus* sp. DD4, a cometabolic dioxane degrader. When fed with propane as the auxiliary substrate, DD4 was able to sustain its activity to degrade dioxane. After the course of aerobic bioaugmentation, the dominance of DD4 (~ 6%) in the microbial community was revealed by our qPCR assay using the biomarker specific to the toluene monooxygenase gene responsible for dioxane degradation in DD4. Even better, DD4 can also entail a concurrent biotransformation of both cDCE and VC and eliminate residuals of these undesirable products from the preceding reductive dehalogenation process. Presence of relatively high concentrations of cDCE and VC (e.g., 1 mg/L as in the aqueous phase) greatly inhibited the propane assimilation and growth of DD4. However, DD4 was able to overcome the hindrance and cometabolize VC and cDCE in sequence. Dioxane degradation was resumed once cDCE and VC were mostly depleted. This is the first report to demonstrate the feasibility of a treatment train combining reductive dehalogenation and aerobic co-oxidation processes in tandem to not only effectively clean up prevalent co-contamination

of TCE and dioxane but also mitigate less-chlorinated products (e.g., cDCE and VC) when reductive dehalogenation is incomplete.

REFERENCES

1. Lourenco, A., Research on polyatomic compounds. *Annals of Chemistry and of Physics* **1863,** *3*, (67), 257-339.

2. Mohr, T. K.; Stickney, J. A.; DiGuiseppi, W. H., *Environmental investigation and remediation: 1, 4-dioxane and other solvent stabilizers*. CRC Press: Boca Raton, FL, 2016.

3. Burrill, A. B.; Johnson, P. M., The ionization potential and ground state cation vibrational structure of 1, 4-dioxane. *Chemical Physics Letters* **2001,** *350*, (5-6), 473-478.

4. Anderson, R. H.; Anderson, J. K.; Bower, P. A., Co-occurrence of 1, 4-dioxane with trichloroethylene in chlorinated solvent groundwater plumes at US Air Force installations: Fact or fiction. *Integrated Environmental Assessment and Management* **2012,** *8*, (4), 731-737.

5. Toxicological Profile for 1, 4-dioxane. In Agency for Toxic Substances and Disease Registry Ed. Division of Toxicology and Environmental Medicine/Applied Toxicology Branch: Atlanta, Georgia, April 2012.

6. Abe, A., Distribution of 1,4-dioxane in relation to possible sources in the water environment. *Science of The Total Environment* **1999,** *227*, (1), 41-47.

7. Adamson, D. T.; Piña, E. A.; Cartwright, A. E.; Rauch, S. R.; Hunter Anderson, R.; Mohr, T.; Connor, J. A., 1,4-Dioxane drinking water occurrence data from the third unregulated contaminant monitoring rule. *Science of The Total Environment* **2017,** *596-597*, 236-245.

8. Adamson, D. T.; Mahendra, S.; Walker Jr, K. L.; Rauch, S. R.; Sengupta, S.; Newell, C. J., A multisite survey to identify the scale of the 1, 4-dioxane problem at contaminated groundwater sites. *Environmental Science and Technology Letters* **2014,** *1*, (5), 254-258.

9. Adamson, D. T.; de Blanc, P. C.; Farhat, S. K.; Newell, C. J., Implications of matrix diffusion on 1, 4-dioxane persistence at contaminated groundwater sites. *Science of the Total Environment* **2016,** *562*, 98-107.

10. Stepien, D. K.; Diehl, P.; Helm, J.; Thoms, A.; Püttmann, W., Fate of 1,4-dioxane in the aquatic environment: From sewage to drinking water. *Water Research* **2014,** *48*, 406-419.

11. The third unregulated contaminant monitoring rule (UCMR 3): data summary, January 2017. In United States Environmental Protection Agency, Ed. Office of Water, United States Environmental Protection Agency: 2017.

12. Adamson, D. T.; Anderson, R. H.; Mahendra, S.; Newell, C. J., Evidence of 1, 4-dioxane attenuation at groundwater sites contaminated with chlorinated solvents and 1, 4-dioxane. *Environmental Science and Technology* **2015,** *49*, (11), 6510-6518.

13. The drinking water standards and health advisories. In 2012 edition ed.; United States Environmental Protection Agency, Ed. Washington, DC, 2012.

14. European Union Risk Assessment Report. In European Commission, Institute for Health and Consumer Protection, European Chemicals Bureau, European Chemicals Bureau Ed. Office for Official Publications of the European Communities: Luxembourg, 2002; Vol. 21.

15. Criteria for a recommended standard occupational exposure to dioxane. In U.S. Department of Health Education and Welfare Center for Disease Control, Ed. National Institute for Occupational Safety and Health: Cincinnati, 1977.

16. Frank R. Lautenberg chemical safety for the 21st century act. In the United States of America, 2016.

17. 1,4-Dioxane in Drinking-water: Background document for development of WHO Guidelines for Drinking-water Quality. In World Health Organization Water Sanitation and Health: Irvine, CA, 2005.

18. 1,4-Dioxane (CASRN 123-91-1). In United States Environmental Protection Agency: 2013.

19. Protection, T. N. J. D. o. E., Ground Water Quality Standard 1,4‐Dioxane. In New Jersey Department of Environmental Protection, Ed. Trenton, NJ, 2015.

20. Stroo, H.; Ward, C., Future directions and research needs for chlorinated solvent plumes. In *In Situ Remediation of Chlorinated Solvent Plumes*, Springer: 2010; pp 699-725.

21. Adamson, D. T.; Mahendra, S.; Walker, K. L.; Rauch, S. R.; Sengupta, S.; Newell, C. J., A multisite survey to identify the scale of the 1,4-dioxane problem at contaminated groundwater sites. *Environmental Science & Technology Letters* **2014,** *1*, (5), 254-258.

22. Technical fact sheet-1,4-dioxane. In USEPA, Ed. Office of Land and Emergency, United States Environmental Protection Agency: 2017.

23. Woodard, S.; Mohr, T.; Nickelsen, M. G., Synthetic Media: A Promising New Treatment Technology for 1, 4‐Dioxane. *Remediation Journal* **2014,** *24*, (4), 27-40.

24. Li, W.; Patton, S.; Gleason, J. M.; Mezyk, S. P.; Ishida, K. P.; Liu, H., UV Photolysis of Chloramine and Persulfate for 1, 4-Dioxane Removal in Reverse-Osmosis Permeate for Potable Water Reuse. *Environmental Science and Technology* **2018**.

25. Nyer, E. K., *Groundwater treatment technology*. John Wiley & Sons: Hoboken, NJ, 1992.

26. Corin, N.; Backlund, P.; Kulovaara, M., Degradation products formed during UV-irradiation of humic waters. *Chemosphere* **1996,** *33*, (2), 245-255.

27. Andaluri, G.; Suri, R., Removal of 1, 4-dioxane and volatile organic compounds from groundwater using ozone-based advanced oxidation process. *Ozone: Science and Engineering* **2017,** *39*, (6), 423-434.

28. Li, M.; Liu, Y.; He, Y.; Mathieu, J.; Hatton, J.; DiGuiseppi, W.; Alvarez, P. J. J., Hindrance of 1,4-dioxane biodegradation in microcosms biostimulated with inducing or non-inducing auxiliary substrates. *Water Research* **2017,** *112*, 217-225.

29. Li, W.; Xu, E.; Schlenk, D.; Liu, H., Cyto-and Geno-Toxicity of 1, 4-Dioxane and Its Transformation Products during Ultraviolet-Driven Advanced Oxidation Processes. *Environmental Science: Water Research and Technology* **2018**.

30. Li, M.; Mathieu, J.; Liu, Y.; Van Orden, E. T.; Yang, Y.; Fiorenza, S.; Alvarez, P. J. J., The abundance of tetrahydrofuran/dioxane monooxygenase genes (*thmA*/*dxmA*) and 1,4-dioxane degradation activity are significantly correlated at various impacted aquifers. *Environmental Science and Technology Letters* **2014,** *1*, (1), 122-127.

31. Li, M.; Van Orden, E. T.; DeVries, D. J.; Xiong, Z.; Hinchee, R.; Alvarez, P. J., Bench-scale biodegradation tests to assess natural attenuation potential of 1, 4-dioxane at three sites in California. *Biodegradation* **2015,** *26*, (1), 39-50.

32. Li, M.; Mathieu, J.; Yang, Y.; Fiorenza, S.; Deng, Y.; He, Z.; Zhou, J.; Alvarez, P. J. J., Widespread distribution of soluble di-iron monooxygenase (SDIMO) genes in arctic groundwater impacted by 1,4-dioxane. *Environmental Science and Technology* **2013,** *47*, (17), 9950-9958.

33. Favara, P.; Tunks, J.; Hatton, J.; DiGuiseppi, W., Sustainable Remediation Considerations for Treatment of 1, 4‐Dioxane in Groundwater. *Remediation Journal* **2016,** *27*, (1), 133-158.

34. Orden, E. T. V. Microcosm Assessment of Aerobic Intrinsic Bioremediation and Mineralization Potential for three 1,4 Dioxane-Impacted Sites. Rice University, Houston, TX, 2013.

35. He, Y.; Mathieu, J.; Yang, Y.; Yu, P.; da Silva, M. L.; Alvarez, P. J., 1, 4-Dioxane biodegradation by *Mycobacterium dioxanotrophicus* PH-06 is associated with a group-6 soluble di-iron monooxygenase. *Environmental Science and Technology Letters* **2017,** *4*, (11), 494-499.

36. Deng, D.; Li, F.; Li, M., A novel propane monooxygenase initiating degradation of 1, 4-dioxane by *Mycobacterium dioxanotrophicus* PH-06. *Environmental Science and Technology Letters* **2017,** *5*, (2), 86-91.

37. Deng, D.; Li, F.; Wu, C.; Li, M., Synchronic Biotransformation of 1, 4-Dioxane and 1, 1-Dichloroethylene by a Gram-Negative Propanotroph *Azoarcus* sp. DD4. *Environmental Science and Technology Letters* **2018,** *5*, (8), 526-532.

38. Li, F.; Deng, D.; Li, M., Distinct Catalytic Behaviors between Two 1,4-Dioxane-Degrading Monooxygenases: Kinetics, Inhibition, and Substrate Range. *Environmental Science and Technology* **2020,** *54*, (3), 1898-1908.

39. Bennett, P.; Hyman, M.; Smith, C.; El Mugammar, H.; Chu, M.-Y.; Nickelsen, M.; Aravena, R., Enrichment with carbon-13 and deuterium during monooxygenase-mediated biodegradation of 1, 4-dioxane. *Environmental Science and Technology Letters* **2018,** *5*, (3), 148-153.

40. Chu, M. Y. J.; Bennett, P. J.; Dolan, M. E.; Hyman, M. R.; Peacock, A. D.; Bodour, A.; Anderson, R. H.; Mackay, D. M.; Goltz, M. N., Concurrent treatment of 1, 4-dioxane and chlorinated aliphatics in a groundwater recirculation system via aerobic cometabolism. *Groundwater Monitoring and Remediation* **2018,** *38*, (3), 53-64.

41. Li, M.; Fiorenza, S.; Chatham, J. R.; Mahendra, S.; Alvarez, P. J., 1, 4-Dioxane biodegradation at low temperatures in Arctic groundwater samples. *Water Research* **2010,** *44*, (9), 2894-2900.

42. Bell, C.; McDonough, J.; Houston, K. S.; Gerber, K., Stable Isotope Probing to Confirm Field-Scale Co-Metabolic Biodegradation of 1, 4-Dioxane. *Remediation Journal* **2016,** *27*, (1), 47-59.

43. Renn, T. In *Field-Scale In Situ Biostimulation Pilot Study for 1, 4-Dioxane Groundwater Plume Source Area*, Remediation of Chlorinated and Recalcitrant Compounds, Monterey, CA, 2012; Monterey, CA, 2012.

44. Rolston, H. M. Experimental demonstration and modeling of aerobic cometabolism of 1,4-dioxane by isobutane-utilizing microorganisms in aquifer microcosms. Oregon State University, 2018.

45. Rolston, H. M.; Hyman, M. R.; Semprini, L., Aerobic cometabolism of 1,4-dioxane by isobutane-utilizing microorganisms including *Rhodococcus rhodochrous* strain 21198 in aquifer microcosms: Experimental and modeling study. *Science of The Total Environment* **2019**, 133688.

46. DiGuiseppi, W.; Walecka-Hutchison, C.; Hatton, J., 1, 4-dioxane treatment technologies. *Remediation Journal* **2016,** *27*, (1), 71-92.

47. Lippincott, D.; Streger, S. H.; Schaefer, C. E.; Hinkle, J.; Stormo, J.; Steffan, R. J., Bioaugmentation and propane biosparging for *in situ* biodegradation of 1, 4-dioxane. *Groundwater Monitoring and Remediation* **2015,** *35*, (2), 81-92.

48. Isaka, K.; Udagawa, M.; Sei, K.; Ike, M., Pilot test of biological removal of 1, 4-dioxane from a chemical factory wastewater by gel carrier entrapping *Afipia* sp. strain D1. *Journal of Hazardous Materials* **2016,** *304*, 251-258.

49. Isaka, K.; Udagawa, M.; Kimura, Y.; Sei, K.; Ike, M., Biological wastewater treatment of 1, 4-dioxane using polyethylene glycol gel carriers entrapping *Afipia* sp. D1. *Journal of Bioscience and Bioengineering* **2016,** *121*, (2), 203-208.

50. Isaka, K.; Udagawa, M.; Kimura, Y.; Sei, K.; Ike, M., Biological 1, 4-dioxane wastewater treatment by immobilized *Pseudonocardia* sp. D17 on lower 1, 4-dioxane concentration. *Journal of Water and Environment Technology* **2016,** *14*, (4), 289-301.

51. Han, T.-H.; Han, J.-S.; So, M.-H.; Seo, J.-W.; Ahn, C.-M.; Min, D. H.; Yoo, Y. S.; Cha, D. K.; Kim, C. G., The removal of 1, 4-dioxane from polyester manufacturing process wastewater using an up-flow biological aerated filter (UBAF) packed with tire chips. *Journal of Environmental Science and Health, Part A* **2012,** *47*, (1), 117-129.

52. Plaehn, W. In *Full-Scale Treatment of 1, 4-Dioxane Using a Bioreactor: Progress Report*, Sixth International Conference on Remediation of Chlorinated and Recalcitrant Compounds, Monterey, CA, 2008; Monterey, CA, 2008.

53. Cordone, L.; Carlson, C.; Plaehn, W.; Shangraw, T.; Wilmoth, D., Case Study and Retrospective: Aerobic Fixed Film Biological Treatment Process for 1,4-Dioxane at the Lowry Landfill Superfund Site. *Remediation Journal* **2016,** *27*, (1), 159-172.

54. Mackay, D. M.; Cherry, J. A., Groundwater contamination: pump-and-treat remediation. *Environmental Science and Technology* **1989,** *23*, (6), 630-636.

55. Grostern, A.; Sales, C. M.; Zhuang, W.-Q.; Erbilgin, O.; Alvarez-Cohen, L., Glyoxylate metabolism is a key feature of the metabolic degradation of 1, 4-dioxane by *Pseudonocardia dioxanivorans* strain CB1190. *Applied and Environmental Microbiology* **2012,** *78*, (9), 3298-3308.

56. Mahendra, S.; Petzold, C. J.; Baidoo, E. E.; Keasling, J. D.; Alvarez-Cohen, L., Identification of the intermediates of in vivo oxidation of 1, 4-dioxane by monooxygenase-containing bacteria. *Environmental Science and Technology* **2007,** *41*, (21), 7330-7336.

57. Sales, C. M.; Grostern, A.; Parales, J. V.; Parales, R. E.; Alvarez-Cohen, L., Oxidation of the cyclic ethers 1, 4-dioxane and tetrahydrofuran by a monooxygenase in two *Pseudonocardia* species. *Applied and Environmental Microbiology* **2013,** *79*, (24), 7702-7708.

58. Kim, Y.-M.; Jeon, J.-R.; Murugesan, K.; Kim, E.-J.; Chang, Y.-S., Biodegradation of 1, 4-dioxane and transformation of related cyclic compounds by a newly isolated *Mycobacterium* sp. PH-06. *Biodegradation* **2009,** *20*, (4), 511.

59. Huang, H.; Shen, D.; Li, N.; Shan, D.; Shentu, J.; Zhou, Y., Biodegradation of 1, 4-dioxane by a novel strain and its biodegradation pathway. *Water, Air, and Soil Pollution* **2014,** *225*, (9), 2135.

60. Vainberg, S.; McClay, K.; Masuda, H.; Root, D.; Condee, C.; Zylstra, G. J.; Steffan, R. J., Biodegradation of ether pollutants by *Pseudonocardia* sp. strain ENV478. *Applied and Environmental Microbiology* **2006,** *72*, (8), 5218-5224.

61. Sei, K.; Oyama, M.; Kakinoki, T.; Inoue, D.; Ike, M., Isolation and characterization of tetrahydrofuran-degrading bacteria for 1, 4-dioxane-containing wastewater treatment by co-metabolic degradation. *Journal of Water and Environment Technology* **2013,** *11*, (1), 11-19.

62. Zhang, S.; Gedalanga, P. B.; Mahendra, S., Advances in bioremediation of 1, 4-dioxane-contaminated waters. *Journal of Environmental Management* **2017,** *204*, 765-774.

63. Coleman, N. V.; Bui, N. B.; Holmes, A. J., Soluble di-iron monooxygenase gene diversity in soils, sediments and ethene enrichments. *Environmental Microbiology* **2006,** *8*, (7), 1228-1239.

64. Mahendra, S.; Alvarez-Cohen, L., Kinetics of 1, 4-dioxane biodegradation by monooxygenase-expressing bacteria. *Environmental Science and Technology* **2006,** *40*, (17), 5435-5442.

65. Mahendra, S.; Grostern, A.; Alvarez-Cohen, L., The impact of chlorinated solvent co-contaminants on the biodegradation kinetics of 1, 4-dioxane. *Chemosphere* **2013,** *91*, (1), 88-92.

66. Grostern, A.; Alvarez-Cohen, L., RubisCO-based CO_2 fixation and C1 metabolism in the actinobacterium P seudonocardia dioxanivorans CB 1190. *Environmental Microbiology* **2013,** *15*, (11), 3040-3053.

67. Zhang, S.; Gedalanga, P. B.; Mahendra, S., Biodegradation kinetics of 1, 4-dioxane in chlorinated solvent mixtures. *Environmental Science and Technology* **2016,** *50*, (17), 9599-9607.

68. Wilson, J. T.; Mills, J. C.; Wilson, B. H.; Ferrey, M. L.; Freedman, D. L.; Taggart, D., Using qPCR Assays to Predict Rates of Cometabolism of TCE in Aerobic Groundwater. *Groundwater Monitoring and Remediation* **2019,** *39*, (2), 53-63.

69. Barajas-Rodriguez, F. J.; Freedman, D. L., Aerobic biodegradation kinetics for 1, 4-dioxane under metabolic and cometabolic conditions. *Journal of Hazardous Materials* **2018,** *350*, 180-188.

70. Kotani, T.; Kawashima, Y.; Yurimoto, H.; Kato, N.; Sakai, Y., Gene structure and regulation of alkane monooxygenases in propane-utilizing *Mycobacterium* sp. TY-6 and *Pseudonocardia* sp. TY-7. *Journal of Bioscience and Bioengineering* **2006,** *102*, (3), 184-192.

71. Deng, D.; Li, F.; Li, M., A Novel Propane Monooxygenase Initiating Degradation of 1,4-Dioxane by Mycobacterium dioxanotrophicus PH-06. *Environmental Science & Technology Letters* **2018,** *5*, (2), 86-91.

72. Tupa, P. R.; Masuda, H., Genomic analysis of propane metabolism in methyl *tert*-butyl ether-degrading *Mycobacterium* sp. strain ENV421. *Journal of Genomics* **2018,** *6*, 24-29.

73. Tupa, P. R.; Masuda, H., Comparative proteomic analysis of propane metabolism in *Mycobacterium* sp. strain ENV421 and *Rhodococcus* sp. strain ENV425. *Journal of Molecular Microbiology and Biotechnology* **2018,** *28*, (3), 107-115.

74. Masuda, H.; McClay, K.; Steffan, R. J.; Zylstra, G. J., Characterization of three propane-inducible oxygenases in *Mycobacterium* sp. strain ENV421. *Letters in Applied Microbiology* **2012,** *55*, (3), 175-181.

75. Young, J.; Braun, W.; Gehring, P.; Horvath, B.; Daniel, R., 1, 4-Dioxane and β-hydroxyethoxyacetic acid excretion in urine of humans exposed to dioxane vapors. *Toxicology and Applied Pharmacology* **1976,** *38*, (3), 643-646.

76. Young, J.; Braun, W.; Gehring, P., Dose-dependent fate of 1, 4-dioxane in rats. *Journal of Toxicology and Environmental Health,* **1978,** *4*, (5-6), 709-726.

77. Braun, W.; Young, J., Identification of β-hydroxyethoxyacetic acid as the major urinary metabolite of 1, 4-dioxane in the rat. *Toxicology and Applied Pharmacology* **1977,** *39*, (1), 33-38.

78. Woo, Y.-t.; Arcos, J. C.; Argus, M. F.; Griffin, G. W.; Nishiyama, K., Metabolism in vivo of dioxane: identification of p-dioxane-2-one as the major urinary metabolite. *Biochemical Pharmacology* **1977,** *26*, (16), 1535-1538.

79. Wenderoth, D.; Rosenbrock, P.; Abraham, W.-R.; Pieper, D.; Höfle, M., Bacterial community dynamics during biostimulation and bioaugmentation experiments aiming at chlorobenzene degradation in groundwater. *Microbial Ecology* **2003,** *46*, (2), 161-176.

80. Dalton, H.; Stirling, D., Co-metabolism. *Philosophical Transactions of the Royal Society of London. B, Biological Sciences* **1982,** *297*, (1088), 481-496.

81. Soil Screening Guidance: Technical background document. In Second Edition ed.; Agency, E. P., Ed. Office of Solid Waste and Emergency Response, United States Environmental Protection Agency: Washington, DC, 1996.

82. McCarty, P. L., In situ bioremediation of chlorinated solvents. *Current Opinion in Biotechnology* **1993,** *4*, (3), 323-330.

83. The drinking water standards and health advisories. In 2004 ed..; Office of Water, Ed. United States Environmental Protection Agency: Washington, DC, 2004.

84. Maymó-Gatell, X.; Chien, Y.-t.; Gossett, J. M.; Zinder, S. H., Isolation of a bacterium that reductively dechlorinates tetrachloroethene to ethene. *Science* **1997,** *276*, (5318), 1568-1571.

85. Vogel, T. M.; McCARTY, P. L., Biotransformation of tetrachloroethylene to trichloroethylene, dichloroethylene, vinyl chloride, and carbon dioxide under methanogenic conditions. *Applied Environmental Microbiology* **1985,** *49*, (5), 1080-1083.

86. Dang, H.; Kanitkar, Y. H.; Stedtfeld, R. D.; Hatzinger, P. B.; Hashsham, S. A.; Cupples, A. M., Abundance of Chlorinated Solvent and 1, 4-Dioxane Degrading Microorganisms at Five Chlorinated Solvent Contaminated Sites Determined via Shotgun Sequencing. *Environmental Science and Technology* **2018,** *52*, (23), 13914-13924.

87. Mattes, T. E.; Alexander, A. K.; Coleman, N. V., Aerobic biodegradation of the chloroethenes: pathways, enzymes, ecology, and evolution. *FEMS Microbiology Reviews* **2010,** *34*, (4), 445-475.

88. He, J.; Ritalahti, K. M.; Yang, K.-L.; Koenigsberg, S. S.; Löffler, F. E., Detoxification of vinyl chloride to ethene coupled to growth of an anaerobic bacterium. *Nature* **2003,** *424*, (6944), 62.

89. Vainberg, S.; Condee, C. W.; Steffan, R. J., Large-scale production of bacterial consortia for remediation of chlorinated solvent-contaminated groundwater. *Journal of Industrial Microbiology and Biotechnology* **2009,** *36*, (9), 1189-1197.

90. Schaefer, C. E.; Towne, R. M.; Vainberg, S.; McCray, J. E.; Steffan, R. J., Bioaugmentation for treatment of dense non-aqueous phase liquid in fractured sandstone blocks. *Environmental Science and Technology* **2010,** *44*, (13), 4958-4964.

91. Shen, W.; Chen, H.; Pan, S., Anaerobic biodegradation of 1,4-dioxane by sludge enriched with iron-reducing microorganisms. *Bioresource Technology* **2008,** *99*, (7), 2483-2487.

92. Parales, R. E.; Adamus, J. E.; White, N.; May, H. D., Degradation of 1,4-dioxane by an actinomycete in pure culture. *Applied and Environmental Microbiology* **1994,** *60*, (12), 4527-4530.

93. Li, M.; Yang, Y.; He, Y.; Mathieu, J.; Yu, C.; Li, Q.; Alvarez, P. J. J., Detection and cell sorting of Pseudonocardia species by fluorescence in situ hybridization and flow cytometry using 16S rRNA-targeted oligonucleotide probes. *Applied Microbiology and Biotechnology* **2018,** *102*, (7), 3375-3386.

94. Mahendra, S.; Alvarez-Cohen, L., *Pseudonocardia dioxanivorans* sp. nov., a novel actinomycete that grows on 1, 4-dioxane. *International Journal of Systematic and Evolutionary Microbiology* **2005,** *55*, (2), 593-598.

95. He, Y.; Wei, K.; Si, K.; Mathieu, J.; Li, M.; Alvarez, P. J., Whole-Genome Sequence of the 1, 4-Dioxane-Degrading Bacterium *Mycobacterium dioxanotrophicus* PH-06. *Genome Announcements* **2017,** *5*, (35), e00625-17.

96. Leahy, J. G.; Batchelor, P. J.; Morcomb, S. M., Evolution of the soluble diiron monooxygenases. *FEMS Microbiology Reviews* **2003,** *27*, (4), 449-479.

97. Holmes, A. J.; Coleman, N. V., Evolutionary ecology and multidisciplinary approaches to prospecting for monooxygenases as biocatalysts. *Antonie Van Leeuwenhoek* **2008,** *94*, (1), 75-84.

98. Gedalanga, P.; Madison, A.; Miao, Y. R.; Richards, T.; Hatton, J.; DiGuiseppi, W. H.; Wilson, J.; Mahendra, S., A Multiple Lines of Evidence Framework to Evaluate Intrinsic Biodegradation of 1, 4-Dioxane. *Remediation Journal* **2016,** *27*, (1), 93-114.

99. Li, M.; Liu, Y.; He, Y.; Mathieu, J.; Hatton, J.; DiGuiseppi, W.; Alvarez, P. J., Hindrance of 1, 4-dioxane biodegradation in microcosms biostimulated with inducing or non-inducing auxiliary substrates. *Water Research* **2017,** *112*, 217-225.

100. He, Y.; Mathieu, J.; da Silva, M. L. B.; Li, M.; Alvarez, P. J. J., 1,4-Dioxane-degrading consortia can be enriched from uncontaminated soils: prevalence of *Mycobacterium* and soluble di-iron monooxygenase genes. *Microbial Biotechnology* **2018,** *11*, (1), 189-198.

101. Furuya, T.; Hayashi, M.; Semba, H.; Kino, K., The mycobacterial binuclear iron monooxygenases require a specific chaperonin-like protein for functional expression in a heterologous host. *The FEBS Journal* **2013,** *280*, (3), 817-826.

102. Ly, M. A.; Liew, E. F.; Le, N. B.; Coleman, N. V., Construction and evaluation of pMycoFos, a fosmid shuttle vector for Mycobacterium spp. with inducible gene expression and copy number control. *Journal of Microbiological Methods* **2011,** *86*, (3), 320-326.

103. Cheung, S.; McCarl, V.; Holmes, A. J.; Coleman, N. V.; Rutledge, P. J., Substrate range and enantioselectivity of epoxidation reactions mediated by the ethene-oxidising Mycobacterium strain NBB4. *Applied Microbiology and Biotechnology* **2013,** *97*, (3), 1131-1140.

104. Laemmli, U. K., Cleavage of structural proteins during the assembly of the head of bacteriophage T4. *Nature* **1970,** *227*, (5259), 680-685.

105. Furuya, T.; Hirose, S.; Osanai, H.; Semba, H.; Kino, K., Identification of the monooxygenase gene clusters responsible for the regioselective oxidation of phenol to hydroquinone in mycobacteria. *Applied and Environmental Microbiology* **2011,** *77*, (4), 1214-1220.

106. Martin, K. E.; Ozsvar, J.; Coleman, N. V., SmoXYB1C1Z of *Mycobacterium* sp. strain NBB4: a soluble methane monooxygenase (sMMO)-like enzyme, active on C_2 to C_4 alkanes and alkenes. *Applied and Environmental Microbiology* **2014,** *80*, (18), 5801-5806.

107. Cheung, S.; McCarl, V.; Holmes, A. J.; Coleman, N. V.; Rutledge, P. J., Substrate range and enantioselectivity of epoxidation reactions mediated by the ethene-oxidising *Mycobacterium* strain NBB4. *Applied Microbiology Biotechnology* **2013,** *97*, (3), 1131-1140.

108. Kim, Y.; Arp, D. J.; Semprini, L., Kinetic and inhibition studies for the aerobic cometabolism of 1, 1, 1-trichloroethane, 1, 1-dichloroethylene, and 1, 1-dichloroethane by a butane-grown mixed culture. *Biotechnology and Bioengineering* **2002,** *80*, (5), 498-508.

109. Kim, Y.; Arp, D. J.; Semprini, L., A combined method for determining inhibition type, kinetic parameters, and inhibition coefficients for aerobic cometabolism of 1, 1, 1-trichloroethane by a butane-grown mixed culture. *Biotechnology and Bioengineering* **2002,** *77*, (5), 564-576.

110. Bradford, M. M., A rapid and sensitive method for the quantitation of microgram quantities of protein utilizing the principle of protein-dye binding. *Analytical Biochemistry* **1976,** *72*, (1-2), 248-254.

111. Gossett, J. M., Measurement of Henry's law constants for C1 and C2 chlorinated hydrocarbons. *Environmental Science and Technology* **1987,** *21*, (2), 202-208.

112. Darling, A. C.; Mau, B.; Blattner, F. R.; Perna, N. T., Mauve: multiple alignment of conserved genomic sequence with rearrangements. *Genome Research* **2004,** *14*, (7), 1394-1403.

113. Li, M.; Conlon, P.; Fiorenza, S.; Vitale, R. J.; Alvarez, P. J., Rapid analysis of 1, 4-dioxane in groundwater by frozen micro-extraction with gas chromatography/mass spectrometry. *Groundwater Monitoring and Remediation* **2011,** *31*, (4), 70-76.

114. Grady Jr, C. L.; Smets, B. F.; Barbeau, D. S., Variability in kinetic parameter estimates: a review of possible causes and a proposed terminology. *Water Research* **1996,** *30*, (3), 742-748.

115. Dolan, M. E.; McCarty, P. L., Methanotrophic chloroethene transformation capacities and 1,1-dichloroethene transformation product toxicity. *Environmental Science and Technology* **1995,** *29*, (11), 2741-2747.

116. Anderson, J. E.; McCarty, P. L., Effect of three chlorinated ethenes on growth rates for a methanotrophic mixed culture. *Environmental Science and Technology* **1996,** *30*, (12), 3517-3524.

117. Doughty, D. M.; Sayavedra-Soto, L. A.; Arp, D. J.; Bottomley, P. J., Effects of dichloroethene isomers on the induction and activity of butane monooxygenase in the alkane-oxidizing bacterium "*Pseudomonas butanovora*". *Applied and Environmental Microbiology* **2005,** *71*, (10), 6054-6059.

118. Ely, R. L.; Williamson, K. J.; Hyman, M. R.; Arp, D. J., Cometabolism of chlorinated solvents by nitrifying bacteria: kinetics, substrate interactions, toxicity effects, and bacterial response. *Biotechnology and Bioengineering* **1997,** *54*, (6), 520-534.

119. Arias, H. R.; Bhumireddy, P.; Bouzat, C., Molecular mechanisms and binding site locations for noncompetitive antagonists of nicotinic acetylcholine receptors. *The International Journal of Biochemistry and Cell Biology* **2006,** *38*, (8), 1254-1276.

120. Keenan, J.; Strand, S.; Stensel, H., Degradation kinetics of chlorinated solvents by a propane-oxidizing enrichment culture. In *Bioremediation of Chlorinated and Polycyclic Aromatic Hydrocarbon Compunds*, Lewis Publishers: 1994; pp 1-11.

121. Grostern, A.; Chan, W. W. M.; Edwards, E. A., 1,1,1-Trichloroethane and 1,1-dichloroethane reductive dechlorination kinetics and co-contaminant effects in a *Dehalobacter*-containing mixed culture. *Environmental Science and Technology* **2009,** *43*, (17), 6799-6807.

122. Halsey, K. H.; Sayavedra-Soto, L. A.; Bottomley, P. J.; Arp, D. J., Trichloroethylene degradation by butane-oxidizing bacteria causes a spectrum of toxic effects. *Applied Microbiology and Biotechnology* **2005,** *68*, (6), 794-801.

123. Lontoh, S.; Semrau, J. D., Methane and trichloroethylene degradation by *Methylosinus trichosporium* OB3b dxpressing particulate methane monooxygenase. *Applied and Environmental Microbiology* **1998,** *64*, (3), 1106-1114.

124. Atkins, G. L.; Nimmo, I. A., Current trends in the estimation of Michaelis-Menten parameters. *Analytical Biochemistry* **1980,** *104*, (1), 1-9.

125. Belpoggi, F.; Soffritti, M.; Maltoni, C., Methyl-tertiary-butyl ether (MTBE)—a gasoline additive—causes testicular and lympho haematopoietic cancers in rats. *Toxicology and Industrial Health* **1995,** *11*, (2), 119-149.

126. Coleman, N. V.; Yau, S.; Wilson, N. L.; Nolan, L. M.; Migocki, M. D.; Ly, M.-a.; Crossett, B.; Holmes, A. J., Untangling the multiple monooxygenases of *Mycobacterium chubuense* strain NBB4, a versatile hydrocarbon degrader. *Environmental Microbiology Reports* **2011,** *3*, (3), 297-307.

127. Steffan, R. J.; McClay, K.; Vainberg, S.; Condee, C. W.; Zhang, D., Biodegradation of the gasoline oxygenates methyl *tert*-butyl ether, ethyl *tert*-butyl ether, and *tert*-amyl methyl ether by propane-oxidizing bacteria. *Applied and Environmental Microbiology* **1997,** *63*, (11), 4216-4222.

128. Shields-Menard, S. A.; Brown, S. D.; Klingeman, D. M.; Indest, K.; Hancock, D.; Wewalwela, J. J.; French, W. T.; Donaldson, J. R., Draft genome sequence of *Rhodococcus rhodochrous* strain ATCC 21198. *Genome Announcements* **2014,** *2*, (1), e00054-14.

129. Cappelletti, M.; Presentato, A.; Milazzo, G.; Turner, R. J.; Fedi, S.; Frascari, D.; Zannoni, D., Growth of *Rhodococcus* sp. strain BCP1 on gaseous n-alkanes: new metabolic insights and transcriptional analysis of two soluble di-iron monooxygenase genes. *Frontiers in Microbiology* **2015,** *6*, 393.

130. Frascari, D.; Pinelli, D.; Nocentini, M.; Fedi, S.; Pii, Y.; Zannoni, D., Chloroform degradation by butane-grown cells of *Rhodococcus aetherovorans* BCP1. *Applied Microbiology and Biotechnology* **2006,** *73*, (2), 421-428.

131. Sales, C. M.; Mahendra, S.; Grostern, A.; Parales, R. E.; Goodwin, L. A.; Woyke, T.; Nolan, M.; Lapidus, A.; Chertkov, O.; Ovchinnikova, G., Genome Sequence of the 1, 4-Dioxane-Degrading *Pseudonocardia dioxanivorans* Strain CB1190. *Journal of Bacteriology* **2011,** *193*, (17), 4549-4550.

132. Yamamoto, N.; Saito, Y.; Inoue, D.; Sei, K.; Ike, M., Characterization of newly isolated *Pseudonocardia* sp. N23 with high 1, 4-dioxane-degrading ability. *Journal of Bioscience and Bioengineering* **2018,** *125*, (5), 552-558.

133. Kohlweyer, U.; Thiemer, B.; Schräder, T.; Andreesen, J. R., Tetrahydrofuran degradation by a newly isolated culture of *Pseudonocardia* sp. strain K1. *FEMS Microbiology Letters* **2000,** *186*, (2), 301-306.

134. Thiemer, B.; Andreesen, J. R.; Schräder, T., Cloning and characterization of a gene cluster involved in tetrahydrofuran degradation in *Pseudonocardia* sp. strain K1. *Archives of Microbiology* **2003,** *179*, (4), 266-277.

135. Masuda, H.; McClay, K.; Steffan, R. J.; Zylstra, G. J., Biodegradation of tetrahydrofuran and 1, 4-dioxane by soluble diiron monooxygenase in *Pseudonocardia* sp. strain ENV478. *Journal of Molecular Microbiology and Biotechnology* **2012,** *22*, (5), 312-316.

136. Yao, Y.; Lv, Z.; Min, H.; Lv, Z.; Jiao, H., Isolation, identification and characterization of a novel *Rhodococcus* sp. strain in biodegradation of tetrahydrofuran and its medium optimization using sequential statistics-based experimental designs. *Bioresource Technology* **2009,** *100*, (11), 2762-2769.

137. Rojo, F., Enzymes for aerobic degradation of alkanes. In *Handbook of hydrocarbon and lipid microbiology*, 2010; pp 781-797.

138. Zhou, Y.; Huang, H.; Shen, D., Multi-substrate biodegradation interaction of 1, 4-dioxane and BTEX mixtures by *Acinetobacter baumannii* DD1. *Biodegradation* **2016,** *27*, (1), 37-46.

139. Paul Hare, M. H. In *Aerobic degradation of 1,4-dioxane in a fixed-film bioreactor with toluene, other volatiles and phenolics as co-contaminants*, Eleventh (11th) International Conference on the Remediation of Chlorinated and Recalcitrant Compounds, Palm Springs, California, 2018; Palm Springs, California, 2018.

140. Bartsch, H.; Montesano, R., Mutagenic and carcinogenic effects of vinyl chloride. *Mutation Research/Reviews in Genetic Toxicology* **1975,** *32*, (2), 93-113.

141. Griffin, B. M.; Tiedje, J. M.; Löffler, F. E., Anaerobic microbial reductive dechlorination of tetrachloroethene to predominately *trans*-1,2-dichloroethene. *Environmental Science and Technology* **2004,** *38*, (16), 4300-4303.

142. Toxicological profile for benzene. In Services, U. S. D. o. H. a. H., Ed. Atlanta, Georgia, 2007.

143. Alvarez, P. J.; Illman, W. A., *Bioremediation and natural attenuation: process fundamentals and mathematical models*. John Wiley & Sons: 2005; Vol. 27.

144. Holmes, A. J., The diversity of soluble di-iron monooxygenases with bioremediation applications. In *Advances in Applied Bioremediation*, Singh, A.; Kuhad, R. C.; Ward, O. P., Eds. Springer Berlin Heidelberg: Berlin, Heidelberg, 2009; pp 91-102.

145. Gaze, W. H.; Zhang, L.; Abdouslam, N. A.; Hawkey, P. M.; Calvo-Bado, L.; Royle, J.; Brown, H.; Davis, S.; Kay, P.; Boxall, A. B., Impacts of anthropogenic activity on the ecology of class 1 integrons and integron-associated genes in the environment. *The ISME Journal* **2011,** *5*, (8), 1253.

146. Gaze, W. H.; Krone, S. M.; Larsson, D. J.; Li, X.-Z.; Robinson, J. A.; Simonet, P.; Smalla, K.; Timinouni, M., Influence of humans on evolution and mobilization of environmental antibiotic resistome. *Emerging Infectious Diseases* **2013,** *19*, (7).

147. Hatzinger, P. B.; Banerjee, R.; Rezes, R.; Streger, S. H.; McClay, K.; Schaefer, C. E., Potential for cometabolic biodegradation of 1,4-dioxane in aquifers with methane or ethane as primary substrates. *Biodegradation* **2017,** *28*, (5), 453-468.

148. Notomista, E.; Lahm, A.; Di Donato, A.; Tramontano, A., Evolution of bacterial and archaeal multicomponent monooxygenases. *Journal of Molecular Evolution* **2003,** *56*, (4), 435-445.

149. Osborne, C. D.; Haritos, V. S., Beneath the surface: Evolution of methane activity in the bacterial multicomponent monooxygenases. *Molecular Phylogenetics and Evolution* **2019,** *139*, 106527.

150. Madhavan, A.; Sindhu, R.; Parameswaran, B.; Sukumaran, R. K.; Pandey, A., Metagenome Analysis: a Powerful Tool for Enzyme Bioprospecting. *Applied Biochemistry and Biotechnology* **2017,** *183*, (2), 636-651.

151. Rosenzweig, A. C.; Frederick, C. A.; Lippard, S. J., Crystal structure of a bacterial non-haem iron hydroxylase that catalyses the biological oxidation of methane. *Nature* **1993,** *366*, (6455), 537-543.

152. Edgar, R. C., MUSCLE: multiple sequence alignment with high accuracy and high throughput. *Nucleic Acids Research* **2004,** *32*, (5), 1792-1797.

153. Guindon, S.; Dufayard, J.-F.; Lefort, V.; Anisimova, M.; Hordijk, W.; Gascuel, O., New algorithms and methods to estimate maximum-likelihood phylogenies: assessing the performance of PhyML 3.0. *Systematic Biology* **2010,** *59*, (3), 307-321.

154. Darriba, D.; Taboada, G. L.; Doallo, R.; Posada, D., ProtTest 3: fast selection of best-fit models of protein evolution. *Bioinformatics* **2011,** *27*, (8), 1164-1165.

155. Letunic, I.; Bork, P., Interactive tree of life (iTOL) v3: an online tool for the display and annotation of phylogenetic and other trees. *Nucleic Acids Research* **2016,** *44*, (W1), W242-W245.

156. Kotani, T.; Yamamoto, T.; Yurimoto, H.; Sakai, Y.; Kato, N., Propane monooxygenase and NAD+-dependent secondary alcohol dehydrogenase in propane metabolism by Gordonia sp. strain TY-5. *Journal of Bacteriology* **2003,** *185*, (24), 7120-7128.

157. Sharp, J. O.; Sales, C. M.; Alvarez-Cohen, L., Functional characterization of propane-enhanced N-nitrosodimethylamine degradation by two actinomycetales. *Biotechnology and Bioengineering* **2010,** *107*, (6), 924-932.

158. Robrock, K. R.; Mohn, W. W.; Eltis, L. D.; Alvarez-Cohen, L., Biphenyl and ethylbenzene dioxygenases of *Rhodococcus jostii* RHA1 transform PBDEs. *Biotechnology and Bioengineering* **2011,** *108*, (2), 313-321.

159. Weerdenburg, E. M.; Abdallah, A. M.; Rangkuti, F.; Otto, T. D.; El Ghany, M. A.; Adroub, S. A.; Molenaar, D.; Ummels, R.; ter Veen, K.; van Stempvoort, G., Pathogenic mycobacteria customize their virulence mechanisms for intracellular replication in different hosts. In 2014; pp 115-143.

160. Amábile-Cuevas, C. F.; Chicurel, M. E., Bacterial plasmids and gene flux. *Cell* **1992,** *70*, (2), 189-199.

161. Ochman, H.; Lawrence, J. G.; Groisman, E. A., Lateral gene transfer and the nature of bacterial innovation. *Nature* **2000,** *405*, (6784), 299.

162. Nordlund, I.; Powlowski, J.; Shingler, V., Complete nucleotide sequence and polypeptide analysis of multicomponent phenol hydroxylase from *Pseudomonas* sp. strain CF600. *Journal of Bacteriology* **1990,** *172*, (12), 6826-6833.

163. Shingler, V.; Franklin, F. C. H.; Tsuda, M.; Holroyd, D.; Bagdasarian, M., Molecular analysis of a plasmid-encoded phenol hydroxylase from *Pseudomonas* CF600. *Microbiology* **1989,** *135*, (5), 1083-1092.

164. Herrmann, H.; Janke, D.; Krejsa, S.; Kunze, I., Involvement of the plasmid pPGH1 in the phenol degradation of Pseudomonas putida strain H. *FEMS Microbiology Letters* **1987,** *43*, (2), 133-137.

165. Herrmann, H.; Müller, C.; Schmidt, I.; Mahnke, J.; Petruschka, L.; Hahnke, K., Localization and organization of phenol degradation genes of *Pseudomonas putida* strain H. *Molecular and General Genetics MGG* **1995,** *247*, (2), 240-246.

166. Ng, L. C.; Shingle, V.; Sze, C. C.; Poh, C. L., Cloning and sequences of the first eight genes of the chromosomally encoded (methyl) phenol degradation pathway from *Pseudomonas putida* P35X. *Gene* **1994,** *151*, (1-2), 29-36.

167. Ehrt, S.; Schirmer, F.; Hillen, W., Genetic organization, nucleotide sequence and regulation of expression of genes encoding phenol hydroxylase and catechol 1, 2-dioxygenase in *Acinetobacter calcoaceticus* NCIB8250. *Molecular Microbiology* **1995,** *18*, (1), 13-20.

168. Horinouchi, M.; Kasuga, K.; Nojiri, H.; Yamane, H.; Omori, T., Cloning and characterization of genes encoding an enzyme which oxidizes dimethyl sulfide in *Acinetobacter* sp. strain 20B. *FEMS Microbiology Letters* **1997,** *155*, (1), 99-105.

169. Iwashita, S.; Shim, H.; Wood, T. K., Directed evolution of toluene ortho-monooxygenase for enhanced 1-naphthol synthesis and chlorinated ethene degradation. *Journal of Bacteriology* **2002,** *184*, (2), 344-349.

170. Shields, M.; Reagin, M.; Gerger, R.; Campbell, R.; Somerville, C., TOM, a new aromatic degradative plasmid from Burkholderia (*Pseudomonas*) *cepacia* G4. *Applied and Environmental Microbiology* **1995,** *61*, (4), 1352-1356.

171. Johnson, G. R.; Olsen, R. H., Nucleotide sequence analysis of genes encoding a toluene/benzene-2-monooxygenase from *Pseudomonas* sp. strain JS150. *Applied and Environmental Microbiology* **1995,** *61*, (9), 3336-3346.

172. Arai, H.; Akahira, S.; Ohishi, T.; Maeda, M.; Kudo, T., Adaptation of *Cornamonas testosteroni* TAM1 to utilize phenol: organization and regulation of the genes involved in phenol degradatio. *Microbiology* **1998,** *144*, (10), 2895-2903.

173. Teramoto, M.; Futamata, H.; Harayama, S.; Watanabe, K., Characterization of a high-affinity phenol hydroxylase from *Comamonas testosteroni* R5 by gene cloning, and expression in Pseudomonas aeruginosa PAO1c. *Molecular and General Genetics MGG* **1999,** *262*, (3), 552-558.

174. Hino, S.; Watanabe, K.; Takahashi, N., Phenol hydroxylase cloned from *Ralstonia eutropha* strain E2 exhibits novel kinetic properties. *Microbiology* **1998,** *144*, (7), 1765-1772.

175. Yen, K.-M.; Karl, M. R.; Blatt, L. M.; Simon, M. J.; Winter, R. B.; Fausset, P. R.; Lu, H. S.; Harcourt, A. A.; Chen, K. K., Cloning and characterization of a *Pseudomonas mendocina* KR1 gene cluster encoding toluene-4-monooxygenase. *Journal of Bacteriology* **1991,** *173*, (17), 5315-5327.

176. Yen, K.; Karl, M. R., Identification of a new gene, tmoF, in the *Pseudomonas mendocina* KR1 gene cluster encoding toluene-4-monooxygenase. *Journal of Bacteriology* **1992,** *174*, (22), 7253-7261.

177. Bertoni, G.; Martino, M.; Galli, E.; Barbieri, P., Analysis of the gene cluster encoding toluene/o-xylene monooxygenase from *Pseudomonas stutzeri* OX1. *Applied and Environmental Microbiology* **1998,** *64*, (10), 3626-3632.

178. Byrne, A. M.; Olsen, R. H., Cascade regulation of the toluene-3-monooxygenase operon (*tbuA1UBVA2C*) of *Burkholderia pickettii* PKO1: role of the *tbuA1* promoter (PtbuA1) in the expression of its cognate activator, TbuT. *Journal of Bacteriology* **1996,** *178*, (21), 6327-6337.

179. Zhou, N.-Y.; Jenkins, A.; Chion, C. K. C. K.; Leak, D. J., The alkene monooxygenase from *Xanthobacter* strain Py2 is closely related to aromatic monooxygenases and catalyzes aromatic monohydroxylation of benzene, toluene, and phenol. *Applied and Environmental Microbiology* **1999,** *65*, (4), 1589-1595.

180. Krum, J. G.; Ensign, S. A., Evidence that a Linear Megaplasmid Encodes Enzymes of Aliphatic Alkene and Epoxide Metabolism and Coenzyme M (2-Mercaptoethanesulfonate) Biosynthesis in *Xanthobacter* Strain Py2. *Journal of Bacteriology* **2001,** *183*, (7), 2172-2177.

181. Ayoubi, P. J.; Harker, A. R., Whole-cell kinetics of trichloroethylene degradation by phenol hydroxylase in a *Ralstonia eutropha* JMP134 derivative. *Applied and Environmental Microbiology* **1998,** *64*, (11), 4353-4356.

182. van Hylckama Vlieg, J. E.; Leemhuis, H.; Spelberg, J. H. L.; Janssen, D. B., Characterization of the gene cluster involved in isoprene metabolism in *Rhodococcus* sp. strain AD45. *Journal of Bacteriology* **2000,** *182*, (7), 1956-1963.

183. Millacura, F. A.; Cardenas, F.; Mendez, V.; Seeger, M.; Rojas, L. A., Degradation of benzene by the heavy-metal resistant bacterium *Cupriavidus metallidurans* CH34 reveals its catabolic potential for aromatic compounds. *bioRxiv* **2017**, 164517.

184. Bouhajja, E.; McGuire, M.; Liles, M. R.; Bataille, G.; Agathos, S. N.; George, I. F., Identification of novel toluene monooxygenase genes in a hydrocarbon-polluted sediment using sequence-and function-based screening of metagenomic libraries. *Applied Microbiology and Biotechnology* **2017,** *101*, (2), 797-808.

185. Deng, D.; Li, F.; Ye, L.; Li, M., Complete Genome Sequence of *Azoarcus* sp. Strain DD4, a Gram-Negative Propanotroph That Degrades 1,4-Dioxane and 1,1-Dichloroethylene. *Microbiology Resource Announcements* **2019,** *8*, (33), e00775-19.

186. Stainthorpe, A.; Lees, V.; Salmond, G. P.; Dalton, H.; Murrell, J. C., The methane monooxygenase gene cluster of *Methylococcus capsulatus* (Bath). *Gene* **1990,** *91*, (1), 27-34.

187. Stainthorpe, A. C.; Murrell, J. C.; Salmond, G. P.; Dalton, H.; Lees, V., Molecular analysis of methane monooxygenase from *Methylococcus capsulatus* (Bath). *Archives of Microbiology* **1989,** *152*, (2), 154-159.

188. Shigematsu, T.; Hanada, S.; Eguchi, M.; Kamagata, Y.; Kanagawa, T.; Kurane, R., Soluble methane monooxygenase gene clusters from trichloroethylene-degrading *Methylomonas* sp. strains and detection of methanotrophs during in situ bioremediation. *Applied and Environmental Microbiology* **1999,** *65*, (12), 5198-5206.

189. Cardy, D.; Laidler, V.; Salmond, G.; Murrell, J., Molecular analysis of the methane monooxygenase (MMO) gene cluster of *Methylosinus trichosporium* OB3b. *Molecular Microbiology* **1991,** *5*, (2), 335-342.

190. Cardy, D.; Laidler, V.; Salmond, G.; Murrell, J., The methane monooxygenase gene cluster of *Methylosinus trichosporium*: cloning and sequencing of the *mmoC* gene. *Microbiology* **1991,** *156*, (6), 477-483.

191. McDonald, I.; Uchiyama, H.; Kambe, S.; Yagi, O.; Murrell, J., The soluble methane monooxygenase gene cluster of the trichloroethylene-degrading methanotroph *Methylocystis* sp. strain M. *Applied and Environmental Microbiology* **1997,** *63*, (5), 1898-1904.

192. Grosse, S.; Laramee, L.; Wendlandt, K.-D.; McDonald, I. R.; Miguez, C. B.; Kleber, H.-P., Purification and Characterization of the Soluble Methane Monooxygenase of the Type II Methanotrophic Bacterium *Methylocystis* sp. Strain WI 14. *Applied and Environmental Microbiology* **1999,** *65*, (9), 3929-3935.

193. Saitoh, S.; Aoyama, H.; Akutsu, M.; Nakano, K.; Shinzato, N.; Matsui, T., Genomic sequencing-based detection of large deletions in *Rhodococcus rhodochrous* strain B-276. *Journal of Bioscience and Bioengineering* **2013,** *116*, (3), 309-312.

194. Garcia, M. J.; Gola, S., Gene and whole genome analyses reveal that the mycobacterial strain JS 623 is not a member of the species *Mycobacterium smegmatis*. *Microbial Biotechnology* **2016,** *9*, (2), 269-274.

195. Mattes, T. E.; Coleman, N. V.; Spain, J. C.; Gossett, J. M., Physiological and molecular genetic analyses of vinyl chloride and ethene biodegradation in *Nocardioides* sp. strain JS614. *Archives of Microbiology* **2005,** *183*, (2), 95-106.

196. Kurokawa, S.; Kabayama, J.; Hwang, S. D.; Nho, S. W.; Hikima, J.-i.; Jung, T. S.; Kondo, H.; Hirono, I.; Takeyama, H.; Mori, T., Whole genome analyses of marine fish pathogenic isolate, *Mycobacterium* sp. 012931. *Marine Biotechnology* **2014,** *16*, (5), 572-579.

197. Rhodes, M. W.; Kator, H.; McNabb, A.; Deshayes, C.; Reyrat, J.-M.; Brown-Elliott, B. A.; Wallace Jr, R.; Trott, K. A.; Parker, J. M.; Lifland, B., Mycobacterium pseudoshottsii sp. nov., a slowly growing chromogenic species isolated from Chesapeake Bay striped bass (Morone saxatilis). *International Journal of Systematic and Evolutionary Microbiology* **2005,** *55*, (3), 1139-1147.

198. Das, S.; Pettersson, B. F.; Behra, P. R. K.; Mallick, A.; Cheramie, M.; Ramesh, M.; Shirreff, L.; DuCote, T.; Dasgupta, S.; Ennis, D. G., Extensive genomic diversity among Mycobacterium marinum strains revealed by whole genome sequencing. *Scientific Reports* **2018,** *8*, (1), 1-15.

199. Saad, J.; Combe, M.; Hammoudi, N.; Couppié, P.; Blaizot, R.; Jedir, F.; Gozlan, R. E.; Drancourt, M.; Bouam, A., Whole-Genome Sequence of Mycobacterium ulcerans CSURP7741, a French Guianan Clinical Isolate. *Microbiology Resource Announcements* **2019,** *8*, (29), e00215-19.

200. Phelippeau, M.; Croce, O.; Robert, C.; Raoult, D.; Drancourt, M., Draft Genome Sequence of *Mycobacterium lentiflavum* CSUR P1491. *Genome Announcements* **2015,** *3*, (4), e00817-15.

201. Guéret, C.; Daroux, M.; Billaud, F., Methane pyrolysis: thermodynamics. *Chemical Engineering Science* **1997,** *52*, (5), 815-827.

202. Kopp, D. A.; Lippard, S. J., Soluble methane monooxygenase: activation of dioxygen and methane. *Current Opinion in Chemical Biology* **2002,** *6*, (5), 568-576.

203. Rosenzweig, A. C., Breaking methane. *Nature* **2015,** *518*, (7539), 309-310.

204. Dean, J. A., *Lange's handbook of chemistry*. Sixteenth Edition ed.; New york; London: McGraw-Hill, Inc.: New York, 1999.

205. Kerr, J., Bond dissociation energies by kinetic methods. *Chemical Reviews* **1966,** *66*, (5), 465-500.

206. Gurvich, L.; Karachevtsev, G.; Kondrat'ev, V.; Lebedev, Y. A.; Medvedev, V.; Potapov, V.; Khodeev, Y. S., Ionization potentials and electron affinity. In *Breaking Energy of Chemical Bonds*, Nauka, Moscow, 1974.

207. Gribov, L.; Novakov, I.; Pavlyuchko, A.; Kulago, I.; Orlinson, B., "Spectroscopic" Calculations of CH Bond Dissociation Energies for Ethane, Propane, Butane, Isobutane, Pentane, Hexane, and Neopentane Using Fundamental Vibration Frequencies. *Journal of Structural Chemistry* **2003,** *44*, (6), 961-969.

208. Battin, F.; Marquaire, P.; Baronnet, F.; Come, G., Products of the gas-phase pyrolysis of 1, 4-dioxane. *Journal of Analytical and Applied Pyrolysis* **1989,** *16*, (4), 345-354.

209. Cruickshank, F. R.; Benson, S. W., Kinetics and mechanism of the reaction of iodine with tetrahydrofuran. Carbon-hydrogen bond dissociation energy in tetrahydrofuran. *Journal of the American Chemical Society* **1969,** *91*, (6), 1289-1292.

210. Harley, C. B.; Reynolds, R. P., Analysis of E. coli pormoter sequences. *Nucleic Acids Research* **1987,** *15*, (5), 2343-2361.

211. Schumacher, J.; Zhang, X.; Jones, S.; Bordes, P.; Buck, M., ATP-dependent transcriptional activation by bacterial PspF AAA+ protein. *Journal of Molecular Biology* **2004,** *338*, (5), 863-875.

212. Neuwald, A. F.; Aravind, L.; Spouge, J. L.; Koonin, E. V., AAA+: A class of chaperone-like ATPases associated with the assembly, operation, and disassembly of protein complexes. *Genome Research* **1999,** *9*, (1), 27-43.

213. Bush, M.; Dixon, R., The role of bacterial enhancer binding proteins as specialized activators of σ54-dependent transcription. *Microbiology and Molecular Biology Reviews* **2012,** *76*, (3), 497-529.

214. Csaki, R.; Bodrossy, L.; Klem, J.; Murrell, J. C.; Kovacs, K. L., Genes involved in the copper-dependent regulation of soluble methane monooxygenase of *Methylococcus capsulatus* (Bath): cloning, sequencing and mutational analysis. *Microbiology* **2003,** *149*, (7), 1785-1795.

215. Stafford, G. P.; Scanlan, J.; McDonald, I. R.; Murrell, J. C., *rpoN, mmoR and mmoG*, genes involved in regulating the expression of soluble methane monooxygenase in *Methylosinus trichosporium* OB3b. *Microbiology* **2003,** *149*, (7), 1771-1784.

216. Rippe, K.; Guthold, M.; von Hippel, P. H.; Bustamante, C., Transcriptional activation via DNA-looping: visualization of intermediates in the activation pathway of *E.* coli RNA polymerase· σ54 holoenzyme by scanning force microscopy. *Journal of Molecular Biology* **1997,** *270*, (2), 125-138.

217. Su, W.; Porter, S.; Kustu, S.; Echols, H., DNA-looping and enhancer activity: association between DNA-bound NtrC activator and RNA polymerase at the bacterial glnA promoter. *Proceedings of the National Academy of Sciences* **1990,** *87*, (14), 5504-5508.

218. Claverie-Martin, F.; Magasanik, B., Positive and negative effects of DNA bending on activation of transcription from a distant site. *Journal of molecular biology* **1992,** *227*, (4), 996-1008.

219. Perez-Martin, J.; De Lorenzo, V., Integration host factor suppresses promiscuous activation of the sigma 54-dependent promoter *Pu* of *Pseudomonas putida*. *Proceedings of the National Academy of Sciences* **1995,** *92*, (16), 7277-7281.

220. Swanberg, S. L.; Wang, J. C., Cloning and sequencing of the Escherichia coli gyrA gene coding for the a subunit of DNA gyrase. *Journal of Molecular Biology* **1987,** *197*, (4), 729-736.

221. Shingler, V.; Bartilson, M.; Moore, T., Cloning and nucleotide sequence of the gene encoding the positive regulator (DmpR) of the phenol catabolic pathway encoded by pVI150 and identification of DmpR as a member of the NtrC family of transcriptional activators. *Journal of Bacteriology* **1993,** *175*, (6), 1596-1604.

222. Ng, L. C.; Poh, C. L.; Shingler, V., Aromatic effector activation of the NtrC-like transcriptional regulator PhhR limits the catabolic potential of the (methyl) phenol degradative pathway it controls. *Journal of bacteriology* **1995,** *177*, (6), 1485-1490.

223. Arenghi, F. L.; Pinti, M.; Galli, E.; Barbieri, P., Identification of the Pseudomonas stutzeri OX1 toluene–o-xylene monooxygenase regulatory gene (touR) and of its cognate promoter. *Applied and Environmental Microbiology* **1999,** *65*, (9), 4057-4063.

224. Murrell, J. C.; McDonald, I. R.; Gilbert, B., Regulation of expression of methane monooxygenases by copper ions. *Trends in Microbiology* **2000,** *8*, (5), 221-225.

225. Bock, C.; Kroppenstedt, R.; Diekmann, H., Degradation and bioconversion of aliphatic and aromatic hydrocarbons by Rhodococcus ruber 219. *Applied Microbiology and Biotechnology* **1996,** *45*, (3), 408-410.

226. Inoue, D.; Tsunoda, T.; Sawada, K.; Yamamoto, N.; Saito, Y.; Sei, K.; Ike, M., 1, 4-Dioxane degradation potential of members of the genera *Pseudonocardia* and *Rhodococcus*. *Biodegradation* **2016,** *27*, (4-6), 277-286.

227. van Beilen, J. B.; Holtackers, R.; Lüscher, D.; Bauer, U.; Witholt, B.; Duetz, W. A., Biocatalytic production of perillyl alcohol from limonene by using a novel *Mycobacterium* sp. cytochrome P450 alkane hydroxylase expressed in *Pseudomonas putida*. *Applied and Environmental Microbiology* **2005,** *71*, (4), 1737-1744.

228. Deng, D.; Li, F.; Wu, C.; Li, M., Synchronic Biotransformation of 1, 4-Dioxane and 1, 1-Dichloroethylene by a Gram-Negative Propanotroph *Azoarcus* sp. DD4. *Environmental Science & Technology Letters* **2018**.

229. Deng, D.; Pham, D. N.; Li, F.; Li, M., Discovery of an Inducible Toluene Monooxygenase that Co-oxidizes 1, 4-Dioxane and 1, 1-Dichloroethylene in Propanotrophic *Azoarcus* sp. DD4. *Applied and Environmental Microbiology* **2020**.

230. Hatzinger, P. B.; Banerjee, R.; Rezes, R.; Streger, S. H.; McClay, K.; Schaefer, C. E., Potential for cometabolic biodegradation of 1, 4-dioxane in aquifers with methane or ethane as primary substrates. *Biodegradation* **2017,** *28*, (5-6), 453-468.

231. Li, W.; Jaroszewski, L.; Godzik, A., Clustering of highly homologous sequences to reduce the size of large protein databases. *Bioinformatics* **2001,** *17*, (3), 282-283.

232. Li, W.; Godzik, A., Cd-hit: a fast program for clustering and comparing large sets of protein or nucleotide sequences. *Bioinformatics* **2006,** *22*, (13), 1658-1659.

233. Moriya, Y.; Itoh, M.; Okuda, S.; Yoshizawa, A. C.; Kanehisa, M., KAAS: an automatic genome annotation and pathway reconstruction server. *Nucleic Acids Research* **2007,** *35*, W182-5.

234. Ricken, B.; Kolvenbach, B. A.; Bergesch, C.; Benndorf, D.; Kroll, K.; Strnad, H.; Vlček, Č.; Adaixo, R.; Hammes, F.; Shahgaldian, P.; Schäffer, A.; Kohler, H.-P. E.; Corvini, P. F. X., $FMNH_2$-dependent monooxygenases initiate catabolism of sulfonamides in *Microbacterium* sp. strain BR1 subsisting on sulfonamide antibiotics. *Scientific Reports* **2017,** *7*, (1), 15783.

235. Valton, J.; Filisetti, L.; Fontecave, M.; Nivière, V., A Two-component Flavin-dependent Monooxygenase Involved in Actinorhodin Biosynthesis in Streptomyces coelicolor. *Journal of Biological Chemistry* **2004,** *279*, (43), 44362-44369.

236. Singh, R.; Lemire, J.; Mailloux, R. J.; Chénier, D.; Hamel, R.; Appanna, V. D., An ATP and oxalate generating variant tricarboxylic acid cycle counters aluminum toxicity in *Pseudomonas fluorescens*. *PLoS one* **2009,** *4*, (10), e7344.

237. Chang, Y.-Y.; Wang, A.-Y.; Cronan, J. E., Molecular cloning, DNA sequencing, and biochemical analyses of *Escherichia coli* glyoxylate carboligase. An enzyme of the acetohydroxy acid synthase-pyruvate oxidase family. *Journal of Biological Chemistry* **1993,** *268*, (6), 3911-3919.

238. Pellicer, M. T.; Badía, J.; Aguilar, J.; Baldomà, L., *glc* locus of *Escherichia coli*: characterization of genes encoding the subunits of glycolate oxidase and the glc regulator protein. *Journal of Bacteriology* **1996,** *178*, (7), 2051.

239. Gedalanga, P. B.; Pornwongthong, P.; Mora, R.; Chiang, S.-Y. D.; Baldwin, B.; Ogles, D.; Mahendra, S., Identification of Biomarker Genes To Predict Biodegradation of 1,4-Dioxane. *Applied and Environmental Microbiology* **2014,** *80*, (10), 3209.

240. Kelley, S. L.; Aitchison, E. W.; Deshpande, M.; Schnoor, J. L.; Alvarez, P. J., Biodegradation of 1, 4-dioxane in planted and unplanted soil: effect of bioaugmentation with *Amycolata* sp. CB1190. *Water Research* **2001,** *35*, (16), 3791-3800.

241. Masuda, H. Identification and characterization of monooxygenase enzymes involved in 1, 4-dioxane degradation in *Pseudonocardia* sp. strain ENV478, *Mycobacterium* sp. strain ENV421, and *Nocardia* sp. strain ENV425. Rutgers University, New Brunswick, 2009.

242. Newman, L. M.; Wackett, L. P., Purification and characterization of toluene 2-monooxygenase from *Burkholderia cepacia* G4. *Biochemistry* **1995,** *34*, (43), 14066-14076.

243. Paune, F.; Caixach, J.; Espadaler, I.; Om, J.; Rivera, J., Assessment on the removal of organic chemicals from raw and drinking water at a Llobregat river water works plant using GAC. *Water Research* **1998,** *32*, (11), 3313-3324.

244. Kim, Y. M.; Jeon, J. R.; Murugesan, K.; Kim, E. J.; Chang, Y. S., Biodegradation of 1,4-dioxane and transformation of related cyclic compounds by a newly isolated *Mycobacterium sp.* PH-06. *Biodegradation* **2009,** *20*, (4), 511-519.

245. Park, J.-W.; Krumins, V.; Kjellerup, B. V.; Fennell, D. E.; Rodenburg, L. A.; Sowers, K. R.; Kerkhof, L. J.; Häggblom, M. M., The effect of co-substrate activation on indigenous and bioaugmented PCB dechlorinating bacterial communities in sediment microcosms. *Applied Microbiology and Biotechnology* **2011,** *89*, (6), 2005-2017.

246. Větrovský, T.; Baldrian, P., The variability of the 16S rRNA gene in bacterial genomes and its consequences for bacterial community analyses. *PloS one* **2013,** *8*, (2).

247. Yu, Y.; Lee, C.; Kim, J.; Hwang, S., Group-specific primer and probe sets to detect methanogenic communities using quantitative real-time polymerase chain reaction. *Biotechnology and Bioengineering* **2005,** *89*, (6), 670-679.

248. Martin, M., Cutadapt removes adapter sequences from high-throughput sequencing reads. *EMBnet. Journal* **2011,** *17*, (1), 10-12.

249. Rognes, T.; Flouri, T.; Nichols, B.; Quince, C.; Mahé, F., VSEARCH: a versatile open source tool for metagenomics. *PeerJ* **2016,** *4*, e2584.

250. Caporaso, J. G.; Kuczynski, J.; Stombaugh, J.; Bittinger, K.; Bushman, F. D.; Costello, E. K.; Fierer, N.; Pena, A. G.; Goodrich, J. K.; Gordon, J. I., QIIME allows analysis of high-throughput community sequencing data. *Nature Methods* **2010,** *7*, (5), 335.

251. Wang, Q.; Garrity, G. M.; Tiedje, J. M.; Cole, J. R., Naive Bayesian classifier for rapid assignment of rRNA sequences into the new bacterial taxonomy. *Applied and Environmental Microbiology* **2007,** *73*, (16), 5261-5267.

252. Müllner, D., fastcluster: Fast hierarchical, agglomerative clustering routines for R and Python. *Journal of Statistical Software* **2013,** *53*, (9), 1-18.

253. Wilkinson, L.; Friendly, M., The history of the cluster heat map. *The American Statistician* **2009,** *63*, (2), 179-184.

254. Volatile organic compounds by gas chromatography/mass spectrometry (GC/MS). In United States Environmental Protection Agency: 2006.

255. Inoue, D.; Tsunoda, T.; Yamamoto, N.; Ike, M.; Sei, K., 1, 4-Dioxane degradation characteristics of *Rhodococcus aetherivorans* JCM 14343. *Biodegradation* **2018,** *29*, (3), 301-310.

256. Cappelletti, M.; Pinelli, D.; Fedi, S.; Zannoni, D.; Frascari, D., Aerobic co-metabolism of 1, 1, 2, 2-tetrachloroethane by *Rhodococcus aetherivorans* TPA grown on propane: kinetic study and bioreactor configuration analysis. *Journal of Chemical Technology & Biotechnology* **2018,** *93*, (1), 155-165.

257. Coleman, N. V.; Le, N. B.; Ly, M. A.; Ogawa, H. E.; McCarl, V.; Wilson, N. L.; Holmes, A. J., Hydrocarbon monooxygenase in Mycobacterium: recombinant expression of a member of the ammonia monooxygenase superfamily. *The ISME Journal* **2012,** *6*, (1), 171-182.

258. Vestal, J.; Perry, J. J., Divergent metabolic pathways for propane and propionate utilization by a soil isolate. *Journal of Bacteriology* **1969,** *99*, (1), 216-221.

259. Vanderberg, L. A.; Perry, J. J., Dehalogenation by *Mycobacterium vaccae* JOB-5: role of the propane monooxygenase. *Canadian Journal of Microbiology* **1994,** *40*, (3), 169-172.

260. Coleman, J.; Perry, J., Purification and characterization of the secondary alcohol dehydrogenase from propane-utilizing *Mycobacterium vaccae* strain JOB-5. *Microbiology* **1985,** *131*, (11), 2901-2907.

261. Girvan, M.; Campbell, C.; Killham, K.; Prosser, J. I.; Glover, L. A., Bacterial diversity promotes community stability and functional resilience after perturbation. *Environmental Microbiology* **2005,** *7*, (3), 301-313.

262. Garbisu, C.; Garaiyurrebaso, O.; Epelde, L.; Grohmann, E.; Alkorta, I., Plasmid-mediated bioaugmentation for the bioremediation of contaminated soils. *Frontiers in Microbiology* **2017,** *8*, 1966.

263. Popa, O.; Hazkani-Covo, E.; Landan, G.; Martin, W.; Dagan, T., Directed networks reveal genomic barriers and DNA repair bypasses to lateral gene transfer among prokaryotes. *Genome Research* **2011,** *21*, (4), 599-609.

264. Goodfellow, M.; Jones, A. L.; Maldonado, L. A.; Salanitro, J., *Rhodococcus aetherivorans* sp. nov., a new species that contains methyl t-butyl ether-degrading actinomycetes. *Systematic and Applied Microbiology* **2004,** *27*, (1), 61-65.

265. He, Z.; Zhang, K.; Wang, H.; Lv, Z., Trehalose promotes *Rhodococcus* sp. strain YYL colonization in activated sludge under tetrahydrofuran (THF) stress. *Frontiers in Microbiology* **2015,** *6*, 438.

266. Hara, T.; Takatsuka, Y.; Niikuni, T., Polychlorinated biphenyl detoxifying complex composition and method for manufacturing same. In Google Patents: 2016.

267. Chong, C. S.; Sabir, D. K.; Lorenz, A.; Bontemps, C.; Andeer, P.; Stahl, D. A.; Strand, S. E.; Rylott, E. L.; Bruce, N. C., Analysis of the xplAB-containing gene cluster involved in the bacterial degradation of the explosive hexahydro-1, 3, 5-trinitro-1, 3, 5-triazine. *Applied and Environmental Microbiology* **2014,** *80*, (21), 6601-6610.

268. Ludwig, B.; Akundi, A.; Kendall, K., A long-chain secondary alcohol dehydrogenase from Rhodococcus erythropolis ATCC 4277. *Applied and Environmental Microbiology* **1995,** *61*, (10), 3729-3733.

269. Kulikova, A.; Bezborodov, A., Assimilation of Propane and Characterization of Propane Monooxygenase from Rhodococcus erythropolis3/89. *Applied Biochemistry and Microbiology* **2001,** *37*, (2), 164-167.

270. Spearman, C., The Proof and Measurement of Association between Two Things. *The American Journal of Psychology* **1904,** *15*, (1), 72-101.

271. Kanitkar, Y. H.; Stedtfeld, R. D.; Steffan, R. J.; Hashsham, S. A.; Cupples, A. M., Loop-mediated isothermal amplification (LAMP) for rapid detection and quantification of *Dehalococcoides* biomarker genes in commercial reductive dechlorinating cultures KB-1 and SDC-9. *Applied and Environmental Microbiology* **2016,** *82*, (6), 1799-1806.

272. Kittelmann, S.; Friedrich, M. W., Novel uncultured Chloroflexi dechlorinate perchloroethene to trans-dichloroethene in tidal flat sediments. *Environmental Microbiology* **2008,** *10*, (6), 1557-1570.

273. MacFarlane, K. D.; Cacciatore, D. A.; Leigh, D. P.; Yurovsky, M. G.; Atta, A., Field-scale evaluation of a biobarrier for the treatment of a trichloroethene plume. *Remediation Journal* **2011,** *22*, (1), 29-41.

274. Abe, Y.; Aravena, R.; Zopfi, J.; Parker, B.; Hunkeler, D., Evaluating the fate of chlorinated ethenes in streambed sediments by combining stable isotope, geochemical and microbial methods. *Journal of Contaminant Hydrology* **2009,** *107*, (1-2), 10-21.

275. Ellis, D. E.; Lutz, E. J.; Odom, J. M.; Buchanan, R. J.; Bartlett, C. L.; Lee, M. D.; Harkness, M. R.; DeWeerd, K. A., Bioaugmentation for Accelerated In Situ Anaerobic Bioremediation. *Environmental Science and Technology* **2000,** *34*, (11), 2254-2260.

276. Conrad, M. E.; Brodie, E. L.; Radtke, C. W.; Bill, M.; Delwiche, M. E.; Lee, M. H.; Swift, D. L.; Colwell, F. S., Field evidence for co-metabolism of trichloroethene stimulated by addition of electron donor to groundwater. *Environmental Science and Technology* **2010,** *44*, (12), 4697-4704.

277. Panagiotakis, I.; Mamais, D.; Pantazidou, M.; Marneri, M.; Parapouli, M.; Hatziloukas, E.; Tandoi, V., Dechlorinating ability of TCE-fed microcosms with different electron donors. *Journal of Hazardous Materials* **2007,** *149*, (3), 582-589.

278. Cupples, A. M.; Spormann, A. M.; McCarty, P. L., Vinyl chloride and cis-dichloroethene dechlorination kinetics and microorganism growth under substrate limiting conditions. *Environmental Science and Technology* **2004,** *38*, (4), 1102-1107.

279. Lovley, D. R.; Phillips, E.; Lonergan, D. J.; Widman, P. K., Fe (III) and S0 reduction by Pelobacter carbinolicus. *Applied and Environmental Microbiology* **1995,** *61*, (6), 2132-2138.

280. Pfennig, N.; Widdel, F.; Trüper, H. G., The dissimilatory sulfate-reducing bacteria. In *The prokaryotes*, Springer: 1981; pp 926-940.

281. Mohr, T. In *1, 4-dioxane and other solvent stabilizers-a ROD re-opener*, Presentation to: United States Environmental Protection Agency Technical Support Project Meeting Sacramento, 2004; 2004.

282. Barajas-Rodriguez, F. J.; Murdoch, L. C.; Falta, R. W.; Freedman, D. L., Simulation of in situ biodegradation of 1, 4-dioxane under metabolic and cometabolic conditions. *Journal of Contaminant Hydrology* **2019,** *223*, 103464.

283. Li, F.; Deng, D.; Li, M., Distinct Catalytic Behaviors between Two 1,4-Dioxane Degrading Monooxygenases: Kinetics, Inhibition, and Substrate Range. *Environmental Science and Technology* **2019**.

284. Polasko, A. L.; Zulli, A.; Gedalanga, P. B.; Pornwongthong, P.; Mahendra, S., A Mixed Microbial Community for the Biodegradation of Chlorinated Ethenes and 1,4-Dioxane. *Environmental Science and Technology Letters* **2019,** *6*, (1), 49-54.

285. Shelton, D. R.; Tiedje, J. M., General method for determining anaerobic biodegradation potential. *Applied and Environmental Microbiology* **1984,** *47*, (4), 850-857.

286. Tedrow, J.; Krieger, R. E., *Soils of New Jersey*. 1986; Vol. 142, p 322.

287. He, Y. T.; Wilson, J. T.; Wilkin, R. T., Impact of iron sulfide transformation on trichloroethylene degradation. *Geochimica et Cosmochimica Acta* **2010,** *74*, (7), 2025-2039.

288. He, J.; Sung, Y.; Krajmalnik‐Brown, R.; Ritalahti, K. M.; Löffler, F. E., Isolation and characterization of *Dehalococcoides* sp. strain FL2, a trichloroethene (TCE)‐and 1, 2‐dichloroethene‐respiring anaerobe. *Environmental Microbiology* **2005,** *7*, (9), 1442-1450.

289. Smidt, H.; de Vos, W. M., Anaerobic microbial dehalogenation. *Annual Review of Microbiology* **2004,** *58*, 43-73.

290. Futagami, T.; Goto, M.; Furukawa, K., Biochemical and genetic bases of dehalorespiration. *The Chemical Record* **2008,** *8*, (1), 1-12.

291. Marcus, D. L.; Bonds, C., Results of the reactant sand-fracking pilot test and implications for the in situ remediation of chlorinated VOCs and metals in deep and fractured bedrock aquifers. *Journal of Hazardous Materials* **1999,** *68*, (1), 125-153.

292. Maymó-Gatell, X.; Nijenhuis, I.; Zinder, S. H., Reductive dechlorination of cis-1, 2-dichloroethene and vinyl chloride by "*Dehalococcoides ethenogenes*". *Environmental Science and Technology* **2001,** *35*, (3), 516-521.

293. Löffler, F. E.; Sun, Q.; Li, J.; Tiedje, J. M., 16S rRNA Gene-Based Detection of Tetrachloroethene-Dechlorinating *Desulfuromonas* and *Dehalococcoides* Species. *Applied and Environmental Microbiology* **2000,** *66*, (4), 1369-1374.

294. Sung, Y.; Ritalahti, K. M.; Sanford, R. A.; Urbance, J. W.; Flynn, S. J.; Tiedje, J. M.; Löffler, F. E., Characterization of two tetrachloroethene-reducing, acetate-oxidizing anaerobic bacteria and their description as *Desulfuromonas michiganensis* sp. nov. *Applied and Environmental Microbiology* **2003,** *69*, (5), 2964-2974.

295. Zhang, T.; Bain, T. S.; Nevin, K. P.; Barlett, M. A.; Lovley, D. R., Anaerobic benzene oxidation by Geobacter species. *Applied and Environmental Microbiology* **2012,** *78*, (23), 8304-8310.

296. Sung, Y.; Fletcher, K. E.; Ritalahti, K. M.; Apkarian, R. P.; Ramos-Hernández, N.; Sanford, R. A.; Mesbah, N. M.; Löffler, F. E., *Geobacter lovleyi* sp. nov. Strain SZ, a Novel Metal-Reducing and Tetrachloroethene-Dechlorinating Bacterium. *Applied and Environmental Microbiology* **2006,** *72*, (4), 2775-2782.

297. Yan, J.; Ritalahti, K. M.; Wagner, D. D.; Löffler, F. E., Unexpected specificity of interspecies cobamide transfer from *Geobacter* spp. to organohalide-respiring Dehalococcoides mccartyi strains. *Applied and Environmental Microbiology* **2012,** *78*, (18), 6630-6636.

298. Löffler, F. E.; Sanford, R. A.; Ritalahti, K. M., Enrichment, cultivation, and detection of reductively dechlorinating bacteria. *Methods in Enzymology* **2005,** *397*, 77-111.

299. Kotik, M.; Davidová, A.; Voříšková, J.; Baldrian, P., Bacterial communities in tetrachloroethene-polluted groundwaters: a case study. *Science of the Total Environment* **2013,** *454*, 517-527.

300. Men, Y.; Feil, H.; VerBerkmoes, N. C.; Shah, M. B.; Johnson, D. R.; Lee, P. K.; West, K. A.; Zinder, S. H.; Andersen, G. L.; Alvarez-Cohen, L., Sustainable syntrophic growth of *Dehalococcoides ethenogenes* strain 195 with *Desulfovibrio vulgaris* Hildenborough and Methanobacterium congolense: global transcriptomic and proteomic analyses. *The ISME journal* **2012,** *6*, (2), 410.

301. Němeček, J.; Dolinová, I.; Macháčková, J.; Špánek, R.; Ševců, A.; Lederer, T.; Černík, M., Stratification of chlorinated ethenes natural attenuation in an alluvial aquifer assessed by hydrochemical and biomolecular tools. *Chemosphere* **2017,** *184*, 1157-1167.

302. Acinas, S. G.; Sarma-Rupavtarm, R.; Klepac-Ceraj, V.; Polz, M. F., PCR-induced sequence artifacts and bias: insights from comparison of two 16S rRNA clone libraries constructed from the same sample. *Applied and Environmental Microbiology* **2005,** *71*, (12), 8966-8969.

303. Hug, L. A.; Beiko, R. G.; Rowe, A. R.; Richardson, R. E.; Edwards, E. A., Comparative metagenomics of three *Dehalococcoides*-containing enrichment cultures: the role of the non-dechlorinating community. *BMC Genomics* **2012,** *13*, (1), 327.

304. Becker, J. G., A modeling study and implications of competition between *Dehalococcoides ethenogenes* and other tetrachloroethene-respiring bacteria. *Environmental Science and Technology* **2006,** *40*, (14), 4473-4480.

305. Aulenta, F.; Beccari, M.; Majone, M.; Papini, M. P.; Tandoi, V., Competition for H2 between sulfate reduction and dechlorination in butyrate-fed anaerobic cultures. *Process Biochemistry* **2008,** *43*, (2), 161-168.

306. Drzyzga, O.; Gerritse, J.; Dijk, J. A.; Elissen, H.; Gottschal, J. C., Coexistence of a sulphate‐reducing Desulfovibrio species and the dehalorespiring *Desulfitobacterium frappieri* TCE1 in defined chemostat cultures grown with various combinations of sulphate and tetrachloroethene. *Environmental Microbiology* **2001,** *3*, (2), 92-99.

307. Fathepure, B. Z.; Elango, V. K.; Singh, H.; Bruner, M. A., Bioaugmentation potential of a vinyl chloride-assimilating Mycobacterium sp., isolated from a chloroethene-contaminated aquifer. *FEMS Microbiology Letters* **2005,** *248*, (2), 227-234.

308. Tiehm, A.; Schmidt, K. R.; Pfeifer, B.; Heidinger, M.; Ertl, S., Growth kinetics and stable carbon isotope fractionation during aerobic degradation of cis-1,2-dichloroethene and vinyl chloride. *Water Research* **2008,** *42*, (10), 2431-2438.

309. Verce, M. F.; Gunsch, C. K.; Danko, A. S.; Freedman, D. L., Cometabolism of cis-1,2-Dichloroethene by Aerobic Cultures Grown on Vinyl Chloride as the Primary Substrate. *Environmental Science and Technology* **2002,** *36*, (10), 2171-2177.

310. Verce, M. F.; Ulrich, R. L.; Freedman, D. L., Characterization of an isolate that uses vinyl chloride as a growth substrate under aerobic conditions. *Applied and Environmental Microbiology* **2000,** *66*, (8), 3535-3542.

311. Schmidt, K. R.; Gaza, S.; Voropaev, A.; Ertl, S.; Tiehm, A., Aerobic biodegradation of trichloroethene without auxiliary substrates. *Water Research* **2014,** *59*, 112-118.

312. Zhao, H.-P.; Schmidt, K. R.; Tiehm, A., Inhibition of aerobic metabolic cis-1, 2-di-chloroethene biodegradation by other chloroethenes. *Water Research* **2010,** *44*, (7), 2276-2282.